ANALYZING THE SUITABILITY OF OPENLISEM HAZARD DEBRIS FLOW MODELLING FOR LAND USE PLANNING IN COLOMBIA

MARIA ISABEL ARANGO CARMONA
August, 2021

SUPERVISORS:
Prof. Dr. Cees Van Westen
Dr. Bastiaan Van den Bout

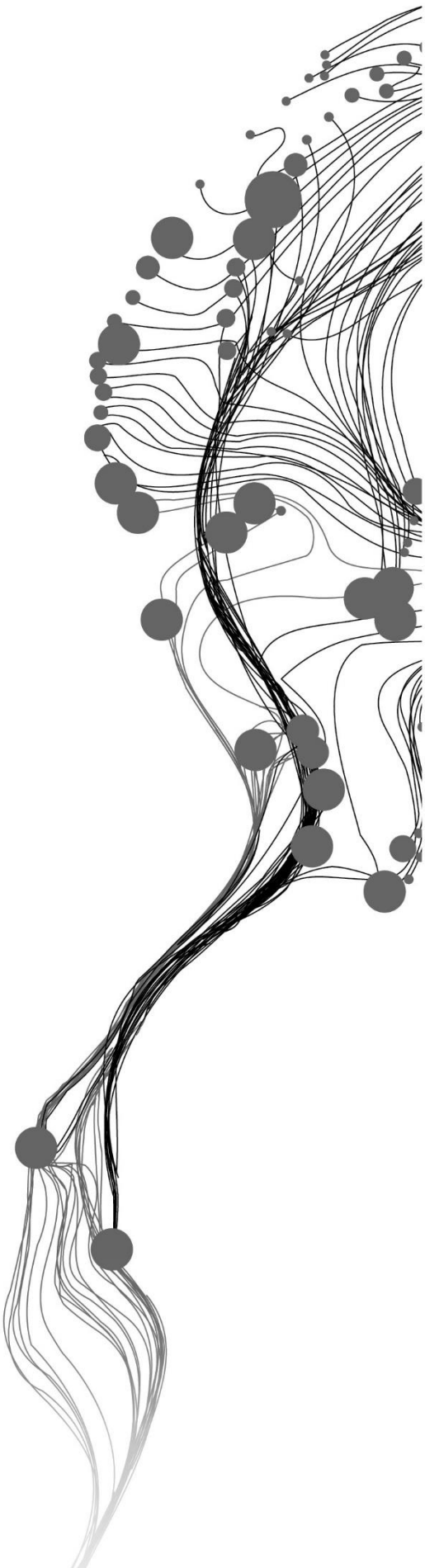

ANALYZING THE SUITABILITY OF OPENLISEM HAZARD DEBRIS FLOW MODELLING FOR LAND USE PLANNING IN COLOMBIA

MARIA ISABEL ARANGO CARMONA

Enschede, The Netherlands, August 2021

Thesis submitted to the Faculty of Geo-Information Science and Earth Observation of the University of Twente in partial fulfilment of the requirements for the degree of Master of Science in Geo-information Science and Earth Observation.
Specialization: Natural Hazards and Disaster Risk Reduction

SUPERVISORS:
Prof. dr. C.J. van Westen
Dr. Bastiaan Van den Bout

THESIS ASSESSMENT BOARD:
Prof. Dr. V.G. Jetten (Chair)
Dr. Rens van Beek (External Examiner, Utrecht University)

ABSTRACT

The Andean region in Colombia is a tropical and mountainous environment where high-intensity rainfall often triggers concatenated phenomena at the catchment scale that includes the coupled or cascading effects of landslides, flash floods, and hyperconcentrated, and debris flows. In Colombia, such events have caused more than 3000 deaths and affected more than 1 million people between 1920 and today.

Recent changes in disaster risk management policies have made it mandatory to include debris flow hazard assessment in the land use planning process. Nevertheless, this analysis has always been evaluated from different approaches, where none of them accounts for its multi-hazard nature and includes all the processes involved in the phenomena. OpenLISEM Hazard is an integrated multi-hazard model that considers and models different hydro-meteorological phenomena and their interactions, like hydrology, runout, slope stability, slope failure, runout, and entrainment. This thesis project aims to analyse the suitability of applying the OpenLISEM Hazard model for developing debris flow hazard maps as a basis for land use planning in Colombia, focusing on evaluating the available datasets influence in terms of resolution and quality. The model was calibrated and validated using two past debris flow events in Colombia with different sources and data quality.

The accuracy assessment of the model was evaluated for each subprocess, including slope failure, runout of hillslope debris flows, and flooding. The process with the higher accuracy is flooding, and the lowest one is the slope failure locations. In general terms, we could not achieve a simulation that represents all the subprocesses with acceptable accuracies in a single run. The calibration of the model included many different variables that were difficult to tune since they influence each sub-process in a different and not traceable way.

This research shows that the main challenges of using multi-hazard modelling with limited information are the propagated uncertainties from unknown or estimated parameters that come into play in the final modelling output. While multi-hazard models show usefulness in research, their application to actual hazard and risk assessment in areas with limited data availability like Colombia should not be undertaken without an improved strategy for dealing with such uncertainties.

ACKNOWLEDGEMENTS

I want to express profound gratitude to my thesis supervisors. To Cees Van Westen for his supportive and patient attitude, improvements in my writing process and keeping my research on track., and to Bastian van den Bout, for guiding me in the technical details of the OpenLISEM Hazard model and support, especially at the end of my thesis process, giving me confidence when I needed it the most. Both cared about me academically and my general well-being, especially during the lockdown period, and I feel fortunate to have them as my supervisors. Also, I would like to thank all the professors from the ESA department of the ITC, who each gave me a piece of knowledge that I'm taking from this experience.

Thanks to professor Edier Aristizábal from the National University of Colombia for encouraging me to work and study with Natural Hazards and his guidance with my thesis when I felt lost. To Federico Gomez and Johnnatan Palacio from the Geohazards group in Medellin for helping me and sharing information about my study cases.

My sincere gratitude to the ITC Faculty of the University of Twente and the Agencia Superior de Medellin - Sapiencia for their financial support during my MSc.

To all the friends I made during my stay in Enschede, for their company and shared experiences. I'm so proud to say I have friends in so many places of the world. Special thanks to Priscilla for becoming my sister and confidant, and Alfredo, my partner and companion, for his patience and love.

I feel especially grateful for my family. Their constant support has given me the courage and confidence to pursue my dreams, and without them, I would not be here. They were my driver in difficult times, and hearing their voices through the phone filled my emotional batteries to continue. Thanks to Iaia and Collin, my piece of family in the Netherlands, for always being there with advice and support, and giving me a place to go when I needed to feel at home.

TABLE OF CONTENTS

LIST OF FIGURES

LIST OF TABLES

1. INTRODUCTION

1.1. Background and Justification

The Andean region in Colombia is a tropical and mountainous environment where high-intensity rainfall episodes are frequent. These rainstorms often trigger progressive and concatenated hydro-meteorological hazardous events locally called *Avenidas Torrenciales*, which translates as "Torrential Avenue", which correspond to the concatenated phenomena at the catchment scale that include the coupled or cascading effects of landslides, flash floods, hyperconcentrated flows, and debris flows. In this work, the different ranges of interactions of such events will be called Debris Flow Processes (DFP). The final stage of such events occurs as the deposition and flooding of fans or low-lying areas that are often populated, resulting in loss of lives and economic damage.

According to the Desinventar database (http://www.desinventar.org/), developed by the Seismological Observatory Corporation of the Colombian Southwest (OSSO) and the Office of the United Nations for Disaster Risk Reduction (UNISDR), there have been 1,387 reports of debris flow processes, including debris floods, debris floods, channelized debris flows, and flash floods between 1921 and April 2020 in Colombia. These events caused at least 3,332 deaths and affected more than 1,152,613 people.

These statistics show the importance of incorporating the hydro-meteorological hazard interactions in susceptibility and hazard assessment as a basis for regional and local land use planning in Colombia. Recent changes in disaster risk management policies have made it mandatory to include floods, landslides, and DFP hazard maps into land-use plans. To guarantee some homogeneity and quality in the elaboration of such analysis, different government institutions have created methodological guidelines for assessing floods and landslides hazard maps, and the guideline for the elaboration of DFP is still under development. This guideline accounts for the multi-hazard nature of the DFP phenomena and suggests using hydrological, slope stability, and flow routing models sequentially. Still, few studies have been carried out that can give insights into the limitations and feasibility of using such methods in the Andean tropical environment.

One recent area of research that is continuously developing is the physically-based coupled models. One of them is the OpenLISEM Hazard, an integrated multi-hazard model that considers and models different hydro-meteorological phenomena and their interactions, like hydrology, runout, slope stability, slope failure, runout, and entrainment. Although integrated physically based models are a promising approach to model hazard interactions, they use many physical parameters and are heavily reliant on data. Such local data is often difficult to obtain when dealing with limited resources or inaccessible locations in study areas.

This thesis project aims to analyse the suitability of applying the OpenLISEM Hazard model for developing DFP hazard maps as a basis for land use planning in Colombia. Because the integration of the hazard and land use plans should be done at the local scale in every municipality of the country, which most lack detailed information, the focus of the analysis is to evaluate the influence of the available datasets in terms of resolution and quality. For this, the model will be calibrated and validated to model two past debris flow events in Colombia using various sets of data, from standard national data to very detailed information.

Integrated models are relatively new and scarce. Understanding the model's capacity and limitations in tropical environments with different data availability will allow us to make more informed decisions about the suitability of this model as input for land management plans.

1.2. Research Objectives and Questions

The research's main objective is to analyse the suitability of the OpenLISEM Hazard tool for modelling debris flow processes as a basis for land use planning in Colombia. Regarding the availability and quality of the information, we will evaluate the main limitations of using the model in a typical Colombian environment. The aim is to assess whether it is a suitable tool to use in areas with limited information and how accurate the results are when modelling with different quality and resolution data.
This main objective is expected to be fulfilled by achieving the following sub-objectives and related research questions:

1. Understand the main implications that modelling with limited input data may have when incorporating such results into land-use plans
   1.1. Does OpenLISEM Hazard provide the type of information that is required in the land use plans?
   1.2. What methodology can be applied to define if the modelling results are acceptable to be incorporated into land use plans?
2. Review the knowledge about the drivers and the occurrence of debris flow processes in Colombia that may influence the methodologies used to model them.
   2.1. What processes and conditions are particular for the occurrence of debris flow processes in Colombia, and which can be modelled with OpenLISEM Hazard?
   2.2. How to design simulation scenarios, including initial and boundary conditions, that capture the range of debris flow events that can occur in the future?
3. Assess the accuracy of the OpenLISEM Hazard model with varying quality and quantity of input data on the various scales in Colombia
   3.1. Are the national and global data sets for parameters like elevation, soils, land use, and rainfall accurate enough to be suitable to model debris flow processes using OpenLISEM Hazard?
   3.2. What sources of information are more reliable to obtain basic input parameters in municipalities with scarce detailed data?
   3.3. How does the resolution and quality of the input data influence the accuracy of the model?
   3.4. What are the most crucial parameters that may cause significant changes in the model's results?
   3.5. Is it better to use other modelling approaches (e.g., empirical approaches) instead of physically-based models when not enough data is available?

1.3. Methodology

Figure 1 shows a flowchart for the proposed methodology. The details of the steps are explained below:

1.3.1. Data acquisition and preparation

The first stage of the methodology includes the compilation and preparation of data for modelling. The analysis is carried out in two different study areas, each of them related to a historical and well documented destructive debris flow event: Salgar and Mocoa.

For the Mocoa case, two sets of data are used for modelling: detailed and coarse. In the case of Salgar, only the coarse dataset is used since no detailed information is available. The detailed dataset includes a higher resolution DEM, rainfall radar or close-by rain gauge rainfall records, local soil and geology maps, and

detailed land use maps. The coarse dataset comprises information extracted from national or global databases, like a global DEM, satellite rainfall information, and national soil and land use maps. In a parallel way, the information concerning the extent and magnitude of the debris flow events of each study area is compiled for calibration and accuracy assessment.

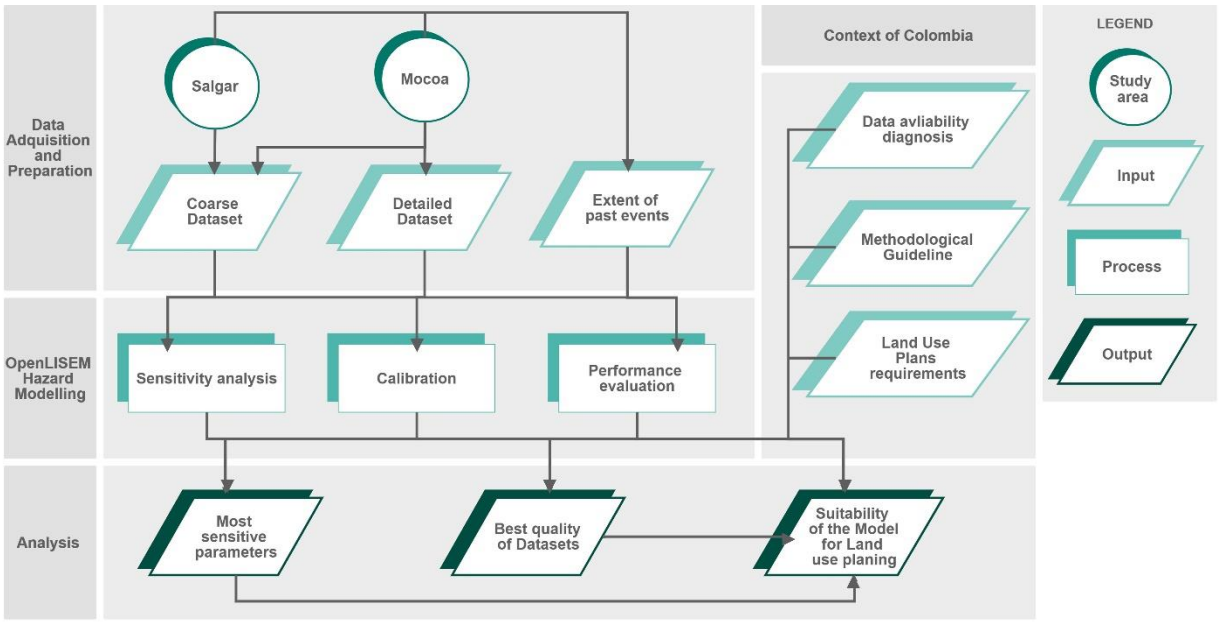

Figure 1. Methodology showing the main phases and processes of the research

1.3.2. OpenLISEM hazard Modelling

The modelling process with OpenLISEM has three main components: Assessing its accuracy with different levels of detail in input information, analysing its sensitivity to different parameters, and calibrating it for the specific case of the study areas.

1.3.2.1. Performance evaluation

The first component is to evaluate the model's performance by comparing the modelling outcomes with the extent of the real events. Three processes will be considered: landslides source areas, propagation of hillslope debris flows, and flood extent. For this, the Receiver Operating Characteristics (ROC) analysis will be carried out. This technique allows the selection of classifiers based on their performance in the prediction, in this case, of unstable cells and areas affected by debris flows and floods. Several ROC indexes have been created to evaluate the performance of a model. All of them uses four variables to measure the accuracy of the results. These variables are True Positives (TP), as the number of cells that the model classifies as unstable or affected and are actually affected. True Negative (TN) is the number of stable cells that the model ranks as stable. False Positives (FP) is the number of cells that the model considers unstable but are stable in reality. Moreover, False Negatives (FN) is the number of cells that the model finds stable but are unstable. The ROC indexes that will be used to evaluate the performance of the model in this study are the False Alarm Rate or False Positive Rate (FPR) and the True Positive Rate or Hit Rate (TPR), defined as:

$$FPR = \frac{FP}{(FP + TN)}$$

$$TPR = \frac{TP}{(TP + FN)}$$

1.3.2.2. Sensitivity Analysis

The sensitivity analysis aims to understand which variables induce instability in the results caused by small changes in their values. Using the datasets with varying resolution and the extent map of the actual events, it is intended to find the most sensitive parameters for each study scale and the critical relationships of parameter calibration at each scale.

1.3.2.3. Calibration

The third component of the modelling process is its calibration for the conditions of the study area. The calibration was first conducted to find the Soil Depth Map and Soil Unit Map that yielded the best results. After this, the calibration was done for the modelling parameters that have the most influence on the results: Cohesion and Internal Friction Angle -that were treated as a single variable- (C-IFA), Soil Depth (SD), Saturated Hydraulic Conductivity (Ksat), and Soil Water Content (Theta).

Table 1. Values used for each calibration parameters for the slope stability analysis.

C- IFA	SD	Ksat	Theta
0.1	1	0.3	1
0.2	1.5	0.6	1.5
0.3	2	1	2
0.6			
1			

The calibration of the modelling parameters was done using the brute force approach, combined with personal criteria. This method enumerates possible combinations of the parameters, using the multiplication factors for each parameter shown in Table 1. The list of possible combinations was iteratively improved based on the observations of previous results and limitations of time and computation resources. All the combinations that were used for each simulation on the study cases are shown in Appendices 7.4, 7.5, and 7.6

Analysis of the context of Colombia

In a parallel way to the modelling process, we analyse the context of incorporating hazard assessment into land use planning in Colombia. This includes diagnosing the scale and quality of available information in the country, focusing on the main input parameters of physically-based models used for debris flow hazard assessments. This analysis also includes examining the requirements of the law that regulate the incorporation of hazard and risk assessment into land use planning and the methodologies that have been suggested to carry out such analysis.

Assessment of the model applicability

By combining the technical analysis of the calibration, sensitivity, and accuracy of the model for the scales of study with the context of the incorporation of hazard analysis in Colombia, the suitability of the OpenLISEM model for land use planning in Colombia is discussed.

2. CONCEPTUAL FRAMEWORK AND BACKGROUND

2.1. Debris Flow phenomena

The classification of hydro-meteorological phenomena that involves a mixture of debris and water is diverse and varies among authors and disciplines. Differences between flow-related phenomena can be determined based on several criteria, like triggering factors, sediment concentration, flow rheology, and momentum transfer. There is a general confusion of terminologies for events composed of mixtures of water and sediments like debris avalanches, mudflows, mudslides, flash floods, hyperconcentrated flows, or lahars (Hungr et al., 2001; Iverson, 1997).

One of the most general definitions of debris flows is proposed by Iverson (1997), who defines them as "mixtures of poorly sorted sediments and water, which rapidly flow downslopes driven by gravity." According to his research, debris flows differ from other flood or landslide related hazards because in debris flows, both the solid and liquid constituents strongly influence the motion. Nettleton et al. (2005) distinguish two forms of debris flows: hillslope debris flows, which form their path down valley slopes as tracks or sheets, and channelised debris flows, which follow existing channel type features. Since these events are closely related to streams, they are often confused with flash floods, debris floods, or floods in disaster reports and databases (Borga et al., 2014).

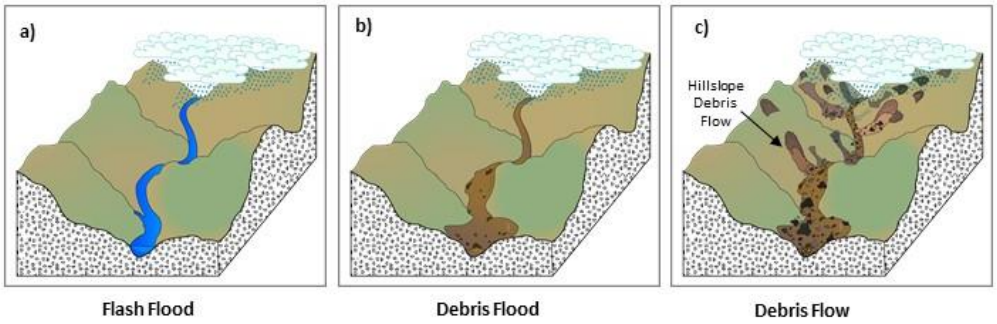

Figure 2. Stages of the formation of debris flow processes in tropical areas.

In the Andean region of Colombia, characterized by tropical weather, deep weathering, and steep slopes, there are often intense and convective rainstorms that are orographically anchored. When falling into steep basins, they generate a rapid runoff concentration that increases the streamflow, generating flash flood events where the steam-driven process dominates (Figure 2a) (Borga et al. 2014). As the flash flood mobilizes downstream, its erosion power increases, remobilizing stream-bed sediments and causing riverbank failures by undermining its channel. These sediments are added to the flow, which becomes a debris flood, a two-phase flow heavily charged with debris (Figure 2b) (Aulitzky 1982; Varnes 1978). The same rainfall event may also trigger, at the same time, one or several landslides in the form of clusters. This phenomenon is defined by Crozier (2005) as Multiple Occurrence Regional Landslide Events (MORLE). When the saturated landslide materials reach the flooded channels, they increase the flow's sediment concentration, altering its rheological properties (Hungr, et al., 2014; J. O'Brien & Julien, 1985). When the flow reaches a very high sediment concentration, flash floods and debris floods become a viscous surge that can range from hyper-concentrated flow to debris flow (Costa 1988; Jakob and Hungr 2005). As the surge moves downstream, erosion power increases, and the stream-bed sediments and the conjunction of small-

scale bank slides or collapses are entrained to the flow (Figure 2c) (Jakob and Hungr 2005). In Colombia, these events are called in technical reports and the media Avenidas Torrenciales, which in English translates literally as "Torrential Avenues", but in this work, they will be designated as debris flow processes (DFP), understanding their variability. They are a concatenated phenomenon in a catchment that includes the coupled or cascading effects of landslides, flash floods, flash floods, and debris flows. The final stage of such events is marked on fans or low-land areas that are often populated, which usually results in being highly affected.

2.2. Modelling approaches of debris flows

Debris flow processes are the result of interactions between various hazardous phenomena at the basin scale. Several approaches have been developed to model such processes independently: hydrology, flooding, slope stability, and debris flow runout. Table 2 shows a review of the modelling approaches. Models can use empirical or physically based equations. The empirical methods rely on field observations and simplified assumptions made from existing cases. They provide general results and are useful when little data is available, and they can be implemented in large areas. Physically-based models use mathematical approaches to model the physical processes that act during the events and clarify the influence of physical parameters in their behaviour (Van den Bout, 2020). Such results are valid only when detailed information about the environment's physical properties is well known, and their computation takes up significant software resources.

Hydrology and flooding models seek to recreate the rainfall-runoff response and assess different properties like depth of water and speed along a flooded channel and its surroundings, based on the topography, soil, land cover, and morphometric characteristics of a basin. Empirical hydrologic and flooding models relate peak flows in a basin and simple parameters like area and shape and calculates possible flooding scenarios based on cross-sections. Physically-based models for flooding intend to solve shallow water equations for a single-phase fluid, determining the characteristics and evolution of large amounts of water moving along different surfaces, either a river channel, a valley, or an urban environment (Alcrudo 2004). They can be classified into one, two, and three dimensional. One-dimensional models represent the channel and floodplain like a sequence of cross-sections where the flow equations are solved for each section. Although they are straightforward and efficient from a computational point of view, they tend to neglect important aspects of flood hydraulics and hydrological processes (Nkwunonwo, Whitworth, and Baily 2020). Examples of such models include HEC-RAS (Bruner 2010) and SOBEK (Deltares 2013). Two-dimensional flooding models consider the topographic features of the channel of the flooding surface. These types of flooding models are widespread nowadays, and they are widely implemented. Some examples include OpenLISEM (De Roo and Jetten 1999), HEC-RAS (Bruner 2010), IBER (Bladé et al. 2014), and MIKE FLOOD (DHI). Three-dimensional flood models solve the flow equations not only on the horizontal but also in the vertical component. They are useful when such dynamics are essential, like in ocean tides or tsunamis. Flow3D (Flow Science) is an example of such an approach.

Slope Stability models include geotechnical and hydrological properties of soil to model the internal forces and find their stability based on the driving and resisting forces as a response to a triggering factor, like rainfall or ground accelerations caused by earthquakes. Physically-based models can use different approaches: they can use finite elements or limit equilibrium. Finite element models divide the mass of a slope into cells or individual units and solve force and strains equations for each component, according to the state of its neighbours (Kanjanakul and Chub-uppakarn 2013). This method can predict particular features like tension cracks and external loads but demands detailed data and computational resources (Ma 2018). Examples of such models are the RS2 (Rocscience) and ADONIS (Mikola 2017) software.

On the other hand, limit equilibrium models use pre-defined potential failure surfaces and calculate their equilibrium based on the Factor of Safety: the ratio between driving and resistive forces. Some of these models use a single scenario for groundwater. In contrast, others are coupled with hydrological models and simulate pore-pressure changes within a storm in the soil and its influence on the slope stability. Infinite slope is the simplest type of limit equilibrium model because they assume a long slip surface and do not calculate lateral forces within the soil. Although they can be used in large areas with varying details, the slip surface is limited to shallow and transitional slip surface (Martin Mergili et al. 2014). Examples of infinite slope models include SHALSTAB (Dietrich and Montgomery 1998), TRIGRS (Baum, Savage, and Godt 2008), and PROBSTAB+STARWARS (Van Beek 2002). Instead, finite slope limit equilibrium models divide the slipping surface into vertical slices, and the Factor of Safety is calculated considering the inter-slice forces. The slip surfaces in finite slope models can vary in depth and shape. The limitations of such models include their inapplicability in GIS environments (Westen and Terlien 1996). Finally, three-dimensional limit equilibrium models use different shapes and depths of slipping surfaces and are fully integrated with GIS interfaces. Examples include Scoops3D (Reid et al. 2015) and r.slope.stability (Martin Mergili et al. 2014).

Runout models intend to reproduce the surface processes that influence the extension, height, and velocity of debris flow depending on the topography and the flow's volume and rheological parameters (Quan 2012). Empirical models rely on field observations and geomorphological features of debris flows and assess the pathways and reaching length or area. Some examples are the one proposed by Heim & Albert (1882) and redefined by Hsu (1975), the Flow-R model (Horton, Jaboyedoff, Rudaz, & Zimmermann, 2013), and the r.randomwalk model (M. Mergili, Krenn, and Chu 2015). Physically-based runout models rely on mass, momentum, and energy conservation equations, in addition to rheological equations that define the velocity, acceleration, and runout distance of the flow. To solve those equations, the models can rely on one and two-dimensional solutions. One dimensional model only considers the cross-section of the travel path to analyse the movement. Two-dimensional models consider the cross-section of the flow, but also the movements from a plan view (Quan 2012). Some examples of two-dimensional, physically-based models are FLO-2D (O'Brien, Julien, & Fullerton, 1993), DAN3D (McDougall and Hungr 2004), and RAMMS (Christen, Kowalski, and Bartelt 2010). Other types of physically-based models for debris flow runout use a discrete approach and are called Cellular Automata. They model the interactions between the constituent elements of a flow, representing them as cells, where each cell's value depends on the adjacent cells' transition functions (Lupiano et al. 2018). The model SCIDDICA (D'Ambrosio et al. 2007) is the most widespread model of this type.

Table 2. Review of the current approaches for modelling processes involved in debris flows

PROCESS	**BASE**	**TYPE**		**EXAMPLES**
Hydrology - Flooding	Physical	1D		HEC-RAS (Bruner, 2010), SOBEK (Deltares, 2013)
		2D		OpenLISEM (De Roo & Jetten, 1999), HEC-RAS (Bruner, 2010), MIKE FLOOD (DHI)
		3D		Flow3D (Flow Science)
Slope Stability	Physical	Finite Elements		RS2 (Rocscience)
		Limit Equilibrium	Infinite Slope	SHALSTAB (Dietrich & Montgomery, 1998), TRIGGRS (Baum, Savage, & Godt, 2008), PROBSTAB+STARWARS (Van Beek, 2002)
			Finite Slope	Slide (Rocscience), ADONIS (Mikola 2017)

			3D	Scoops3D (Reid, Christian, Brien, & Henderson, 2015), r.slope.stability (Mergili et al., 2014).
Runout	Empirical			Mobility Ratio (Heim & Albert 1882), Flow-R (Horton et al. .2013), r.randomwalk v1 (M. Mergili, Krenn, and Chu 2015)
	Physical	2D		Flo-2D (O'Brien, Julien, & Fullerton, 1993), RAMMS (Christen, Kowalski, & Bartelt, 2010), DAN3D (McDougall and Hungr 2004)
		Cellular Automata		SCIDDICA (D'Ambrosio, Iovine, Spataro, & Miyamoto, 2007)
Integrated	Physical			STEP TRAMM (Fan, Lehmann, McArdell, & Or, 2017), r.avaflow (Mergili, Fischer, Krenn, & Pudasaini, 2017), RAMMS (Christen et al., 2010), Flo-2D (K. O'Brien, 1982), OpenLISEM Hazard (Bout et al., 2018), EDDA 2.0 (Shen et al. 2018)

The previously mentioned models focus on single hazards, but single triggering factors like rainfall or earthquake often generate different phenomena that interact with each other. The single hazards can be modelled separately, but their interaction can alter the final event's result. For that reason, understanding how hazards relate in time and space is a crucial step in a complete hazard assessment (Van den Bout, 2020). Some integrated hazards models include STEP TRAMM (Fan et al. 2017) that integrate slope stability and runout. Others, like r.avaflow (Martin Mergili et al. 2017), RAMMS(Christen, Kowalski, and Bartelt 2010), EDDA 2.0 (Shen et al. 2018), and Flo-2D(K. O'Brien 1982), integrate and relate the relationships between different types of mass movements. Finally, OpenLISEM Hazard (Van den Bout, Lombardo, van Westen, & Jetten, 2018) will be used in this study, integrates hydrology, slope stability, runout, flooding, and entrainment of debris into flows.

2.3. OpenLISEM Hazard

OpenLISEM Hazard is a physically-based, multi-hazard model that incorporates hydrological processes like rainfall, interception, infiltration, runoff, and morphological processes like slope stability, slope failure, and debris flow runout. An integrated simulation tool like OpenLISEM Hazard allows understanding the interactions and feedback of all the processes of a concatenated debris flow event until its end into the deposition zone (Van den Bout et al. 2018). It was developed by Bout et al. (2018), based on the Open Source Limburg Soil Erosion Model (OpenLisem), created by De Roo & Jetten (1999), that specializes in event-based runoff, flooding, and erosion at the basin scale, using soil physical information, land cover and terrain properties.

Table 3 shows the processes and sub-processes included in the OpenLISEM Hazard model. The documentation of the model includes an extensive review of the equations for each subprocess (Bout et al. 2018), which are also summarized in the table, with the main input parameters required to compute each process. The model includes four processes: Hydrology, Sediments, Slope Stability, and Mass Movement. The model includes a graphical interface and an interactive map viewer, making it very friendly for new users. All the settings, input maps and parameters can be defined in the interface.

Table 3. Processes and subprocesses included in the OpenLISEM Hazard model.

PROCESS	SUBRPOCESS	MODEL	INPUTS
Hydrology	Interception	Calculated for vegetation, buildings, and rain drums	- Digital Elevation Model - Rainfall intensity - Surface properties (Roughness, Manning's N, vegetated areas, buildings, roads) - Soil Hydraulic parameters - Channels Width and Depth
	Infiltration	Green & Ampt infiltration model, Smith & Parlange model, SWATRE multi-layered soil water model	
	Groundwater flow	Calculation of vertical and lateral flow in the soil using retention curves	
	Surface flow	Sain Venant equations for mass conservation and momentum balance for shallow water flows	
Sediment	Splash detachment	Equation derived from splash tests	- Digital Elevation Model - Rainfall intensity - Vegetation Height - Soil Cohesion - Grain Size Distribution - Soil depth
	Erosion	Transport capacity, flow detachment, sediment deposition and grain settling velocity equations	
	Sediment Transport	Equations of sediment flow in kinematic waves and steady flows.	
	Sediment Diffusion	Diffusion coefficient included in sediment flow computing	
	Two-layer sediment load	Calculation of thickness and transport of two layers of sediments in the channel section: bedload and suspended sediment	
	Multi-class sediment	Overland flow, bed, and suspended load transport using different grain sizes in each run	
Slope Stability	Slope Stability	Infinite slope with planar and shallow failure surface model following Mohr-Coulomb failure criterion	- Digital Elevation Model - Rainfall intensity - Soil Geotechnical parameters (Cohesion, Internal Friction Angle, Saturation level, Root cohesion) - Soil depth
	Iterative failure and slope failure volume	Iterative process of failure depth calculation from toe to top of slopes, including the interaction of inter-slice forcing. The unstable material is removed and considered as failure volume.	
Mass Movement	Rheology	Two-phase equations that contain pressure, gravitational and viscous forces, non-Newtonian viscosity, two-phase drag, and a Mohr-Coulomb type friction force for the solid phase.	- Sediment Density - Average Grain Size - Internal Friction Angle
	Entrainment	Entrainment equations	

2.4. Incorporation of hazard maps for land use planning in Colombia

The "*Plan de Ordenamiento Territorial*" (POT) in Colombia is the primary land management planning tool developed at the municipal scale, which is the second level of administrative units in Colombia (after the Departments). The 1.123 municipalities in Colombia vary significantly in size, with areas ranging from 15 Km^2 in highly populated areas, to more than 65.000 Km^2 in remote regions (Gobierno de Colombia, 2020). Each municipality is responsible for formulating its POT every 12 years, with possible revisions and updates

every four years. Although risk prevention and reduction were a part of Colombia's land use planning since the 1990s, their incorporation policies were unclear (UNGRD, 2015). After the ENSO season of 2010-2011, which left more than USD 4870 billion in economic losses and affected more than 5.2 million people (Serdano-Cruz, Carvajal-Escobar, and Avila Diaz 2013), disaster risk management policies have been specified to fully incorporate floods, landslides, and debris flow hazard maps as a base input for their POT (Ministerio de Vivienda 2014). The "*Corporaciones Autónomas Regionales*" (CAR) are the autonomous regional environmental corporations responsible for approving and monitoring the POT of the municipalities within their jurisdiction.

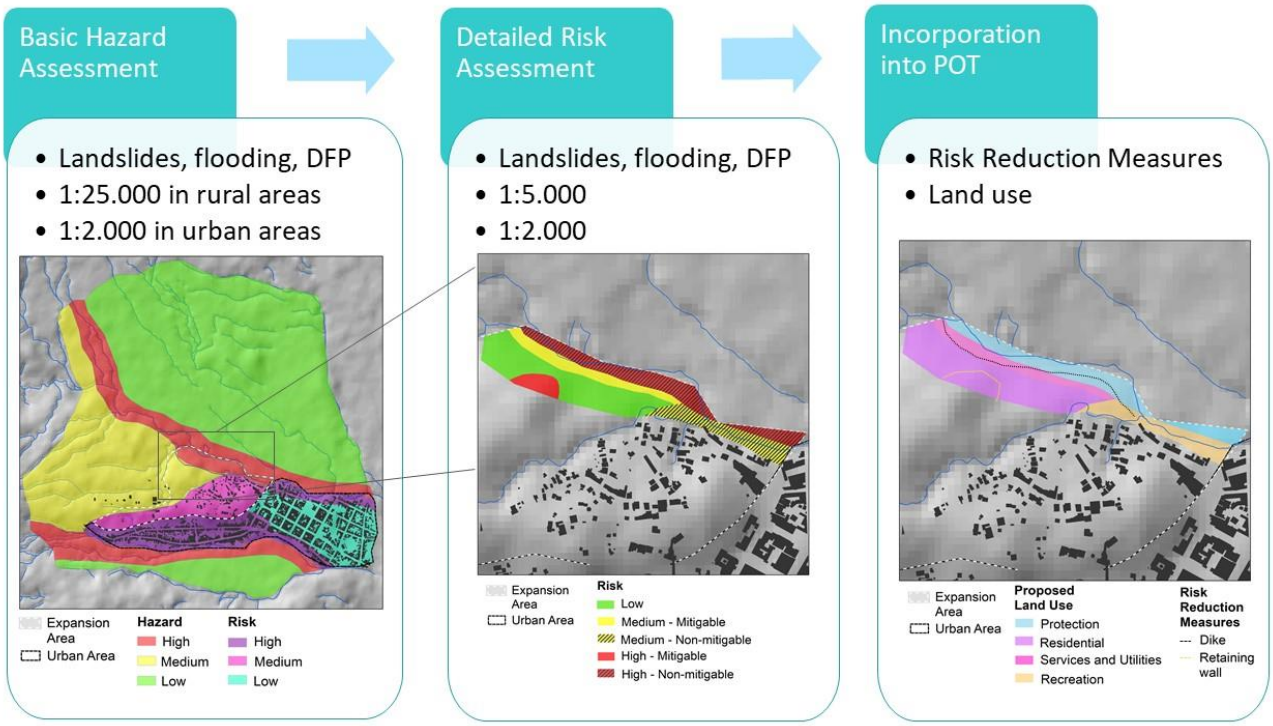

Figure 3. Steps for the incorporation of hazard and risk assessment into Land Use Plans

The new regulation for incorporating hazard assessment into land use planning indicates two levels of hazard analysis (Figure 3). First, a basic hazard assessment is carried out in the whole municipality area on a scale of 1:25.000 in rural areas and 1:5.000 in urban and urban expansion areas. The basic hazard assessment's objective is to divide the municipality between areas with hazardous conditions (non-populated regions with medium or high hazard), areas with risky condition (hazardous conditions in populated areas), and areas with low hazard. Land regulations like use, density or potential are applied in a POT based on the zonation of the basic hazard assessment. The methodologies to assess hazard and criteria to define its level are specified in the methodological guidelines explained in section 2.5. Although following the methodological guidelines is not mandatory, the role of the CARs is to approve the validity of the hazard assessment methods and results.

Whenever the municipality plans to develop an urbanization project on hazardous or risky areas, they must define study polygons and conduct a detailed analysis on a scale of 1:5.000 in rural areas and 1:2.000 in urban and urban expansion areas. This study includes detailed hazard, vulnerability, risk, and mitigation measures assessment. The output of this analysis is the division of the polygons between areas with low, medium, and high risk, divided into mitigable and non-mitigable. Areas considered as high or medium non-mitigable risk

are not candidates for any type of urbanistic development and must be regarded as protected areas. Hazard or vulnerability reduction measures must be proposed for projects in areas considered to have medium or high mitigable risk, together with a definition of other characteristics such as proposed land use, maximum density, occupation, and type of development.

2.5. Methodological Guidelines

After the change of policies for incorporating hazard assessment into land-use planning, it was imperative to standardize and give general guidelines about the methodological framework to carry out such hazard analysis. Several methodological guidelines for floods and landslide hazard maps were created recently (IDEAM & CNM, 2018; SGC, 2015; SGC, 2017). The methodologies that were used during the last decades for assessing debris flows hazard, on the other hand, were very diverse. Since the phenomena were studied from the hydrology and geology standpoints, either slope stability or flooding models were used independently. In general, there was a lack of knowledge about the use of methodologies that acknowledge the multi-hazard nature of these events. Finally, the guideline for developing debris flow hazard maps is under development (SGC & PUJ, 2020). The suggested methodologies of guidelines are described in the following sections.

2.5.1. Landslides

The methodological guidelines for landslide hazard zoning were divided into basic and detailed studies. The Colombian Geological Survey (SGC) is responsible for creating and publishing the guidelines.

2.5.1.1. Methodological Guideline for Landslide hazard assessment at 1:25.000 scale (SGC 2017)

For basic studies, the proposed scale is 1:25.000. The guideline suggests dividing the landslide processes into deep-seated and shallow landslides, falls, creeps, and flows. Flows are compared in this guideline to debris and mudflows.

This guideline proposes to carry out an environmental characterization of the study area, including collecting and elaborating the morpho-dynamic processes inventory and analysis of conditioning and triggering factors. The basic input data for the characterization is shown in Table 4**¡Error! No se encuentra el origen de la referencia.**.

The scale of analysis for the landslide hazard assessment in basic studies is the Geological Superficial Units (UGS), which divides the homogeneous material exposed to the environment in the terrain. Units are primarily classified between soils and rocks, and secondarily according to their origin, composition, engineer properties, geo-mechanic classification, and degree of weathering.

Table 4. Input data for geo-environmental characterization for the landslide hazard assessment

Types	Data
Inventory	Landslide inventory
Geomorphology	Slope
	Curvature
	Morphogenesis
Superficial Geological Units	Rock type
	Weathering
	Discontinuities
	Structural Features
	Falls
	Soil Types
	Soil Depth
	Geotechnical parameters
	Hydrological Parameters
Land use and Cover	Landcover
	Current Land use
	Land use changes
Triggering	Rainfall records
	Earthquake records

For the susceptibility assessment, the guideline proposes using the Weight of Evidence (WoE) bi-variate statistical analysis, whose goal is to assess the relationship between a combination of conditioning factors and landslides occurrence based on past events. For hazard assessment, the frequency of occurrence of the triggering factor is included. Depending on the quality of information available in the study area, other alternatives can be used, such as heuristic or methodological methods, geomorphology, absolute frequencies, relative frequencies, correlation with rainfall threshold, etc.

2.5.1.2. Methodological Guideline for Landslide risk assessment at 1:5.000 scale (SGC 2015)

For detailed studies, the analysis must include hazard, vulnerability, and risk assessment at the scale of 1:5.000 or 1:2.000. This guideline emphasizes that the methodology is unsuitable for debris flow processes since they are not considered a type of landslide, contradicting the guideline for the 1:25.000 scale.

For the hazard assessment, a basic map of Geological Units for Engineering (UGI) must be constructed from information like geology, geomorphology, land use, land cover, and geotechnical soil and rock sampling. For basic studies (1:5.000), the hazard is assessed using physically-based limit equilibrium methods that result in terms of Safety Factor at the pixel scale. For detailed Studies (1:2.000), the hazard is calculated also using physically-based limit equilibrium methods, but the hazard level is assessed in terms of failure probability, computed using different scenarios of soil parameters and triggering factors. The hazard is described in terms of the magnitude, travel distance and velocity of the possible events.

The vulnerability assessment is carried out by computing damage levels with different probability scenarios using information about Elements at Risk and fragility curves regarding buildings, essential infrastructure, and people. Finally, the risk is assessed in terms of life and economic losses expected per time unit.

2.5.2. Methodological guideline for the construction of Flooding Maps (IDEAM & CNM 2018)

They were published by The Colombian Institute of Hydrology, Meteorology and Environmental Studies (IDEAM) and the National Modelling Centre (CNM). Debris flows are not considered in the guideline, but they include Colombia's debris flow susceptibility map into their annexes. This document contains very general guidelines for constructing different flooding maps: susceptibility, events, hazard, hazard zoning, vulnerability, and emergency. For the flooding hazard assessment, the guideline proposes hydrological modelling (using either historical flow record or rainfall-runoff models) and hydraulic modelling (1D, 2D or 3D). The guideline is not very specific on what methods to use, although it gives valuable insights into each methodology's possible options, pros, and cons. The hazard zonation is also very illustrative, showing different international and national standards of flooding hazard zonation (ASCE, FEMA, Australia, IGME and IDEAM), but it doesn't constrain the use of a specific method.

2.5.3. Methodological Guideline for Debris Flow hazard assessment (SGC &PUJ 2020)

This guideline is still under construction, and the methodology described here concerns a preliminary version of the document; therefore, some specific items may vary in the final version. The guideline is constructed by the Colombian Geological Survey (SGC) and the Pontificia Javeriana University (PUJ).

This methodology suggests combining hydrologic and dynamic flow models for creating debris flow hazard maps. To start, they recommend analysing the study area at the scale of 1:25.000 and, based on the results, selecting critical areas like medium and high hazard zones, old torrential deposits, or urban areas for a more detailed analysis 1:2.000 scale.

The assessment steps include the collection and preparation of input data, the modelling of the volume of sediments coming into the flow (called initiation zones), the flow modelling (called transport, drag and deposition), and the hazard computation.

2.5.3.1. Preparation of input data

The inputs for this analysis are listed in Table 5. When no detailed Digital Elevation Model is available in the study area, the guideline proposes using a corrected and re-sampled version of the 12.5m ALOS PALSAR DEM, corrected using interpolation with heights from elements like roads, drainages, or land surveying data.

Table 5. Main inputs for the debris flow hazard assessment

Basic inputs	**Debris Flow Characterization**	**Triggering factors**
Adjusted 12.5m DEM	Geo-environmental characterization	Rainfall Records
Geomorphological and geological map	Debris flow inventory	Soil Hydraulic Parameters
Land use and Land cover maps	Landslide Susceptibility map	Stream Flow Records

The geo-environmental characterization and landslide susceptibility map are extracted from the landslide hazard assessment for the same study area.

For the construction of the flooding hydrographs and the flow series for each return period, an intensity-frequency analysis is carried out using different methods, depending on the quality of the input information available for the study area, as summarized in Table 6. The basic input for the intensity-frequency analysis is rainfall records, obtained from local rain gauges or global satellite products like CHIRPS (Funk et al. 2015). The records must be then used to construct the Intensity-Duration-Frequency curves for the 2.33, 5, 10, 25, 50, 100, 300, and 500 years return periods. The rainfall-runoff and infiltration models can be physically based when enough soil hydraulic parameters and stream flow records are available. Otherwise, the parameters can be estimated using empirical approaches.

Table 6. Data requirements and models proposed for the construction of the flooding hydrographs

Type of Model	**Input**	**Good Quality Input**	**Poor Quality Input**
Design Hydrograph	Rainfall Record	IDEAM National Rainfall Gauges Records	CHIRPS Satellite Rainfall records
Infiltration	Soil Hydraulic Parameters	Physically Based (Green-Ampt or other)	Curve Number (SCS)
Rainfall - Runout	Flow record	Physically Based	Convoluted Synthetic Unitary Hydrograph

2.5.3.2. Assessment of Initiation Zones

This analysis estimates the volume of solids incorporated into the flow, coming from slope erosion, landslides, rockfall and hillslope debris flows.

- Sediments coming from slope erosion: They are estimated using a semi-empirical model that relates the rainfall drop diameter, calculated from the rainfall records, with soil parameters like vegetation cover, slope, and flow depth to estimate the erosion rate due to raindrops impact and runoff.
- Sediments coming from landslides, rockfalls, and hillslope debris flows: The potential areas of sediment sources are the areas considered as high and medium susceptibility in the landslide susceptibility assessment. The sediment volume is estimated using an empirical relationship between the slopes of the main channel and its hillslopes and considering the weathering state of the slopes, based on the predominant lithology of the basin.
- Sediments coming from stream bed undermining: This is only considered when working in the 1:2.000 scale. Potential areas that are susceptible to lateral channel erosion are selected and

mapped based on geomorphological features. The volume of sediments eroded in such areas is computed using physically-based limit-equilibrium models to estimate the critical velocity when the flow starts to undermine its channel. Then, an empirical relationship is applied to estimate the volume of eroded materials considering the amount of time that the flow overcame the critical velocity.

The final output of the assessment of initiation zones is a flooding hydrograph for each return period that contains solid and liquid volumes.

2.5.3.3. Modelling of transport, dragging and deposition

The flow modelling follows a different procedure depending on the scale of analysis:

- 1:25.000: The guideline proposes to use two-dimensional, single-phase physically-based models to assess the hazard. They mention the models FLO-2D, RAMMS, D-Claw, FLATModel, Titan2D, RiverFlow2D, and massmov2D as options to calculate the maximum velocity and flow depth, the parameters that are used for the hazard calculations.
- 1:2.000: They suggest using physically-based models, but they should include the dragging of sediment of the streambed into the flow; therefore, they should model two-phase flows. Some of the models that the guideline suggests including iRIC, r. avaflow, TRENT2D WG and D-Claw. The models should be used to calculate maximum velocity and flow depth for each return period scenario.

2.5.3.4. Hazard assessment

For the hazard assessment, different methodologies were also suggested depending on the scale of the analysis:

- 1:25.000: Hazard is assessed using a matrix that integrates two variables: The Flow Intensity Index, an index that is computed synthetizing all the return period's maximum depth and velocity; and the D_{90} diameter of the typical sediment column of the stream, a parameter that accounts for the magnitude of the event. The hazard is qualified as low, medium, or high.
- 1:2.000: The Flow Intensity Index is also computed, but a single value is calculated for each return period. The information of the flow intensity associated with each return period can be used to create a hazard curve that relates each return period with a flow intensity. The procedure to obtain a final hazard value from the curve is still under debate.

2.6. Related Work

The OpenLISEM Hazard model has been tested in several environments and multi-hazard settings. Bout et al. (2018) tested the OpenLISEM Hazard model's accuracy with a debris flow event in Sicily, Italy, in 2009. Their conclusions include the high reliability of the model in the quality of input information like the Digital Elevation Model, soil properties and landslide susceptibility, and proper calibration of the main parameters with ground truth data. Fonseca (2019) used the OpenLISEM Hazard model to evaluate the multi-hazard risk to debris flow in the Ayurá basin of Antioquia, Colombia. Even though the study area had very detailed input data, the only information about early events in 1927, 1944, 1964, and 1988 are news and disaster database reports. No indication or map of affected areas and landslides is available, so the model's results could not be calibrated, and its performance could not be evaluated. Xiao (2020) tested the OpenLISEM Hazard model's transferability using the debris flow caused by the 2008 earthquake in Wenchuan, China. She calibrated and conducted a sensitivity analysis of the model using the co-seismic debris flows generated by the earthquake in a basin and run the model using the calibrated parameters in a similar watershed. Her findings include the capability of the model of predicting the occurrence, magnitude, and arrival time of debris flow in new study areas using the calibration of similar regions. However, the

volume and arrival time of the events is not very well estimated. The sensitivity of the parameters varied significantly between different study areas.

Other studies that use physically-based models for debris flow hazard maps in tropical areas include the one carried out by Lehmann, von Ruette, & Or (2018), who used two debris flow events in Sierra Leone and Colombia to test the accuracy of the STEP-TRAMM coupled model, and Arango-Carmona, (2019) and Chiang, Chang, Mondini, Tsai, & Chen, (2012) who used slope stability, debris flow routing and flooding propagation models in an integrated way to assess debris flow hazard in topical areas like Taiwan and Colombia, respectively. Gomes et al. (2008) follow a similar approach by combining slope stability with debris flow runout models in Brazil. Shen et al. (2020) used the EDDA 2.0 model to evaluate three entrainment models using data from a debris flow event in Hong Kong, finding the main differences between each model in terms of accuracy in magnitude, deposition volume, and inundation area.

3. STUDY AREA AND DATA COLLECTION

3.1. Colombia

Colombia is located in a complex tectonic setting resulting from the Caribbean Plate moving south-eastward from the North of the South American Plate and the Nazca plate subducting in its western margin (Kellogg, Vega, and Stailings 1995; Taboada et al. 2000; Trenkamp, Kellogg, and Freymueller 2002). The Andean range, the product of the subduction processes, stretches along the Western edge of South America and divides into three mountain ranges in Colombia. The Western Cordillera consists of oceanic blocks accreted in the Cretaceous and Tertiary, composed of mafic and ultramafic rocks with high levels of deformation and shearing. The Central Cordillera is composed of Mesozoic igneous rocks intruded into Precambrian metamorphic rocks with Cenozoic volcanic activity, and the Eastern Cordillera is composed of Palaeozoic to Cenozoic sedimentary rocks. The Cauca – Patía fault separates the Western and Central Cordillera, and the Magdalena valley sedimentary basin separates the central and Eastern Cordilleras. The Eastern Cordillera is separated to the Eastern Orinoco plains and the Amazonian Forest by the Llanero Piedmont fault line (Gomez et al. 2007). In addition to this tectonic setting, the Andean Mountain ranges correspond to the eastern section of the "Pacific Ring of Fire," which extends around the perimeter of the Pacific Ocean and where much of the world's volcanic and earthquake activity is concentrated (Anderson and Decker 1992).

The annual rainfall pattern in Colombia is governed by the passing of the Intertropical Convergence Zone (ITCZ) that oscillates between 5° South latitude in January-February, and 14° North in July and August (Jaramillo-Robledo and Chaves-Córdoba 2000). For Colombia, this means the ITCZ marks a rainy season between December and April in the South. For the rest of the country, including the Andean region, it marks two rainy seasons during April-May and September-November, created by the double-pass of the ITCZ. Nonetheless, the intra-annual weather and rainfall pattern of the country is also influenced by local characteristics like the topographic gradients of the three Andean mountain ranges, crossing from southwest no northeast, the atmospheric circulation patterns over the Pacific and Caribbean sea, and the hydroclimatic dynamics of the Amazon and Orinoco basins (Poveda et al. 2007), while the interannual variability is also marked by the presence of the phases of the El Niño/Southern Oscillation (ENSO), that causes dry and rainy phases (Pabón, Eslava, and Gómez 2001). Also, localized phenomena like strong topographic features induce local atmospheric circulation and topographic peaks, enhancing deep anchored convective systems and leading to highly intense storms in space and time that trigger flash floods, debris flows, and landslides (Álvarez-Villa, Vélez, and Poveda 2011; Poveda 2011).

3.2. Data availability in Colombia

Given that debris flow and landslide hazard assessment studies must be carried out in every country municipality for land use planning, it is essential to understand the availability of the basic input information for carrying out such analysis on the national scale. In this following section, there is a general description of the scale and spatial coverage of some of the datasets that could be used to extract such information.

3.2.1. Basic Cartography

The institution responsible in Colombia for creating and publishing cartographic data is the Agustin Codazzi Geographical Institute (IGAC). In 2018, the institute published a catalogue with the available geographical information for land use planning for each department of Colombia (IGAC 2018). Figure 4 shows a summary of the basic cartographic elements available for each department. The grey dots in the map represent settlements and illustrate where most of the population lives in the country, mainly in the Andean

and Caribbean regions. The Pacific region and Orinoco plains have medium densities of settlements, while the Amazonian area is sparsely populated.

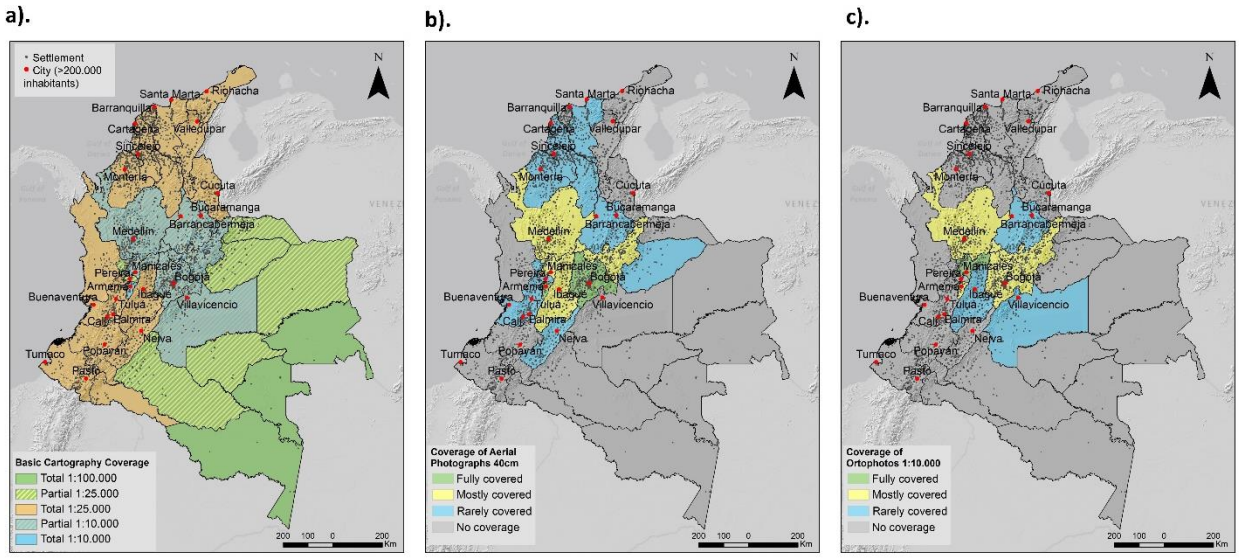

Figure 4. Coverage of basin cartography in each department of Colombia.

Figure 4a shows the best resolution available for basic cartographic maps. These maps contain general information about contour lines, drainages, buildings, control points and vegetation cover. The only available product for the whole country is at 1:100.000 scale, although the most urbanized areas have partial or total coverage with better resolution data (1:25.000 and 1:10.000). A set of maps in 1:2.000 is also available upon request for main cities and large settlements. The data that can be extracted from basic cartographic maps for hazard assessment is the Digital Elevation Model, constructed from the contour lines and infrastructure lines of roads, useful for surface flow modelling. Digital aerial photographs of 40 cm resolution, acquired between 2009 and 2014, are also available in some departments, as shown in Figure 4b. Such images can be used to map surface properties like land use, land cover, and elements like buildings and roads. Another set of aerial photographs of 7 to 15 cm of resolution are also available for main cities. Orthophotos with a scale of 1:10.000 are also available, as shown in Figure 4c. Other datasets of orthophotos at 1:5.000 and 1:2.000 are also available for major cities. Orthophotos can be used in the hazard assessment to map land cover, land use, cartographic elements like buildings and roads, and carry out geologic and geomorphological photo interpretation, which can lead to the construction of maps of soil units, geology, geomorphological units, and morpho-dynamic processes inventories. The aerial photographs and orthophotos are not freely accessible; they must be requested to the IGAC.

3.2.2. Geology, Geomorphology and Geohazards

The Colombian Geological Survey (SGC) is the entity responsible for elaborating and distributing geological, geomorphological, and geo-hazards related maps, among others.

There are currently two freely-available geological maps at the national levels that cover the country at a 1:1.000.000 scale (SGC 2007, 2015b). Figure 5a shows the coverage of the geological cartography at 1:100.000 scale, available for most of the Andean, Caribbean, and Pacific regions. Figure 5b shows the availability of departmental geological maps at intermediate scales. More detailed scales (1:50.000, 1:25.000) are available for specific areas. The geological maps are an essential input for the zonation of soil units, and they can give a broad idea of the geotechnical and hydrologic parameters of the soils.

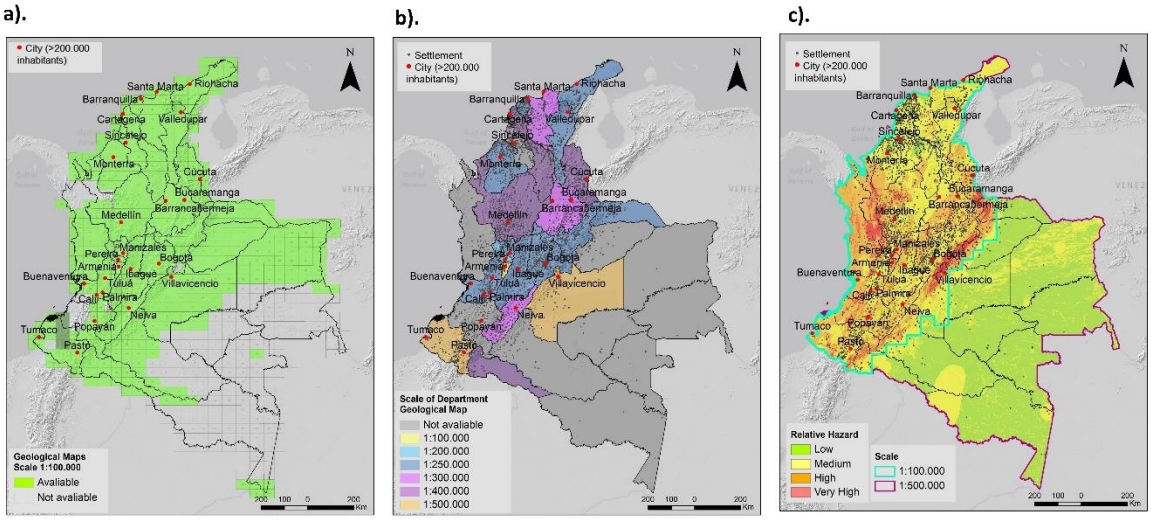

Figure 5. a) Current coverage of geological cartography at 1:100.000 scale, b) Availability of departmental geological maps at intermediate scales, c) Coverage of the relative national hazard and susceptibility landslides map

The Geological Survey and the IDEAM institute, together with six universities of Colombia, created a National Mass Movement Relative Hazard Map at a scale of 1:100.000 (SGC 2016). This project included elaborating the geomorphological units, susceptibility to landslides, and the map of relative hazard to landslides (Figure 5c). Even though this project did not include all the country, the most relevant zones are covered since the Orinoco, and Amazonian plains are areas with low susceptibility to landslides phenomena because of their low slopes. For such sites, the information is available on a scale of 1:500.000.

3.2.3. Land use and Land Cover

The Institute of Hydrology, Meteorology and Environmental Studies (IDEAM) and several national and international institutes have created three national land cover maps: 2000-2000, 2005-2009, and 2010-2012 (IDEAM 2010). These maps have a scale of 1:100.000 and follow the CORINE land cover methodology, adapted for the specific case of Colombia. Such maps can be used to assess the surface parameters of the hazard assessment needed for the hydrologic and hydraulic modelling.

3.2.4. Rainfall and Flow levels

IDEAM is the official institution in charge of the national hydro-meteorological stations network. This network contains around 4.500 meteorological, hydrologic, and hydro-meteorological gauges (Figure 6a). The recorded timespan is very diverse. Some of the gauges date back to the early 1900 years, but most have records since the 1970 and 1980. Around 40% of the stations are currently suspended, but their records are still available. Thyssen polygons were created around every rainfall station to analyse the differences in the spatial distribution of the rain gauges. Figure 6b shows the polygons, and the colour for each department is based on the mean value of the area of the polygons inside it. The departments with larger station densities have around one station per 100 Km^2, and the sparsest ones have one station for around 10.000 or even 20.000 km^2. The rainfall records for all the stations are freely available on the IDEAM website (http://dhime.ideam.gov.co/atencionciudadano/). Also, the institute created Intensity-Duration-Frequency curves for 110 stations that can be freely downloaded (http://www.ideam.gov.co/curvas-idf). The analysis includes curves for return periods from 2 to 100 years. One significant disadvantage of using the rainfall records for extreme rainfall scenarios is that most rain gauges are located in urban areas and settlements, often in low-lying areas; therefore, they don't capture intense rainstorms that often occur in the high part of the catchments. In any case, the records provide essential input for the hazard modelling.

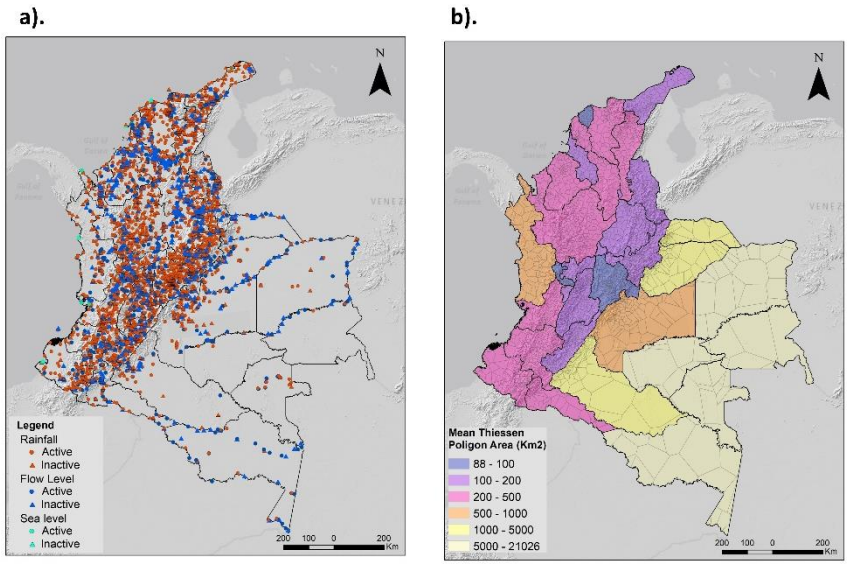

Figure 6. a) Map of the main rainfall, hydrologic and sea level stations of the national network, b) Division of the area between rainfall stations, and categorization of the main area for each department

Other sources for information on rainfall and flow levels are specific departmental and municipal agencies of Colombia's main urban centres, including better resolution data of urban areas. Some examples include the Early Warning System for Medellin and the Aburrá Valley (SIATA). This project consists of a monitoring network of rainfall, meteorologic and flow level stations with measurements with a very detailed scale in time. This project also includes a meteorologic radar covering 90% of the Antioquia department with a temporal resolution of 5 minutes. The project is working since 2007 and contains a web portal where all the information can be freely accessed (https://siata.gov.co/siata_nuevo/). Another example is the Warning System of Bogotá (SAB), a network of 30 hydro-meteorologic gauges and a meteorologic radar covering Bogotá with a temporal resolution of 5 minutes. However, the accessibility to their records is not clear.

3.2.5. Disaster and events inventories

The following sources can be consulted for the construction of inventories. Other sources of information for the inventories include news, reports, the knowledge of the community, the interpretation of remote imagery and fieldwork

3.2.5.1. DESINVENTAR

DesInventar (https://db.desinventar.org/) is a tool developed to generate national disaster inventories, developed by the UNDRR and UNDP, together with Latin-American institutions like The Network of Social Studies for Disaster Prevention (LA RED) and the Colombian Southwest Seismological Observatory (OSSO) corporation. It contains inventories for more than 20 countries now. DesInventar includes 12 inventories in Colombia, with a national inventory in charge of the OSSO corporation, but with other smaller inventories in charge of local authors, universities and government entities, some of which are not updated anymore. The Colombian national inventory contains more than 53.000 disaster records from 1914 to 2020. The events are mainly well described, but they have the format of tables that lack a spatial component, only constrained to the description of the place where it occurred. The localisation description can sometimes be very vague, increasing the chances of misplacing the locations, especially for events like landslides or rockfall. Other local databases of Colombia in Desinventar include the DAPARD database for the Antioquia department, which is constantly updated, the historical inventory of the city of Cali, with registers until 2012, and the Aburrá Valley Metropolitan Area inventory.

3.2.5.2. SIMMA

The Mass Movement Information System (SIMMA) (http://simma.sgc.gov.co/) is an application developed by the Colombian Geological Survey (SGC) to record, store, process and visualize mass movements hazard assessments and records in Colombia. It contains two different databases: the historical catalogue, which includes records obtained by compiling various historical records from emergency offices and local and national disaster management entities. It only contains a description of the place where the events occurred. The second database is the Mass Movement inventory that compiles technical reports of mass movements, including precise location, description and even photographs of the events.

3.2.5.3. GEO-HAZARDS

The Geohazards research group of the Faculty of Mines of the National University of Colombia has recently developed a disaster inventory for Colombia and Antioquia (https://landslides-colombia.herokuapp.com/#/find). This inventory results from several academic projects that include compiling, cleaning, and updating existing databases. The tool also has the option to report events, which are later added to the inventory. The records include the geographical location of the events associated with its level of uncertainty.

3.3. Global Datasets

Whenever a hazard assessment needs to be carried out in an area with scarce detailed information, some global datasets may be used or support voids in local data. A review of the main global datasets with coverage in Colombia is summarized in Table 7

Table 7. Review of the main global datasets to use for hazard modelling in Colombia

Type of Data	Source	Characteristics	Scale	Temporal coverage	Link
Digital Elevation Models	ALOS PALSAR	L-Band Radar Images	12.5 m	2006 - 2011	https://asf.alaska.edu/
	SRTM	X and C band Radar Images	1" (aprox. 30 m)	2000	https://earthexplorer.usgs.gov/
Basic Cartography	OpenStreet Map	Includes basic cartographic elements with varying detail	Varies	Continous	https://www.openstreetmap.org/
	Google Earth and Google Maps	Should only be used for rectification purposes with care of their copyright infringement policies	Varies	Continous	https://earth.google.com/web/
Land Cover	Copernicus Global Land Service Land Cover Map	23 categories of land cover. Created from Sentinel-2 imagery	100 m	2015 - 2919	https://land.copernicus.eu/global/products/lc
	MODIS Land Cover Product	Generated from MODIS images. 6 different land classification systems	500 m	2001 - 2019	https://modis.gsfc.nasa.gov/data/dataprod/mod12.php
Soil Properties	SoilGrids	Information of pH, Organic Carbon Content, Bulk density, and coarse fragment, sand, silt,	250 m with varying accuracies	Continous	https://www.isric.org/explore/soilgrids

		and clay content, among others, at six different depths			
Rainfall Records	CHIRPS	Daily, monthly and yearly scale. Accuracy for Colombia is good in monthly and annual resolutions. Daily measurements soften extreme events. (Urrea, Ochoa, and Mesa 2016)	0.05° (approx. 5.5 km)	1981 - today	https://www.chc.ucsb.edu/data/chirps
	TRMM	Temporal resolution of 3 hours	0.25° (aprox. 27.75 km)	1997.2015	https://gpm.nasa.gov/data/directory

3.4. Study areas

In terms of analysis of debris flow hazards in Colombia, one of the main limitations of research is the lack of properly documented events. The first technical reports of debris flow processes in Colombia date back to the late 1980s and 1990s decade (Caballero and Mejía 1988; Florez and Parra 1988, Cadavid and Hermelín 2005; Hermelín, Curvelo, and Osorio 1992; Piedrahita and Hermelín 2005). Even though these reports included a very detailed description of the triggering effects, presence of landslides and extension of the damages, its extension was not mapped. The two most recent and destructive debris flow events in Colombia, Salgar (2015) and Mocoa (2017), were selected as study areas because they got a lot of media coverage and government support and are subject to technical reports and scientific analysis that give sufficient information for modelling. Still, many smaller-scale debris flow events are occurring in Colombia without a systematic and rigorous post-event technical field analysis.

Another reason for choosing both areas as study cases is that they represent different environments with varying information availability. Mocoa is a medium-size city located in a wide fluvial fan, with a good amount of information. At the same time, Salgar is a small rural settlement located in a deep and V-shaped valley with very limited information.

3.4.1. Debris flow in Mocoa, Putumayo on 31st March 2017

Mocoa is a city of around 25.000 inhabitants located in the Putumayo department, southwest of Colombia, on the piedmont of the Andean range into the Amazonian plains. The Taruca, Sangoyaco and Mulato rivers initiate in the Andean steep mountains, and their confluence into the Mocoa river is located in a large torrential fan in the lowlands of the Amazonian plains, where the city of Mocoa is located (Figure 7). On 31 March 2017, after four days of accumulated rainfall, a heavy rainstorm of 129.3 mm fell in three hours over the city's surrounding area (UNGRD and PUJ 2017). This rainstorm triggered at least 420 landslides in the high slopes of the Taruca, Sangoyaco, and Mulato river catchment areas, which added to the rivers' flooded streams and were mobilized as debris flows, and caused at least 5 channel blockages, that might have increased its intensity (Prada-Sarmiento et al. 2019).. The final deposition of the flows was the city of Mocoa, where they came with enough power and speed to destroy more than 120 houses, killing around 409 people,

and affecting 17 neighbourhoods, according to the DESINVENTAR database (www.desinventar.org) (Figure 7).

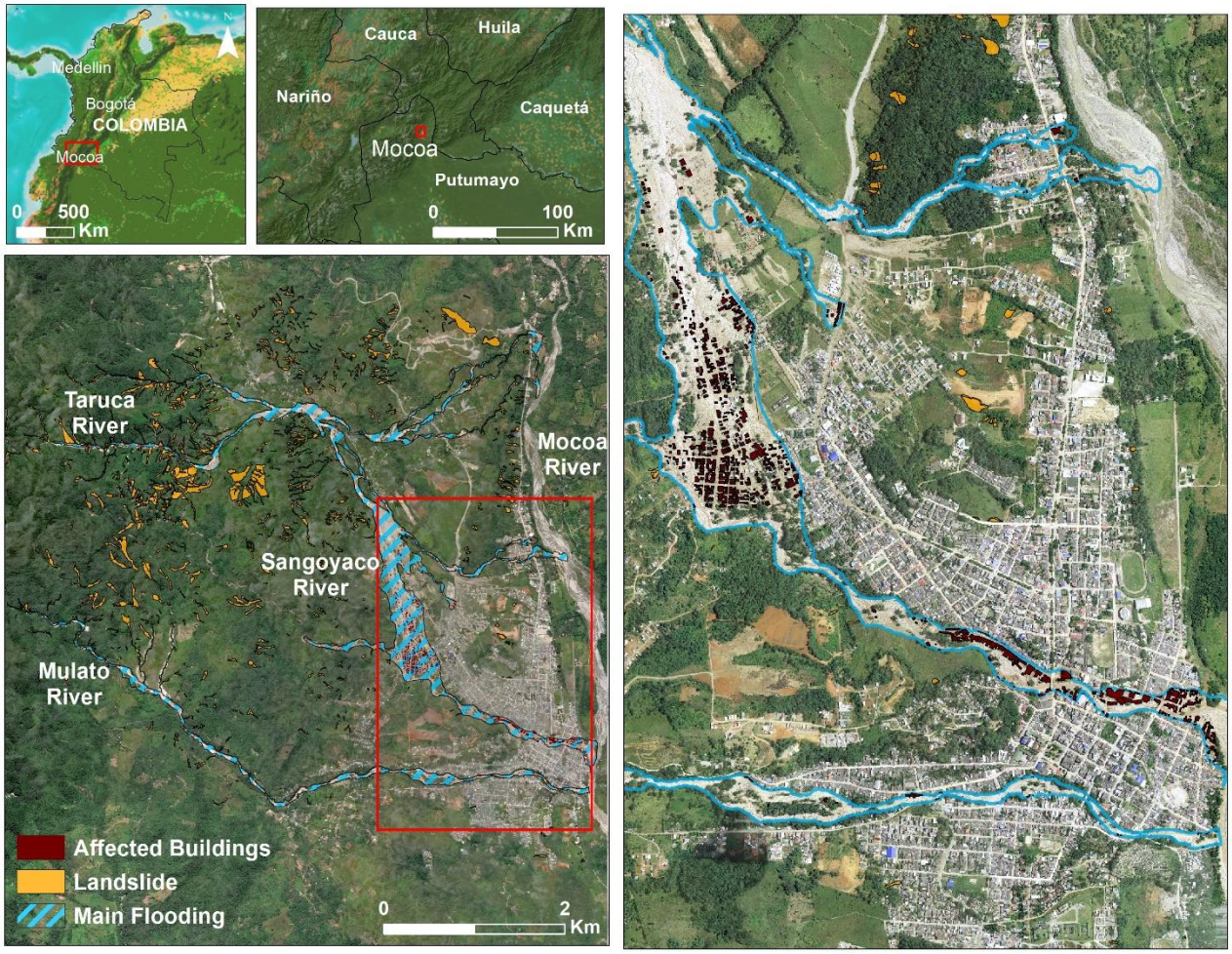

Figure 7. Location of the city of Mocoa and extent of the event with the location of damaged buildings

3.4.2. Debris flow in Salgar, Antioquia on 18th May 2015

Salgar is a rural municipality city located in the Antioquia department, over the eastern flank of the Western Andean Cordillera. The urban area of the municipality, of around 9.000 inhabitants by 2015, is settled in the Liboriana river valley, near its outlet into the Barroso River. The Liboriana river has a basin of 56 km^2 and originates in the Cerro Plateado, a very steep mountain ridge of the Western Cordillera, with an elevation of 3600 masl. The river travels for around 20 kilometres in a steep valley, passing through several small settlements until it reaches the urban area of the Salgar Municipality, where it meets its outlet with the Barroso River, located at 1300 masl. On 18 May 2015, after three days with several rainstorms that accumulated over 180 mm in the upper watershed, a rainfall event of 38 mm triggered a debris flow that initiated in the upper catchment with several landslides that were added to the flooding. Some landslides also caused the damming of the main channel of the river. The flow caused caused more than 100 deaths and leaving 100 destroyed and 219 affected houses. Most of the damages occurred in La Margarita settlement and in the urban area of the municipality (Figure 8) (Velásquez et al. 2020).

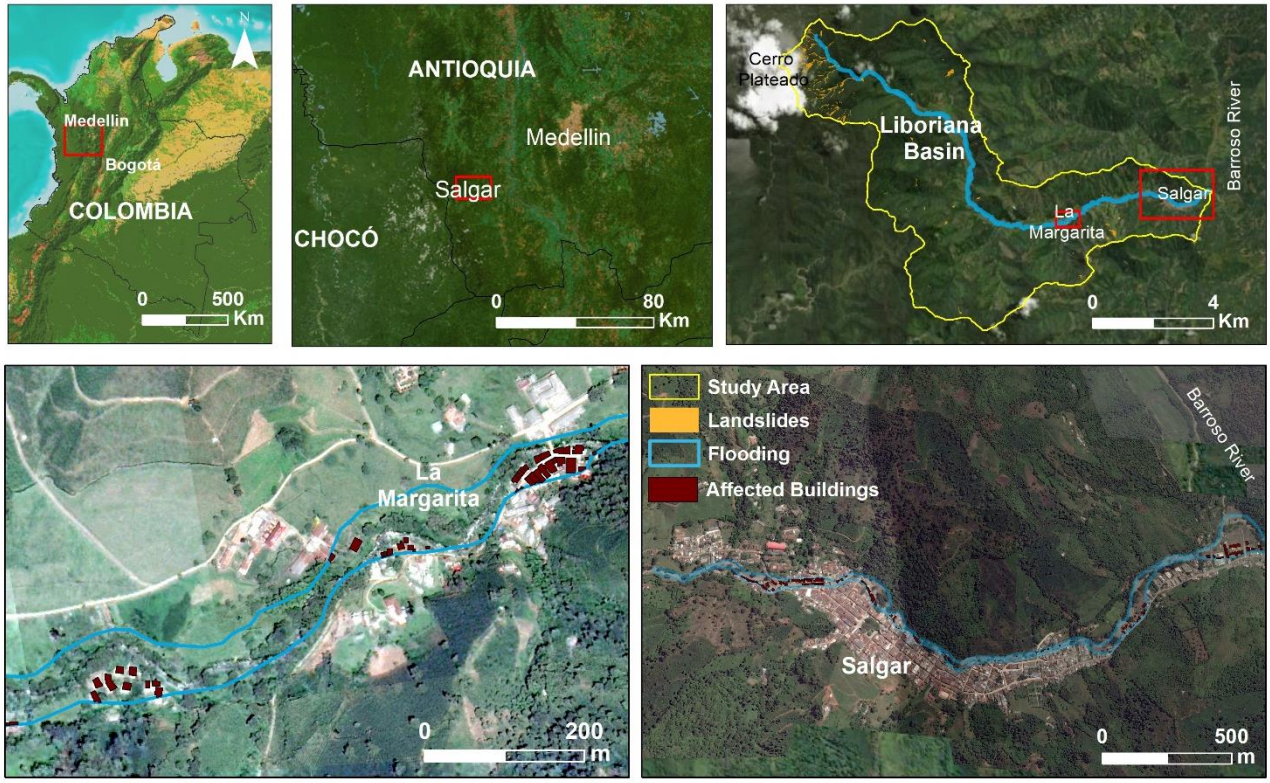

Figure 8. Location of the Liboriana basin and extent of the event with affected buildings

3.5. Previous Studies

3.5.1. Mocoa

Several post-disaster studies with different objectives followed the event of 31 March 2017 in Mocoa:

3.5.1.1. Characterization of the 31st May 2017 debris flow in Mocoa, Putumayo (SGC 2017)

Shortly after the event, the Colombian Geological Survey published this report to describe the main characteristics and extent of the event. The report includes the main observations made by a group of technicians to the city and the higher parts of the Taruca, Taruquita, Sangoyaco and Mulato rivers, the identification of the main triggering factors, the patterns of deposition of the material, flow heights, some empirical analysis to estimate flow velocities, and a classification of the event. Their outputs include the landslide inventory, a map of deposition areas, and a very extensive photograph report. The report, input data and results of this study are freely available.

3.5.1.2. Zoning of Mass Movement Susceptibility and Hazard for the basins of the Taruca, Taruquita, San Antonio, El Carmen, Mulatos and Sangoyaco rivers in the Mocoa Municipality, Putumayo, Scale 1:25.000 (SGC 2017b)

This study aims to create the basic landslide hazard input for the land use plan incorporation in the municipality of Mocoa. This analysis follows the methodology suggested by the methodological guideline for landslide susceptibility and hazard assessment at 1:25.000 scale. They elaborated the Superficial Geological Units (UGS) map, geomorphological units map, and landcover map as inputs for the evaluation. The outputs of this report are the susceptibility and hazard maps for landslides and debris flow phenomena. The report, input data and results of this study are freely available.

3.5.1.3. Debris flow hazard assessment for the basins of the Taruca, Taruquita, San Antonio, El Carmen, Mulatos and Sangoyaco rivers in the Mocoa Municipality, Scale 1:5.000 (SGC 2018a)

This analysis focuses on the hydrological and hydraulic modelling of the debris flow event using the FLO2D model. The objective of the research is to create a detailed debris flow hazard map for the urban area of Mocoa. The report, input data and outputs of this study are freely available

3.5.1.4. Mass movement hazard assessment in the urban, peri-urban and expansion areas of the Mocoa municipality, Putumayo, Scale 1:5.000 (SGC 2018b)

This study aims to create the detailed landslide hazard input for the land use plan incorporation in the urban area of Mocoa. This analysis follows the methodology suggested by the methodological guideline for landslide hazard assessment at 1:5.000 scale. This project included the generation of detailed input data for the urban area, including a Digital Elevation Model, detailed landcover maps and laboratory tests of granulometry and soil mechanical properties. The hazard assessment was done using limit equilibrium models for rainfall and earthquake triggers. This analysis did not include debris flow hazard assessment. The report, input data and outputs of this study are freely available

3.5.1.5. Design studies for the early warning system for debris flows and flash floods in the Mulato, Sangoyaco, Taruca and Taruquita rivers in the municipality of Mocoa, Santander (UNGRD and PUJ 2018)

This document was created by the National Disaster Risk Management Unit (UNGRD) and the Pontificia Javeriana University (PUJ). The project's objective is to model the circumstances leading to the event to propose an early warning system for the city, a system that is operating now. It includes rainfall, geomorphology, geotechnical and hydraulic analysis, and several modelling approaches of the event using two-phase hydraulic software's. The final output of the report is the considerations for creating the Early Warning System. Most of the input information that this project used comes from the analysis carried out by the SGC, but this project's intermediate and output data could not be accessed because of restricted use permits.

3.5.2. Salgar

3.5.2.1. Design studies for the early warning system for debris flows in the Liboriana, La Cara and Barroso rivers in the municipality of Salgar, Antioquia (UNGRD and PUJ 2016)

Following the Salgar event, the UNGRD and PUJ collaborated on a project to implement an early warning system for the municipality. The report includes a collection of secondary data that includes mainly basic cartography, aerial photographs, rain gauge records, and local data related to the municipality's current land use plan at that time. The intermediate information created by the project includes geomorphologic, soil units, and landcover maps, and the methodology included slope stability hydrologic and hydraulic modelling of the event. The components of vulnerability and design of the early warning systems are also included. The intermediate and output data of this project could not be accessed because of restricted use permits.

3.5.2.2. Reconstructing the 2015 Salgar flash flood using radar retrievals and a conceptual modelling framework in an ungauged basin (Velásquez et al. 2020)

This paper reconstructs the debris flow event using radar quantitative precipitation estimation from the SIATA radar, satellite data and post-event field observations as input data for a hydrologic, slope stability and hydraulic modelling of the event.

3.6. Data Acquisition and Preparation

This section contains the details about the data used for the modelling. For Mocoa, this process included creating a coarse and detailed dataset. Since some information was not available on both scales, they were included in both datasets. For the case of Salgar, there is only one dataset.

3.6.1. Mocoa

3.6.1.1. DEM

The detailed DEM was obtained from an X-band Synthetic Aperture Radar from the GeoSAR project with a pixel size of 5 meters. The GeoSAR DEM is generated by combining X-band and P-band data acquired simultaneously and allowed extracting the vegetation and getting a surface model. The SGC (SGC 2018a) processed and corrected the DEM using 215 cross-sections from the Sangoyaco and Taruca river channels. For the urban area, the SGC generated a 2m resolution DEM from orthophotos acquired in 2008 (SGC 2018b). This model was re-sampled to 5 meters and inserted into the final DEM in the urban area. In the final mosaic, there were some steps between the limit of both DEMs. To fix this, we applied a softening filter to the area between them.

The coarse DEM was obtained from ALOS PALSAR High-Terrain Corrected dataset with a pixel size of 12.5 m. We softened the DEM to decrease the number of ponds in the valley area and burned the drainage network from the basic cartography map at a scale of 1:25.000.

3.6.1.2. RAINFALL RECORDS

Figure 9a shows the rain gauge stations from the Hydrology, Meteorology and Environmental Studies Institute of Colombia (IDEAM) in the surrounding area of Mocoa. We used the rainfall record of the Acueducto station for the hazard modelling in the detailed and coarse case since it is the only active station in the area. This station is located in the urban area of Mocoa, which implies that probably the instrument did not acquire the data concerning the storm in the upper part of the basin. This rain gauge has records from 1982 until today and takes automatic daily and 10-minute measurements and. According to the daily records, there was a precipitation of 129.3 mm on the 31st of March, 2017. The 10-minute record shows a rainstorm of 31 mm occurring 24 hours before the disaster and two minor rain episodes during the day. The triggering event started around 8:30 pm on the 31st of March, lowering its intensity at around 12:50 am on the 1st of April and ending completely at 6:30 am, with an accumulated rainfall of 105 mm (Figure 9b).

The SGC also carried out a historical analysis of the Acueducto rain gauge. The mean monthly rainfall of the area is around 300 mm, which means that the triggering rainfall event corresponded to 35% of the mean monthly rainfall. Even though the event is extreme, the return period of a daily rainfall of 129 mm is 5 to 10 years, which don't correspond to an event of such extent. The cumulative rainfall was also analyzed: In the previous 38 days of the event, the accumulated rainfall was 600.6 mm. This amount of rain in 38 days is not extreme, given that it occurs at least once a year. Nevertheless, the combined probability of having a day with 129 mm of rainfall, with 600 mm of rainfall accumulated on the previous 38 days, has a return period of 25 years. This gives an idea about how the moisture condition of the soils before the disaster is a crucial factor to consider for the extreme nature of this event.

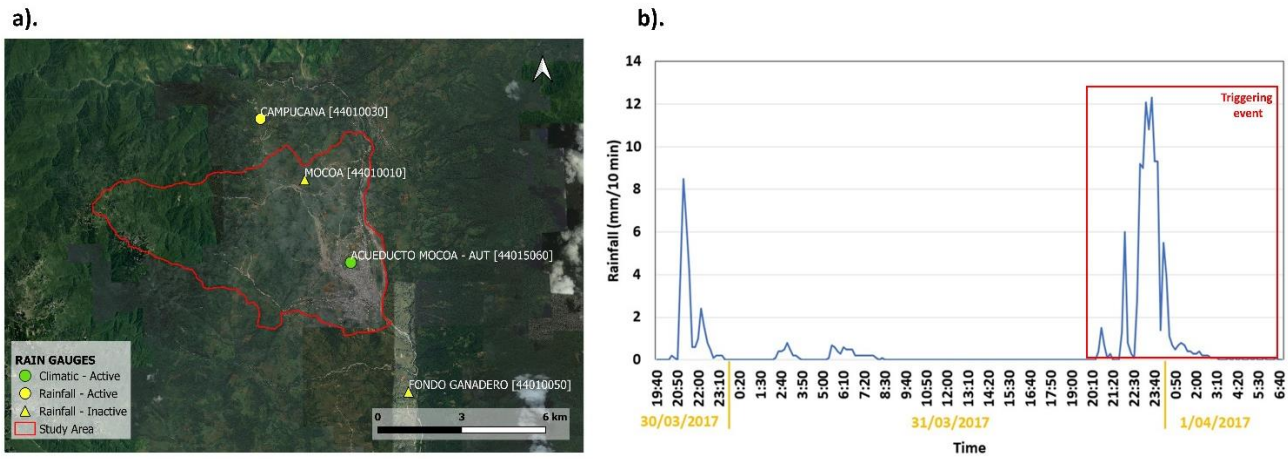

Figure 9. a). Rain gauges from the National Network near the study area. b). Record of the Acueducto rain gauge before and during the main triggering event

3.6.1.3. LANDCOVER INFORMATION

For the detailed case, the landcover was constructed as a collage between detailed information in the urban area and coarse national data for the rest of the study area (Figure 10a). The urban area was classified by the SGC (SGC 2018b) on a scale of 1:5.000 from the interpretation of aerial photographs and corrected during fieldwork. For the rest of the study area and the coarse map, we used the National Cover Map of Colombia on a scale of 1:100.000 (Figure 10b)

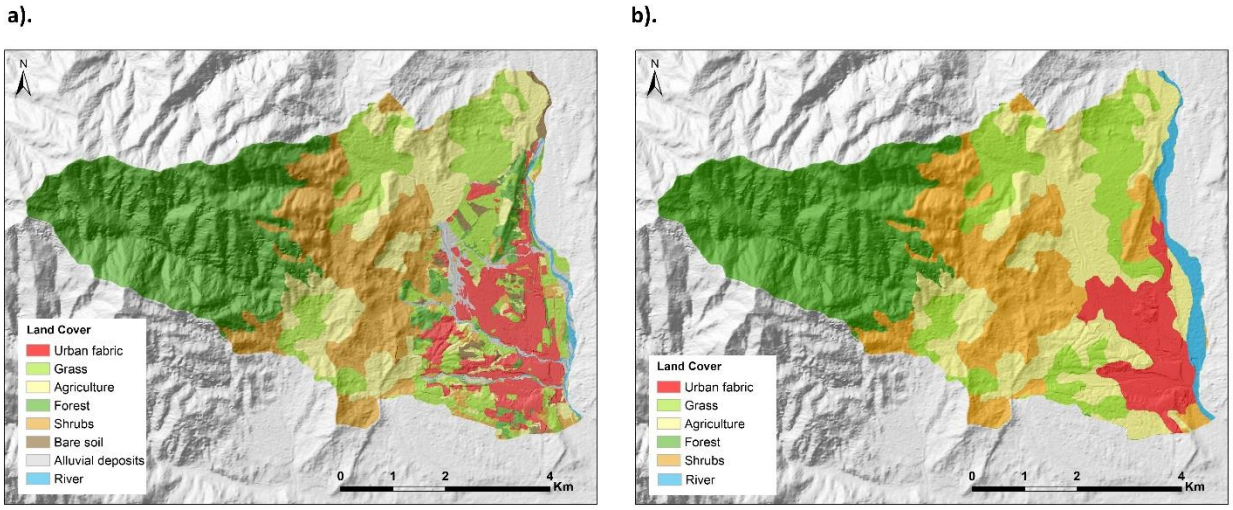

Figure 10. Landcover maps used for the detailed and coarse analysis

This input landcover map is not used directly but is used to spatialize surface properties needed for the hydraulic transit of flows. The variables that were extracted from the land cover maps include:

- Random Roughness (RR): Standard RR values were consulted from Floors et al. (2018) and Bout et al. (2018).
- Manning's roughness coefficient (n): Averaged values of n based on land cover data were extracted from Papaioannou et al. (2018) and Bout et al. (2018).

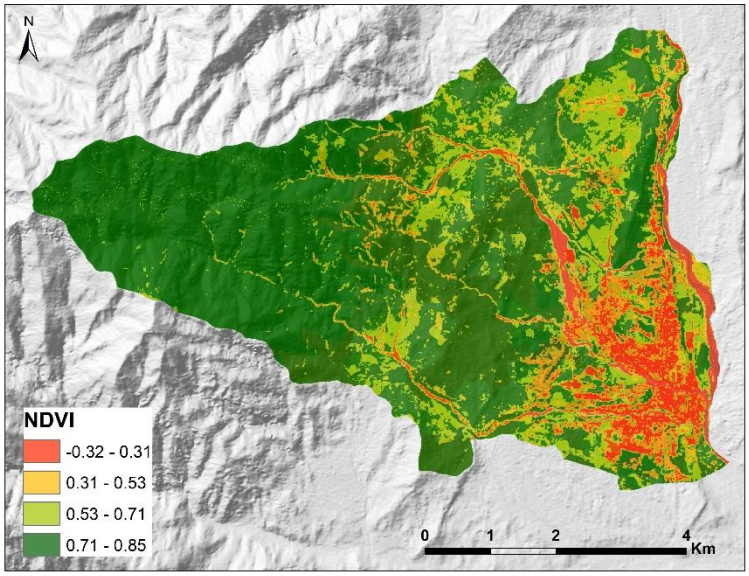

Figure 11. NDVI Map

Additionally, Figure 11 shows the NDVI map calculated from freely available online Sentinel -2 images and re-sampled to 5m for the detailed resolution and 12.5m for the coarse resolution. The NDVI was used to calculate the Vegetation Cover and Leaf Area Index (LAI) using the following equations, suggested by Bout et al. (2018):

$$Vegcover = e^{\frac{-2*NDVI}{1-NDVI}}$$

$$LAI = \frac{\ln(1 - vegcover)}{-0.4}$$

3.6.1.4. GEOTECHNICAL PROPERTIES

Most of the urban area of Mocoa is constructed on transported soil units of fluvio-torrential origin, corresponding to the riverbeds and recent, sub-recent, old, and very old terraces of the Sangoyaco, Taruca and Taruquita rivers. The upper part of the urban area is constituted of sedimentary rocks, ranging from conglomerates, siltstones, mudstones, and shales. In the Western part of the study area, the Mocoa Monzogranite is in contact with the sedimentary rocks through the Mocoa-La Tebaida fault line, which marks the change between the steep slopes of the western part with the more gentle slopes of the sedimentary rocks and the valley. This fault line is responsible for a very intense physical and chemical weathering of the surrounding units.

Two maps with different sets of geotechnical parameters were used in the analysis for calibration purposes. Even though one of the maps contains more details than the other, they were not used separately for the coarse and detailed analysis. Still, they were used in both scales to verify which set of geotechnical parameters yield a better result. Using each soil unit map for each scale of analysis would make both cases very difficult to compare since each soil unit map is associated with geotechnical parameters that are very different.

The first map (Figure 12a) was created merging the Geological Units for Engineering (UGI) at scale 1:5.000 in the urban area from SGC (2018b), with the of Geological Superficial Units (UGS) at scale 1:25.000 in the rest of the study area from (SGC 2017b). In the analysis carried out by SGC (2018b) in the urban area at scale 1:5.000, several laboratory tests were performed on samples taken in the form of drillings, trenches and granulometric samples of soils. The analysis includes a detailed description of drillings and trenches' soil profiles, laboratory tests of classification and physical properties (humidity, consistency limits, granulometry, and unitary and specific weight), and geotechnical properties (Compression, direct shear stress, triaxial test, consolidation test). The samples taken from the deposits of the riverbed were tested for their granulometric curve, humidity, specific gravity, and US soil classification. For these units, the mechanical properties were taken from literature values, based on their granulometric properties. The geotechnical and physical properties of the soil units outside of the urban area were unknown. To assign their properties, we assigned them by relating the units to similar ones from the detailed analysis. For the units that were not similar or relatable to any unit present in the urban area, we obtained their geotechnical parameters from literature, based on the percentage of particle size information from the Putumayo soil map at scale 1:100.000. The description of each soil unit and its properties are shown in Appendix 1.

The second geotechnical unit map (Figure 12b) was taken from the zoning carried out by UNGRD and Pontificia Universidad Javeriana (2018). The properties were assigned to each unit based on laboratory analysis -when available-, literature values and a calibration procedure using a slope stability model of the event conditions. Since this information was not available in shape format, it was digitalized from the study's PDF product, and the properties were assigned based on their values. The description of each soil unit and its properties are shown in Appendix 2.

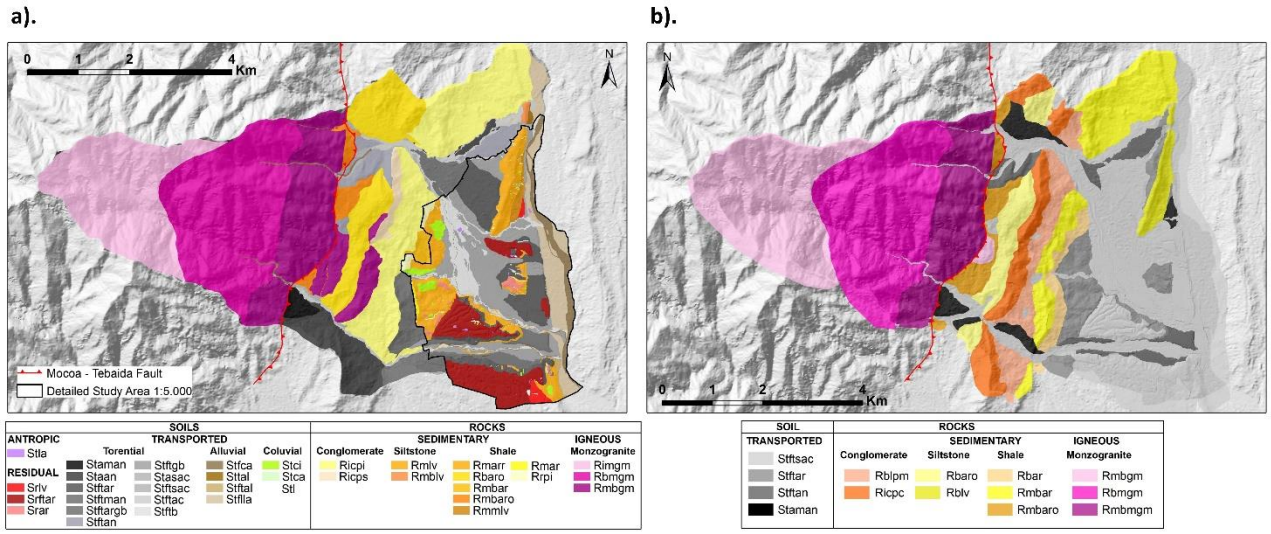

Figure 12. Geotechnical datasets used for calibration

3.6.1.5. SOIL DEPTH MAP

Similar to the geotechnical parameters, two soil depth maps were used for calibration purposes in both scales to assess the soil depth model that yielded the best results.

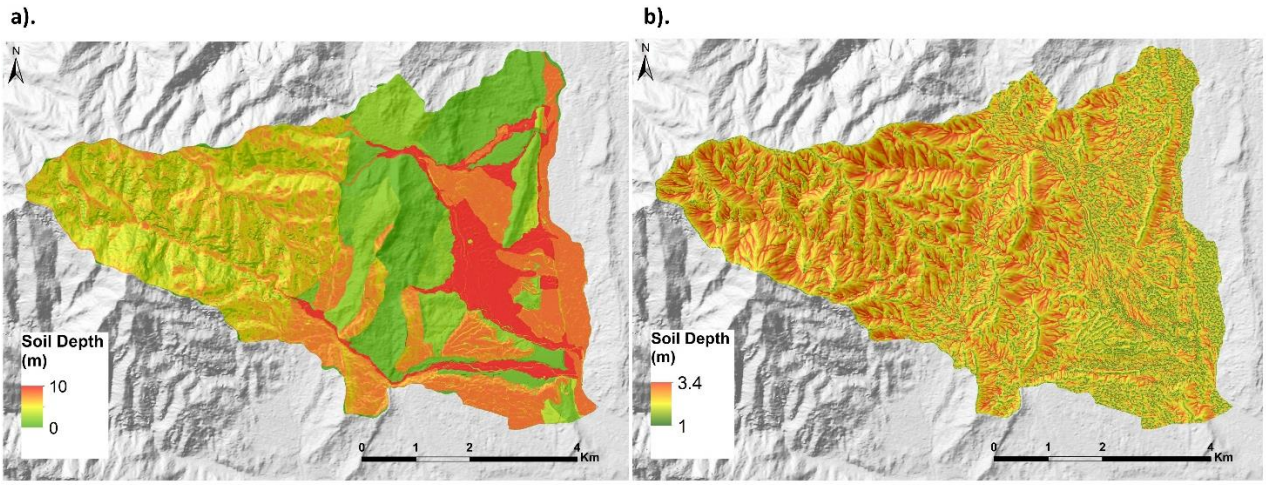

Figure 13. Soil Depth maps used in the model

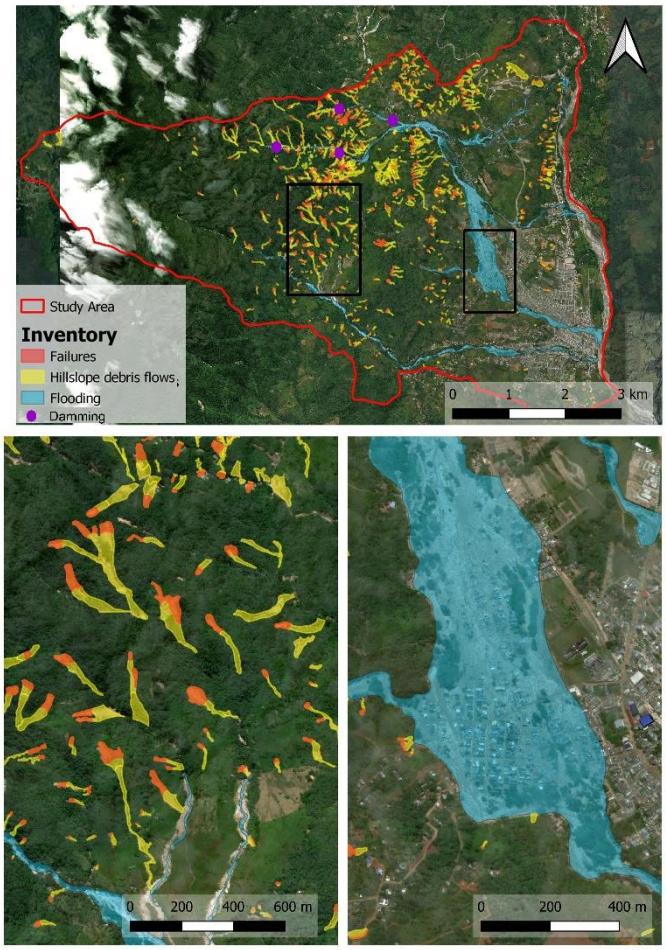

Figure 14. View of the inventory of the event. Bottom left: Zoom into view of the hillslope debris flow failure and runout areas. Bottom right: zoom into the area of largest affectations in the urban centre

The first map (Figure 13a) was calculated using the approach of Catani, Segoni, and Falorni (2010), which uses as inputs the DEM and the Maximum and Minimum soil depth parameters as constrainers. The minimum and maximum soil depth parameters were set for each soil unit based on the descriptions from the field from (SGC 2018b). This map describes the true conditions of the area based on observations but creates sharp limits between units with variable soil depths.

The second map was created using the approach proposed by Stothoff (2008), which assumes steady conditions between soil production rate and erosive processes. The model uses the DEM as unique input, so it doesn't represent the specific weather or lithological conditions of the study area but represents very well the local variations in soil depth.

3.6.1.6. EXTENT OF THE EVENT

Figure 14 shows the channelised debris flow and flooding extent map created by the SGC using aerial photographs obtained after the event. The debris flow polygons were divided between the run-out area and the failure zones using the same photographs.

3.6.2. Salgar

The primary source of information for the Salgar study case was the study carried out by Javeriana (2016). They collected and complied most of the information from secondary coarse data.

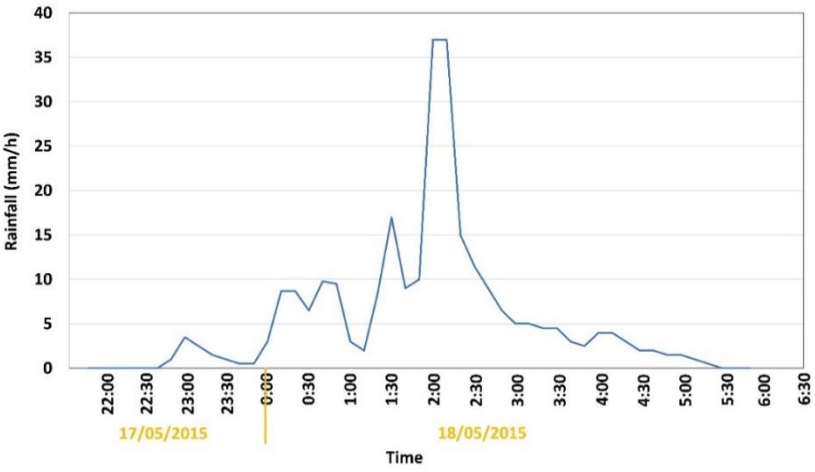

Figure 15. Rainfall event corresponding to the disaster in Salgar

3.6.2.1. DEM

The DEM was obtained from ALOS PALSAR High-Terrain Corrected dataset with a pixel size of 12.5 m.

3.6.2.2. RAINFALL RECORDS

Since there isn't any rain gauge located inside the study area, Hoyos et al. (2019)carried out an analysis of the meteorological conditions leading to the Salgar disaster using information from nearby rainfall gauges and disdrometers and from a Quantitative

Precipitation Estimation from records of the C-band polarimetric Doppler weather radar operated by the Sistema de Alerta Temprana Medellín y el Valle de Aburra (SIATA), located in Medellin. The radar records have a spatial resolution of 128m and a temporal resolution of 5 minutes. According to their analysis, between the 15th and 18th of May 2015, several rainfall episodes occurred in the Liboriana basin. On the day of the event, two rainstorms occurred, the first with an accumulated rainfall of 47mm, and the second one, which was the triggering episode, with 38mm.

According to the rainfall pattern of the region, Hoyos et al. (2019)concluded that none of the single precipitation events occurring on the previous days of the events was large enough to create such an extreme event. However, the combination of a high accumulation of rainfall during the last four days to the event, with a moderate extreme event on the 18th of May, could explain its occurrence. Moreover, the footprint of the triggering rainfall event shows very localized intense convective storms, orographically enhanced by the Cerro Plateado Mountain range, in the upper part of the basin, which ultimately triggered the flood.

For the modelling with OpenLISEM, only the main triggering event was considered. Figure 15**¡Error! No se encuentra el origen de la referencia.** shows the rainfall records of such event, that started at around 11:00 pm on the 17th May and finished at 5:30 am on the 18th May.

3.6.2.3. LANDCOVER INFORMATION

The landcover information was obtained from the semi-detailed land cover map for the Antioquia department for 2007(Figure 16a). The map has a resolution of 1:25.000 and was constructed based on the Corine Land Cover method. The Vegetation Cover and Leaf Area Index parameters were calculated from the NDVI map, constructed from Sentinel-2 images (Figure 16b).

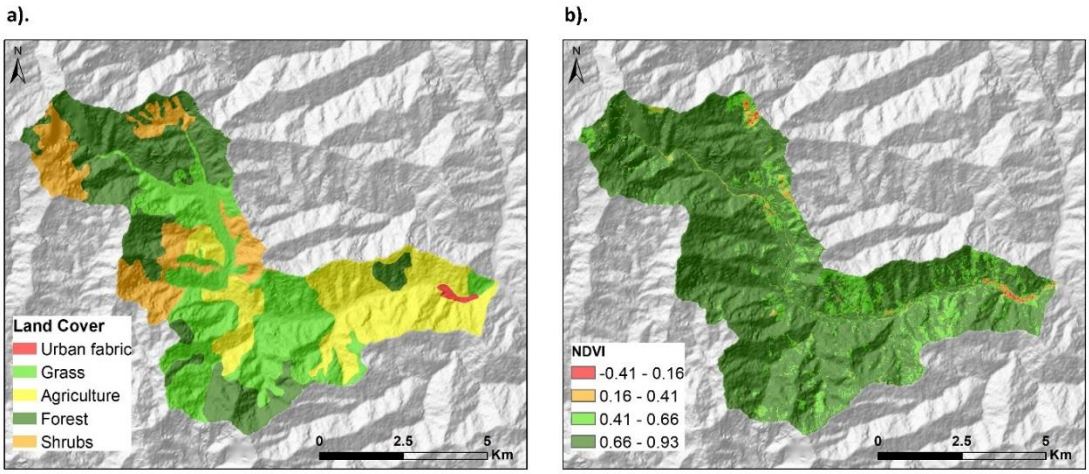

Figure 16. a) Landcover map and b)NDVI map for Salgar

3.6.2.4. GEOTECHNICAL PROPERTIES

The Liboriana basin is constituted in its low and medium zones from the sedimentary Penderisco rock formation that includes shales, siltstones, mudstones, sandstones, cherts and conglomerates, with layers of volcanic stuff. The Penderisco formation has good developed residual soils with high cohesion and slope stability (Cadavid 2014). In the upper part of the basin, they are intruded by the Cerro Plateado Stock, a granitic rock of Cenozoic age that creates very steep slopes with no residual soil, only a layer of organic soil with vegetation that covers the fresh rock, and that have very low to no cohesion. The bottom of the valley is filled with fluvial and fluvio-torrential recent deposits (Cadavid 2014).

The delimitation of soil units and their geotechnical parameters was obtained from the analysis carried out by Javeriana (2016). The soil units were delimited based on the terrain's geomorphological, physiographic, and geological features (Figure 17a). To assign the geotechnical properties to the soil units, they collected and described 11 samples of soils from different units. These samples were tested for humidity, consistency limits, granulometry and specific gravity. Also, direct shear test was applied to 5 samples, and two were used to measure viscosity with a viscometer. The description and characteristics of each soil unit are described in Appendix 3.

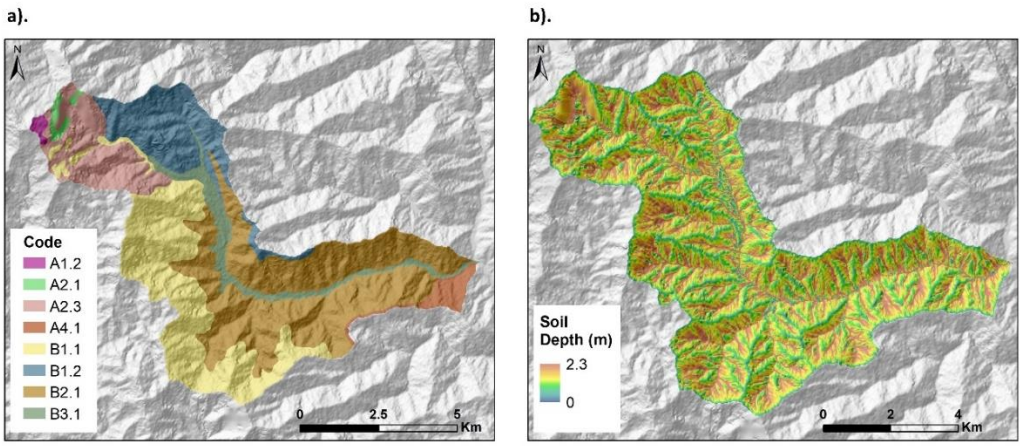

Figure 17. a) Soil unit map and b) Soil depth map of Salgar

3.6.2.5. SOIL DEPTH MAP

The soil depth map was constructed using the same approach as Mocoa, following the method proposed by Stothoff (2008), which uses the DEM as unique input (Figure 17b).

3.6.2.6. EXTENT OF THE EVENT

The extent of the event was digitalized using Google Earth multi-temporal images from the 31st of May of 2015. Given the proximity of the photographs with the occurrence of the event, its extent is visible, and it is possible to delimit the extension of each sub-process.

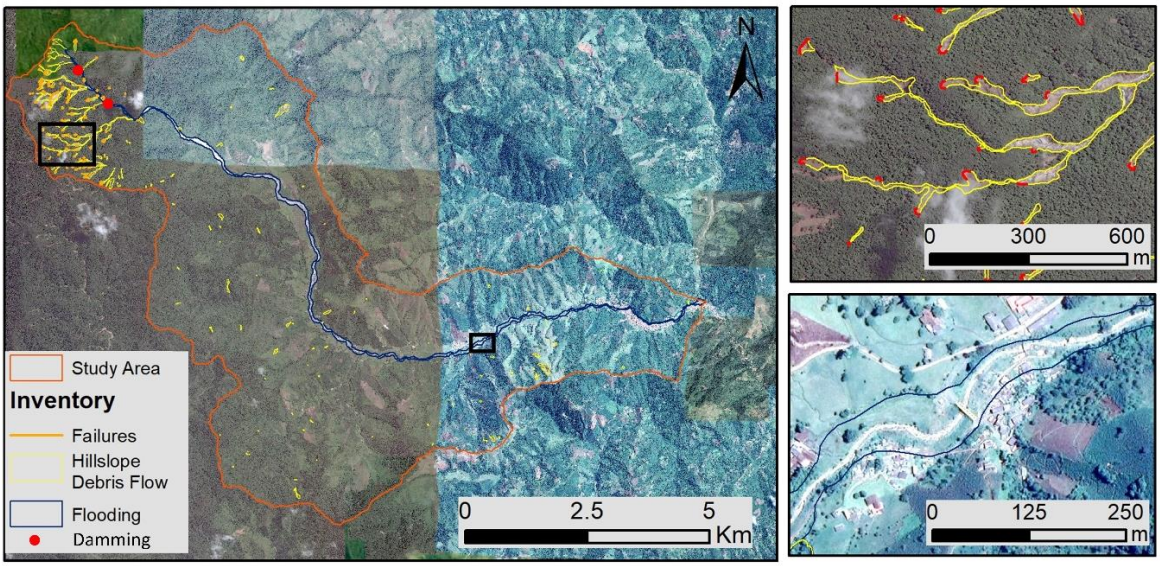

Figure 18. The extent of the Salgar disaster event used for calibration and accuracy analysis

4. RESULTS

This section includes the results of the sensitivity and accuracy assessment. Since the calibration process was more instrumental, its results are explained in a more descriptive way and therefore are included in the Discussion and Conclusions Section.

Table 8 lists the output maps of the OpenLISEM Hazard model. To analyse and evaluate the model's accuracy, four output maps are used and compared to the inventories: Maximum Flood level, Maximum Debris Flow Height, Minimum Safety Factor, and Slope Failure Height. These outputs were converted from their respective units to boolean rasters indicating the presence or absence of the given phenomena at each cell. However, the model does not distinguish between flooding and debris flow. Both phenomena are simulated as flows that vary from clear water to a solid-rich runout using generalized two-phase flow equations. Figure 19a illustrates the overlapping between the flooding and debris flow runout.

Conceptually, the end limit of a hillslope debris flow occurs when it incorporates into a flooded channel. To compare the extent of the hillslope debris flows and flooding with the model's outputs, a slope threshold of 20° was defined based on the observation of the study area to differentiate between these phenomena (Figure 19b). This threshold allows distinguishing the flows that travel in the slopes, usually in steep areas, from the fluvial deposits areas like channels and fans that typically correspond to flooding areas. That way, the criteria to determine the output maps are:

- The maximum flood level map is used to evaluate the flooding extent. A cell was considered flooded when the maximum flood level is more than 0.1m, and its slope is less than 20°.
- The maximum debris flow height map is used to evaluate the runout of the hillslope debris flows. A cell was considered part of the runout when the maximum debris flow height exceeds 0.1m, and its slope is greater than 20°.
- The Slope Failure map is used to evaluate the location of the hillslope debris flows initiation. A cell is considered part of the slope failure area when its slope failure value is greater than 0.1 m.
- The minimum safety factor map was only used to visualise the spatial variation of the slope stability in the calibration process. It was not used to compare with any inventory map. A cell is considered unstable when its minimum safety factor is less than 1.

Table 8. Output maps of the OpenLISEM Hazard Model

Hydrology Maps	**Flood and Channel Maps**	**Sediment Maps**	**Slope Failure and Debris Flows**
• Interception (mm) • Infiltration (mm) • Runoff (m3) • Slope Runoff Fraction • Max Runoff Water Level (m) • Max Discharge in outlets (m3/s)	• Max Flood Level (m) • Flood Duration (min) • Flood Start (min) • Max Flood Velocity (m/s) • Max Water Height (m)	• Detachment • Deposition • Soil Loss Map • Channel Detachment • Channel Deposition	• Maximum Debris Flow Height (m) • Maximum Debris Flow Velocity (m/s) • Debris Flow Start • Entrainment • Slope Failure (m) • Minimum Safety Factor

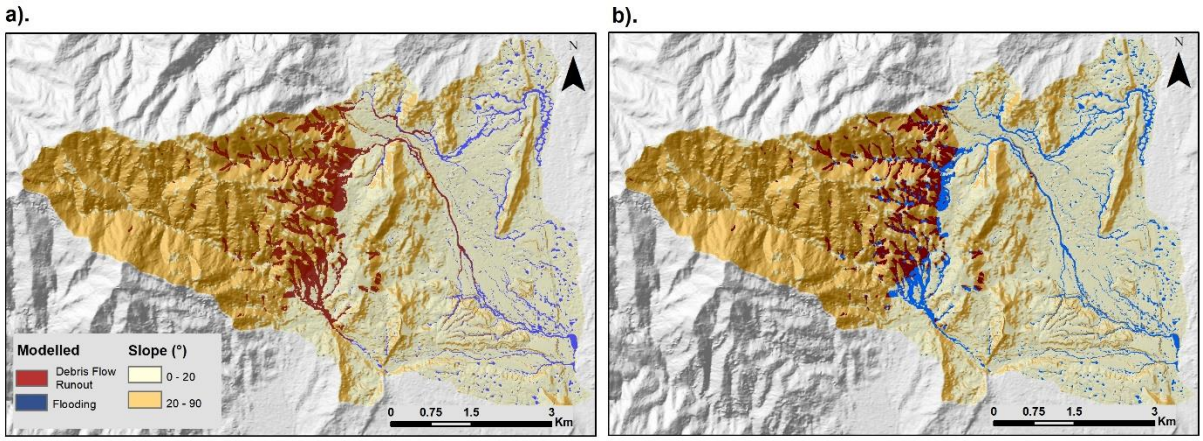

Figure 19. Example of the procedure to differentiate the modelled hillslope debris flows from flooding in the OpenLISEM Hazard output maps

4.1. Results for Mocoa

The Mocoa case study was modelled 50 times with the detailed dataset and 35 times with the coarse dataset. Each run took approximately four days for the detailed and 12 hours for the coarse dataset in a computer with 16 GB RAM and a Core i7 processor. The simulation time step was 10 seconds, with a total modelled time of 1000 minutes (16.7 hours). The input and calibration parameters for each run are specified on Appendices 7.4 and 7.5

4.1.1. Accuracy Analysis

The accuracies for the different subprocesses of the model are shown in Figure 20a for the detailed dataset and Figure 20b for the coarse dataset, where dots represent the False Positive Rate (FPR) and True Positive Rate (TPR) for each run. In this type of graph, a perfectly accurate simulation is located in the upper-left corner of the graph (TPR=1 and FPR=0), and simulations closest to this corner represent the highest accuracy. The flooding extent was the process that reached the highest accuracies in general, while the slope failure is the process with the lowest ones. Many runs did not lead to any slope failures and those who did generally overestimated the failure areas.

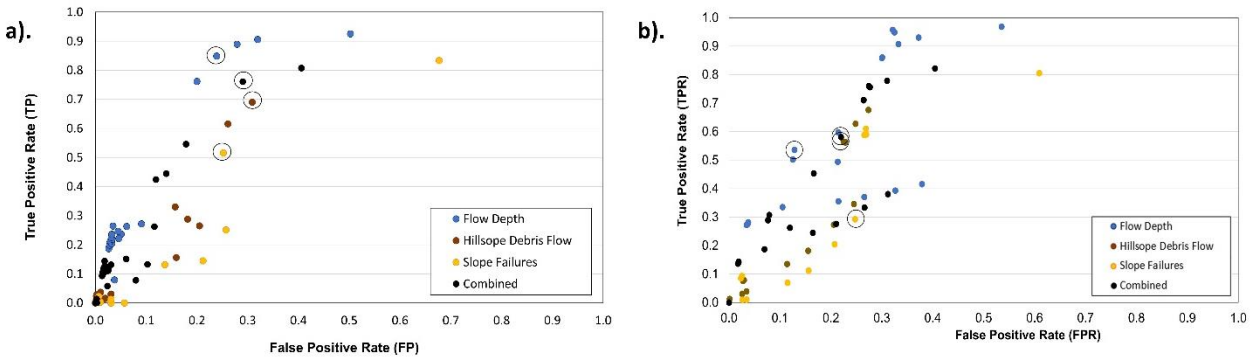

Figure 20. Results of the model performance of the different processes: Flooding, hillslope debris flow runout, slope failure, and an average of the combined processes using the a) detailed and b) coarse dataset

The black circles in Figure 20 indicate the most accurate results for each sub-process: for hillslope debris flow, slope failure, and combined processes for a) the detailed and b) coarse scales (Figure 20b). In both the analysis with the detailed and coarse resolution datasets, the flooding extent was the sub-process with the highest accuracy, followed by the combined processes and debris flow runout. The slope failure was the

process with the lowest accuracies. In both cases, the same run gave the best results for slope failures, hillslope debris flows and combined processes, while the best flooding results correspond to another run.

4.1.1.1. Flooding

Figure 21a shows the best modelling results for flooding extent using the detailed resolution, corresponding to the blue dot inside the black circle in Figure 20a, with a TPR of 0.84 and a FPR of 0.23. The model recreates the extent of the flooding in the urban area (Figure 21a, i) and over-estimates the flooding extent, especially in the northeastern part of the study area (Figure 21a, ii) and in the upslope areas near the first-order drainages.

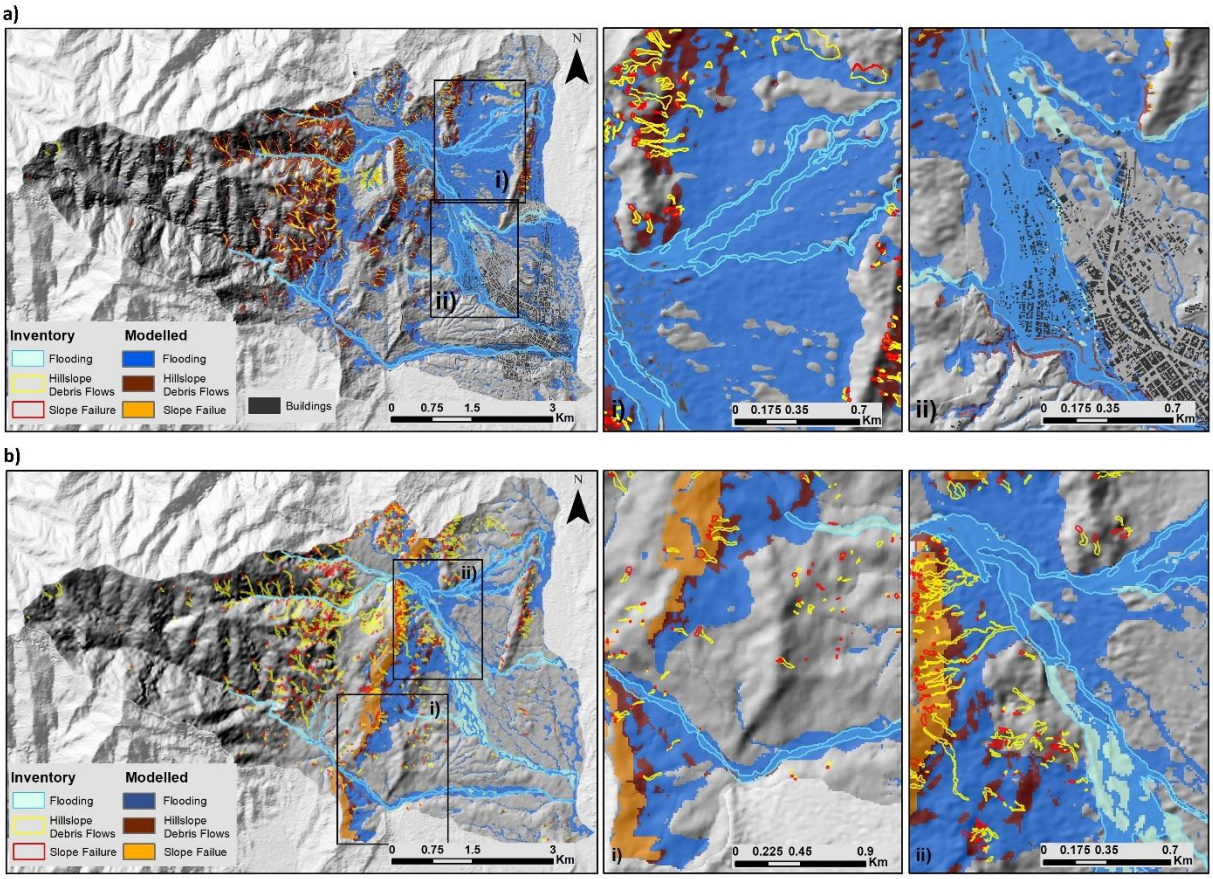

Figure 21. Best modelling results for flooding extent a)Using the detailed dataset, b) Using the coarse dataset

Figure 21b shows the best modelling results for flooding extent using the coarse resolution dataset, corresponding to the blue dot inside the black circle in Figure 20b, with a TPR of 53 and a FPR of 0.13. The flooding originates in the slope failures rather than the streams(Figure 21b, i). It does not have continuity in the terrain, causing its extension to decrease towards the urban area, where it reaches with discontinuous pattern (Figure 21b, ii).

Figure 22 shows the frequency of the flooding extent output of all the modelling runs using the detailed (a) and coarse (b) dataset. For the detailed case, out of the 50 runs, about 30% modelled a flood, while the remaining 70% did not model any channel overflowing. For the coarse scale, from 35 runs, 37% modelled a flood, and the remaining 63% did not. Usually, the absence of flooding in a modelling run is caused by the

lack of slope failures in the corresponding modelling run or the wrong choice of hydraulic soil parameters that did not allow any excess runoff to be created.

For both cases, from the proportion of runs that led to channel overflowing, most of them over-estimate the extent of the flooding in the north-eastern part of the study area (Figure 22a, i) and the extent of the main flooding event downstream of the Taruca an Sangoyaco rivers. On the coarse scale, the flooding areas were concentrated in the floodplains closest to the hillslopes (Figure 22b, ii). They propagated over-land partially to the urbanized areas, indicating that the floods came primarily from the runoff of slope failures. These results suggest that the model tends to either under or overestimate the flooding extent. Finding the right balance between hydrologic and slope stability properties to come out to the proper extent is difficult.

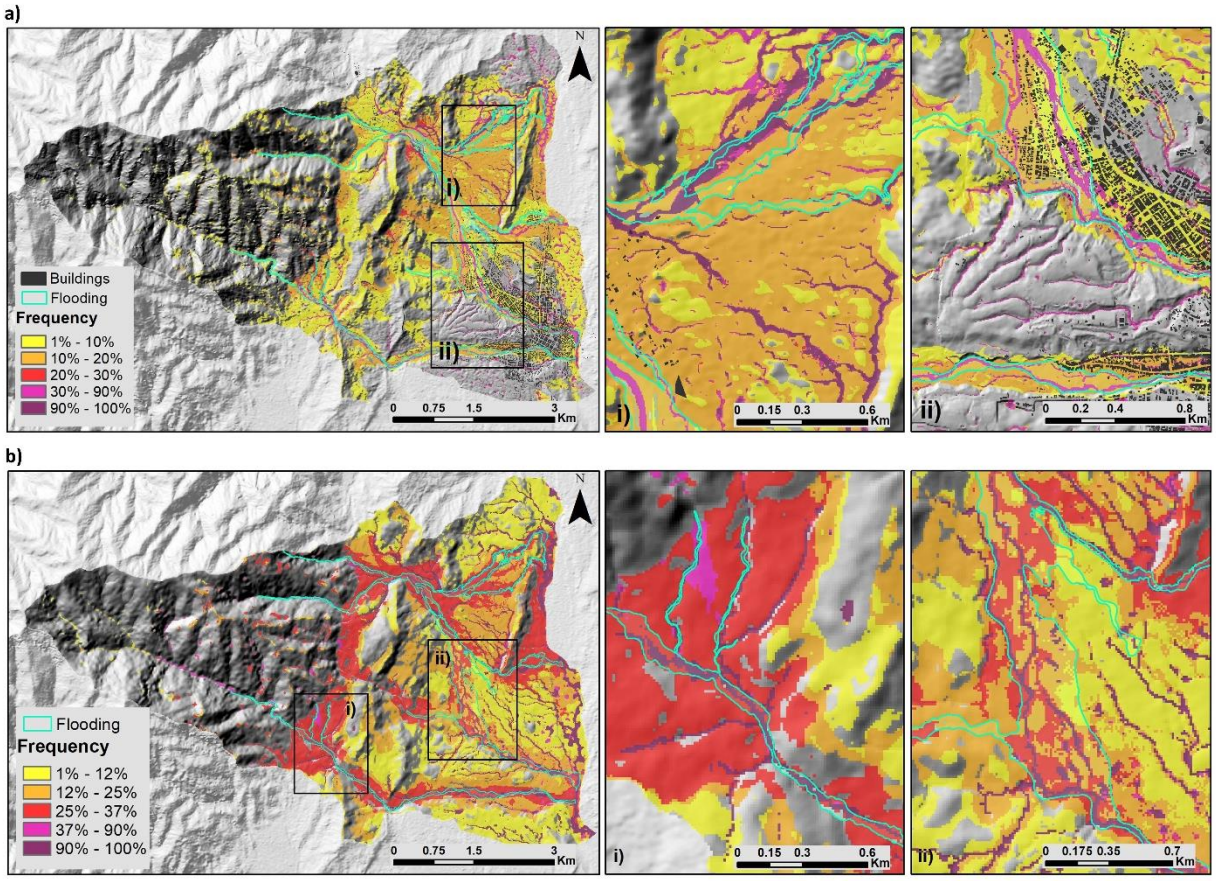

Figure 22. Frequency of flooding extent output of the model runs a) Using the detailed dataset, and b) Using the coarse dataset.

4.1.1.2. Slope Failure, Hillslope Debris Flows, and combined processes

Figure 23 shows the best results for slope failure, hillslope debris flow and combined modelling, corresponding to the brown, yellow and black dots in black circles of Figure 20. Figure 23a corresponds to results with the detailed scale, and Figure 23b with the coarse scale.

For the slope failure, the results have a TPR of 0.51 and a FPR of 0.25 on the detailed, and a TPR of 0.29 and FPR of 0.25 on the coarse scale. The hillslope debris flows modelling had a TPR of 0.69 and a FPR of 0.30 in the detailed, and TPR of 0.56 and a FPR of 0.23 on the coarse scale. For the combined processes, the detailed scale reached a 0.76 TPR and 0.29 FPR, and the coarse scale, a TPR of 0.58 and a FPR of 0.22.

For both scales, this results strongly over-estimate slope failures. On the detailed scale (Figure 23a), the flood extent covers nearly all the bottom of the fan, while the coarse scale (Figure 23b) only generated a flood in the upper part of the basin.

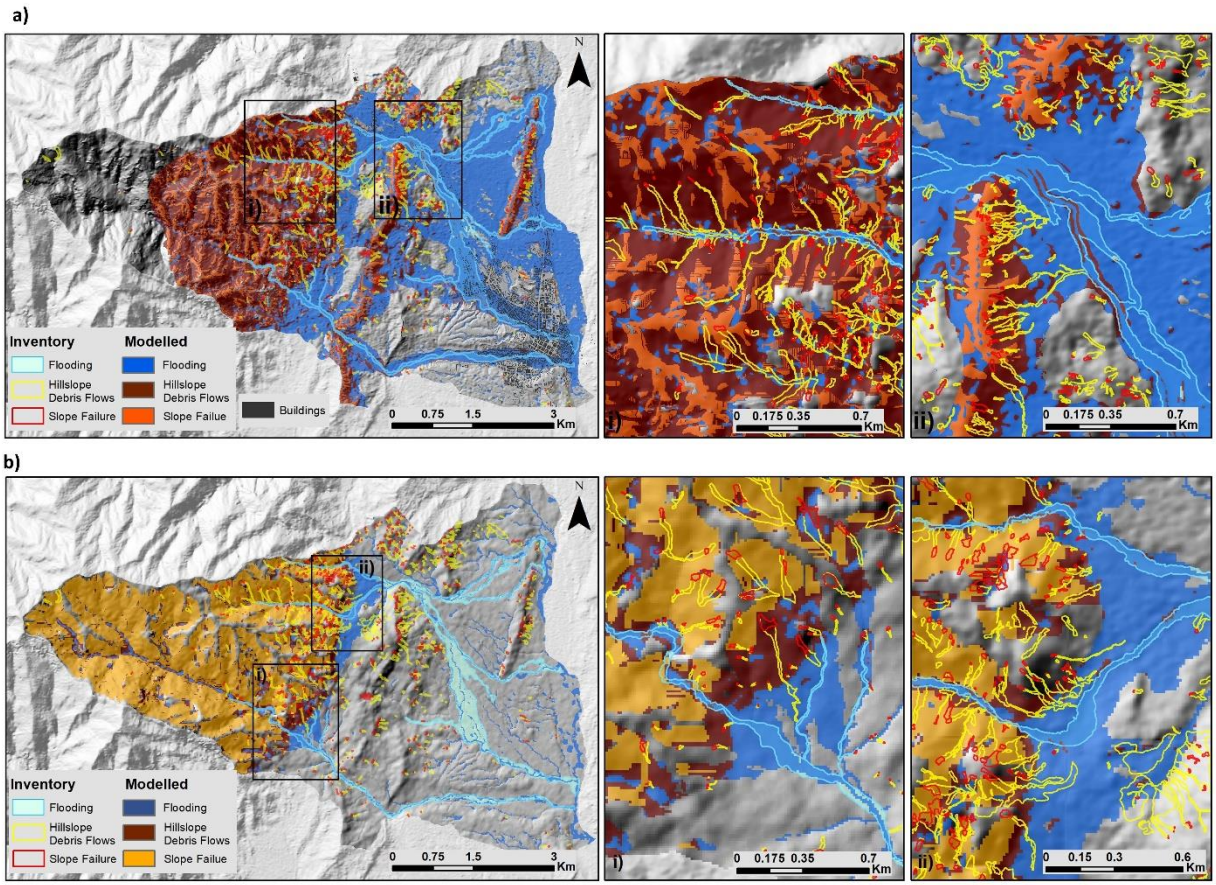

Figure 23. Best modelling results for slope failure and hillslope debris flow runout using a) the detailed dataset and b)the coarse dataset

4.1.2. Sensitivity Analysis

Figure 24 shows, for both scales of study, the changes in the percentages of flooded and unstable cells concerning changes in the values of calibration parameters: Cohesion and Internal Friction Angle -that were treated as a single variable- (C-IFA), Soil Depth (SD), Saturated Hydraulic Conductivity (Ksat), and Soil Water Content (Theta). The trendlines slope indicates the model's sensitivity to the changes in the value of the parameters. It is important to note that, due to limited time and computation capacity, not enough runs were done to vary each parameter individually on each computation; therefore, the variation in the results are the consequence of changing more than one parameter. This means that the sensibility analysis is only indicative and cannot be interpreted as absolute.

For the slope stability modelling, the percentage of cells with a Safety Factor less than 1 was the indicator of the changes in slope stability since it describes better the changes of sensibility of the model.

For both details of the study (Figure 24a for detailed and Figure 24c for coarse), the slope stability modelling is most sensitive to C-IFA, followed by SD. However, the sensitivity for both parameters is stronger for the

detailed case. These results are in accordance with expectations from slope stability theory (Van Beek and Van Asch 2004).

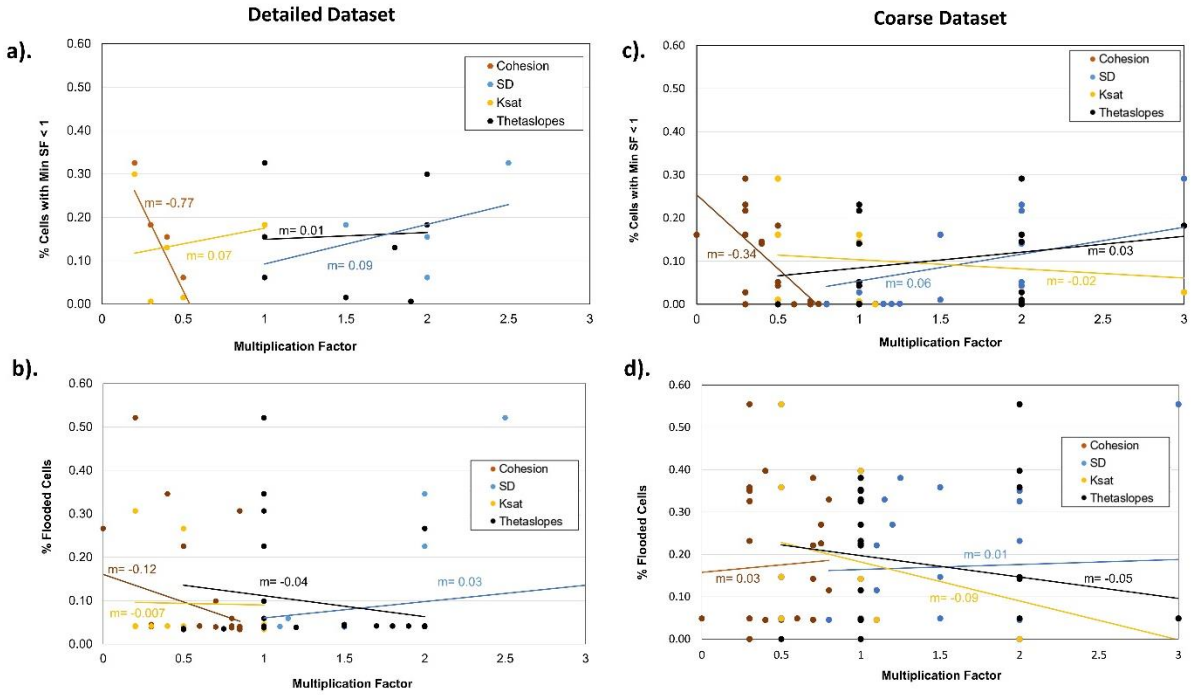

Figure 24. Sensitivity of the flooding and slope stability modelling to each of the calibration variables. a) Slope Stability of detailed dataset, b)Flooding of the detailed dataset, and c)Slope Stability of coarse dataset, and d) Flooding of the coarse dataset

The sensitivity to Ksat and Theta parameters are stronger for the coarse scale than the detailed one. In the coarse scale, the Ksat parameter shows an inverse relationship with the increased flooded cells, meaning that higher values of Ksat generated less stable cells, contrary to the detailed scale, where the relationship between Ksat and unstable cells is direct. This contradiction shows that the influence of the Ksat parameter in the slope stability is not linear, probably due to two competing processes: I) Decreased flood volume due to infiltration limiting available water for surface flow. II) Increased slope failure due to increased infiltration provides additional fluids and solids that run out to downstream areas. Depending on the terrain type and the value of other parameters, either of these processes might dominate the sensitivity results.

In the case of flooding (Figure 24b for detailed and Figure 24d for coarse scales), the detailed scale is most sensitive to C-IFA, followed by Ksat, Theta, and SD. The coarse scale is most sensitive to Ksat, followed by Theta, C-IFA and SD. The high sensitivity of the detailed scale to C-IFA might be related to the presence of slope failures, therefore an increase in the flooding extent. The rest of the trends of the sensibilities are generally observed for flood models (Van den Bout et al. 2018).

4.2. Results for Salgar

The Salgar study case was modelled 50 times. Each run took approximately 12 hours on a computer with 16 GB RAM and a Core i7 processor. The simulation time step was 10 seconds, with a total modelled time of 1000 minutes (16.7 hours).

4.2.1. Accuracy Analysis

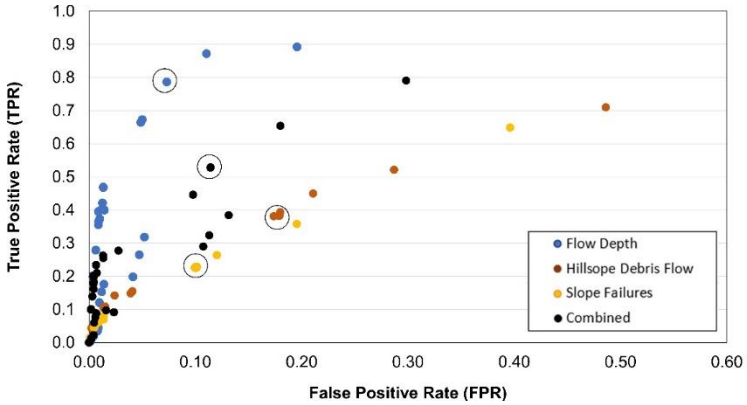

Figure 25. Performance of the model for each sub-process, and combined modelling in the Salgar case study

Figure 25 shows the accuracy of all the sub-processes and combined modelling for Salgar. The graph shows evident accuracy trends for each sub-process. The flooding extent has the highest accuracies, followed by the combined processes results. The hillslope debris flows and slope failures have similar trends but lower accuracies overall. Similar to the case of Mocoa, many runs did not model any slope failures. The black circles in Figure 25 **¡Error! No se encuentra el origen de la referencia.**indicate the most accurate results for each sub-process.

Figure 26 shows the best modelling results for flooding extent, corresponding to the blue dot inside the black circle in Figure 25 with a TPR of 0.78 and a FPR of 0.07. These results model the channel of the river correctly, although they overestimate the extent of the flooding event. The overestimation is especially visible in the tributary drainages, and in the upper part of the basin where the flooding extends in a flood plain (Figure 26a), and in the urban area, where the model covers a large zone (Figure 26b).

Figure 27 shows the best results for slope failure, hillslope debris flow and combined modelling, corresponding to the brown, yellow and black dots in black circles Figure 25, with a TPR of 0.38 and a FPR of 0.18 for hillslope debris flow, TPR of 0.22 and a FPR of 0.1 for slope failure, and 0.52 TPR and 0.11 FPR for combined modelling. Although these results also tend to overestimate the slope failures and hillslope debris flow areas, the unstable cells have a pattern that resembles the real one, and the runout of the landslides is very accurate, too (Figure 27a). The flooding extent is very precise in the upper part of the basin, although it also overestimates the extent in the urban area (Figure 27b).

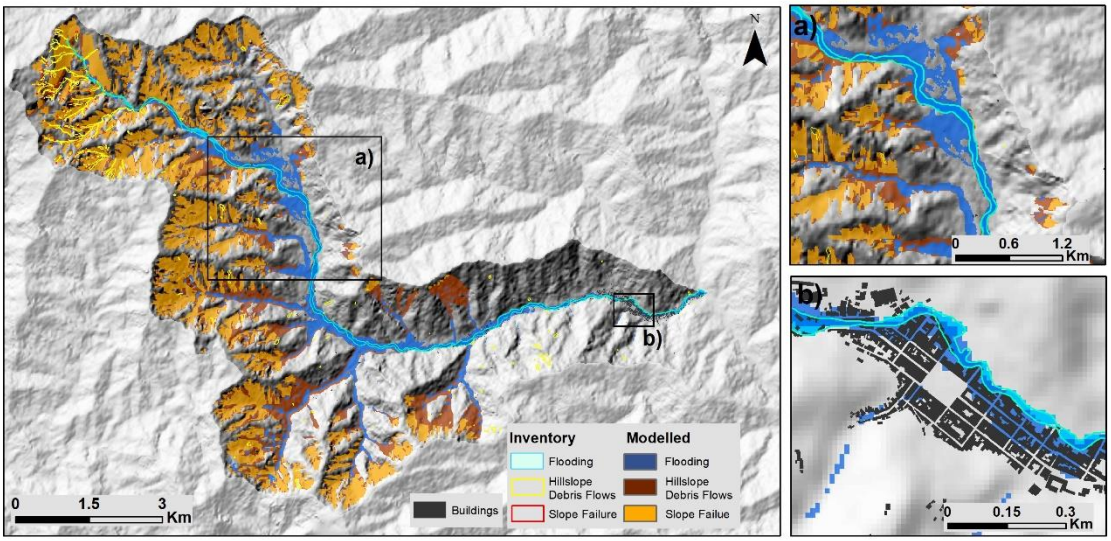

Figure 26. Best modelling results for flooding extent

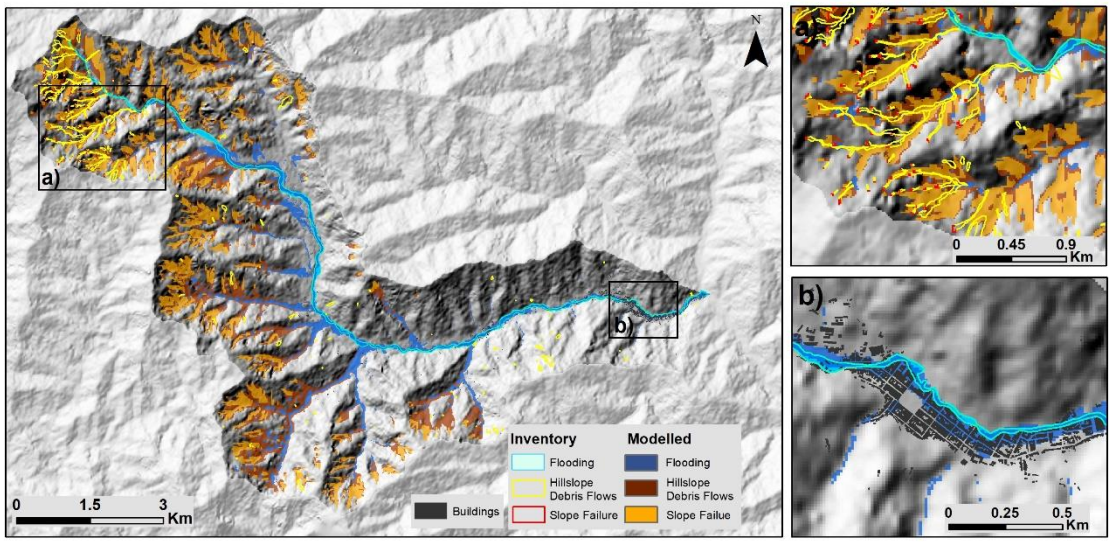

Figure 27.Best modelling results for hillslope debris flows, slope failure, and combined modelling

4.2.2. Sensitivity Analysis

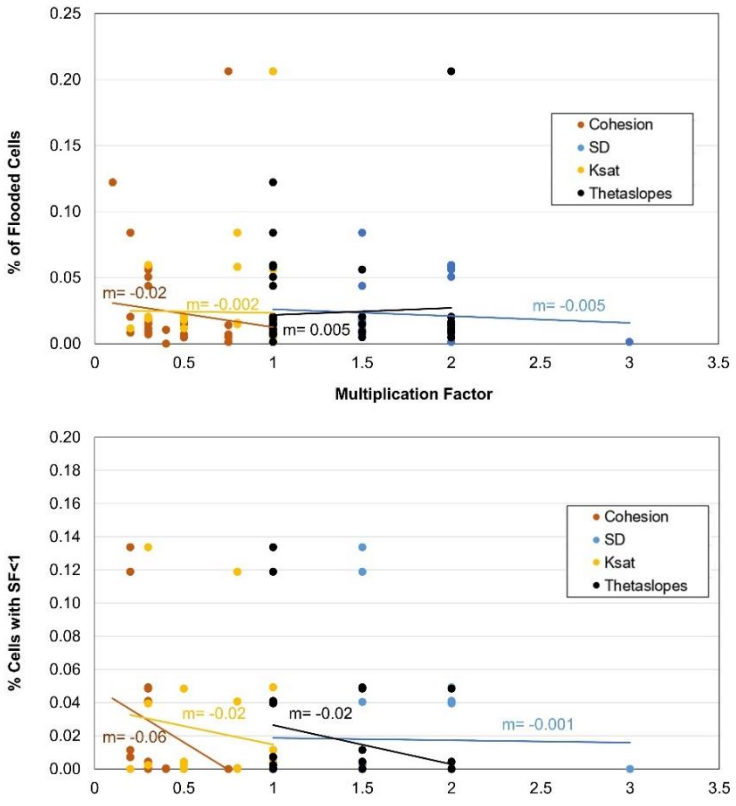

Figure 28. Sensitivity of the flooding and slope stability modelling to each of the calibration variables

Figure 28 shows the changes in the percentages of flooded and unstable cells with respect to changes in the values of calibration parameters: C-IFA, SD, Ksat and Theta. The slope stability modelling (Figure 28**¡Error! No se encuentra el origen de la referencia.**b) is most sensitive to C-IFA, followed by Ksat. Unlike the Mocoa case study, the Slope Stability is not sensitive to the soil depth, and it is not very sensitive to the initial saturation of the slopes (Theta).

In the case of flooding (Figure 28a), the model is not very sensitive to any parameter. C-IFA is also the parameter with the highest sensitivity, while the sensitivity to SD, Theta and Ksat is minimal.

These sensitivity results are quite different from the Mocoa case study, giving the idea that the model's sensitivity to each parameter depends on the study area, not on the model itself. This should not be the case, and this disparity in values may be interpreted as changing several parameters in each simulation. For a more accurate sensitivity analysis in the future, it is essential to carry out a more systematized scheme for the simulations.

5. DISCUSSION AND CONCLUSIONS

5.1. Calibration Process

The process of calibration is instrumental in the application of physically-based modelling. For this reason, the effectiveness and difficulties encountered in doing so are relevant for the suitability of the OpenLISEM multi-hazard model to hazard assessment in the context of Colombia. This section seeks to show the most pertinent findings related to the calibration of each study case.

5.1.1. The calibration of Slope Stability

Slope stability is a critical sub-process in the OpenLISEM hazard modelling. Its importance lies in the fact that the slope failure is a determinant factor in triggering the subsequent process chains, determining the total volume and timing of sediment input in the main flow that impacts the downstream area. When running the model with parameters that do not create slope failures during the calibration, the user carries out a "lost run", where the output corresponds only to a stream flood modelling, usually without any channel overflowing. Since OpenLISEM consumes so many computational and time resources, these lost runs mean a big obstacle for the calibration process. In our case, the number of runs that did not simulate slope failures was 28 out of 50 on the detailed scale, 16 of 35 on the coarse scale, and 35 of 50 for the case of Salgar, that s equals 137 lost days, out of the 242 days of total modelling time.

To overcome this difficulty, a separate analysis was carried out in Mocoa trying to answer the following question: Can we ensure that the slope failures occur, by finding the correct values for the calibration parameters that create slope failures simulating only the initial stability conditions, and then use those same parameters later on to simulate all the processes?

As seen in the sensitivity analysis for the study areas, the slope stability modelling is mainly sensitive to the Cohesion-Angle of friction and Soil depth parameters. The exercise consisted in modelling only the initial slope stability in one timestep for the case of Mocoa while varying the C-IFA and SD calibration factors individually while keeping the rest of the parameters unchanged. Each of these simulations took less than a minute to complete. Figure 29 and Figure 30 show the variation in the Minimum Safety Factor when varying the multiplication factors of the C-IFA and SD parameters, respectively.

The result confirms that cohesion, friction angle, and soil depth are critical parameters in slope stability estimation. The model is more sensitive to changes in soil cohesion and angle of friction and less sensitive to changes in soil depth. From this exercise, the scenario that yielded more accurate slope stability results is shown in Figure 29b, where some areas in the upper basin and high slope zones have Safety Factors less than one and therefore should fail. These parameters were then used to run the model, including all the processes. However, the output of such exercise did not yield any slope failure.

This happens because additional processes such as infiltration and surface flow influence the stability and failure process when switching from static to dynamics simulation of slope stability. This brings us to a critical characteristic of multi-hazard modelling: A single parameter influences several subprocesses differently. As a result, calibration of one individual process does not guarantee a good outcome when simulating a multi-process event. The influence of such complex inter-dependence of variables cannot yet be anticipated. As a result, those "lost runs" were unavoidable.

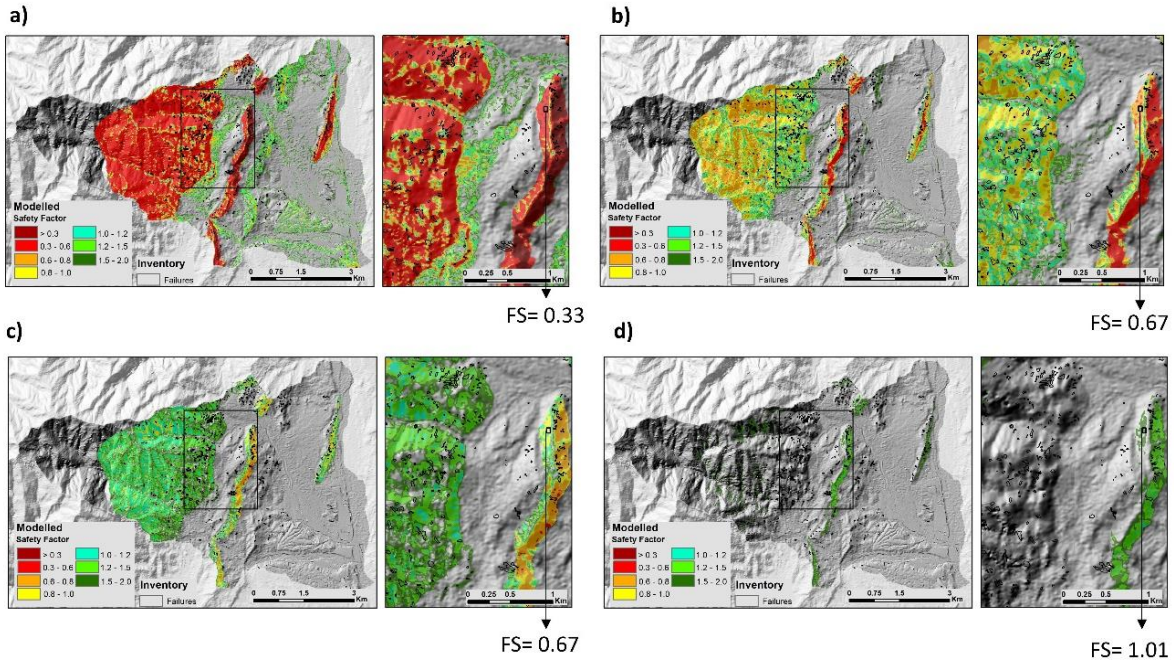

Figure 29. Variation of Minimum safety factor with changes in Soil Cohesion and Friction Angle values. The multiplication factors are a) 0.1, b) 0.2, c) 0.3 and d) 0.6

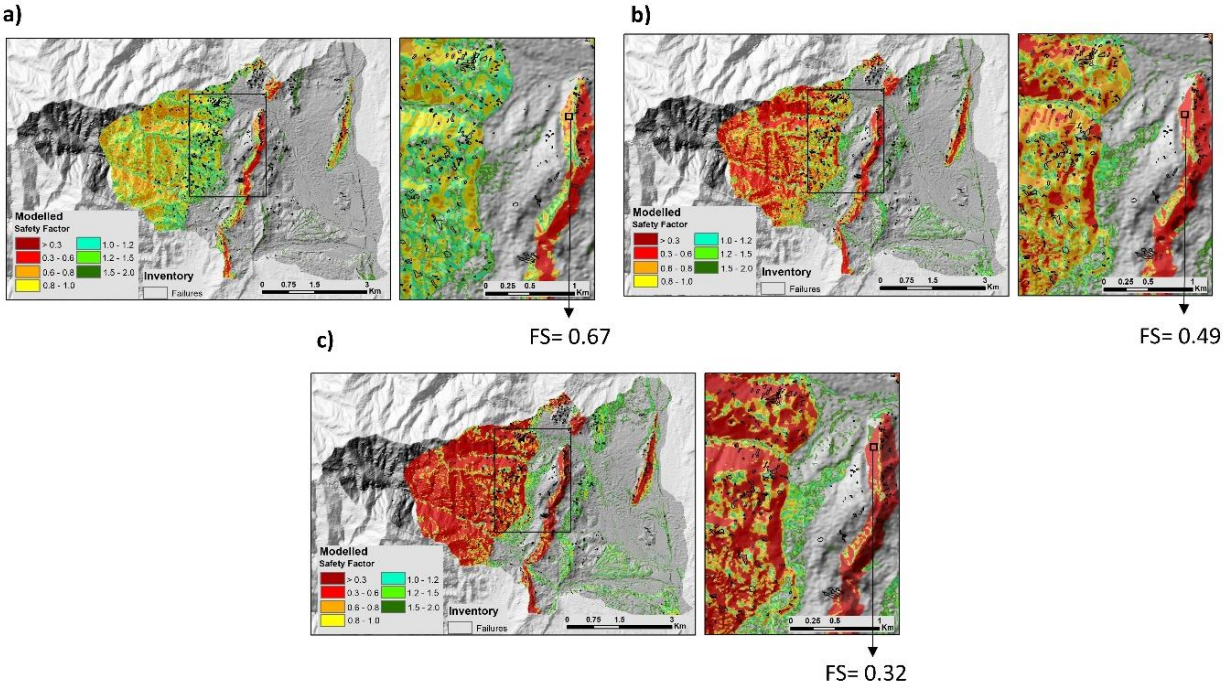

Figure 30. Variation in Minimum Factor or Safety with changes in Soil Depth Values. The multiplication factors are a) 1.0, b) 1.5, and c) 2.0

5.1.2. Relationships between slope failure and slope stability parameters

To understand how the variables relate to slope failures, we created plots relating different combinations of values for calibration parameters and the presence or absence of slope failures for the corresponding simulation. Figure 31a shows the results for the case of Mocoa, where there is a clear trend between the ratio between C-IFA, Soil depth, and slope failure, where greater cohesion values require thicker soil profiles

for slope failures to occur. Some simulations, located on the red box of the figure, had the same C-IFA and SD combinations and had simulations with and without slope failures. In those cases, the presence of slope failures depended on the value of Ksat and Theta (Figure 31b). From this, it is also clear that the Ksat and Theta parameters influence the occurrence of slope failures, where slopes with higher saturated conductivity and lower porosity values start showing slope failures. Due to the complex multi-process nature of the model, with many interdependent processes and input parameters, thresholds for slope failure behaviour are challenging to predict.

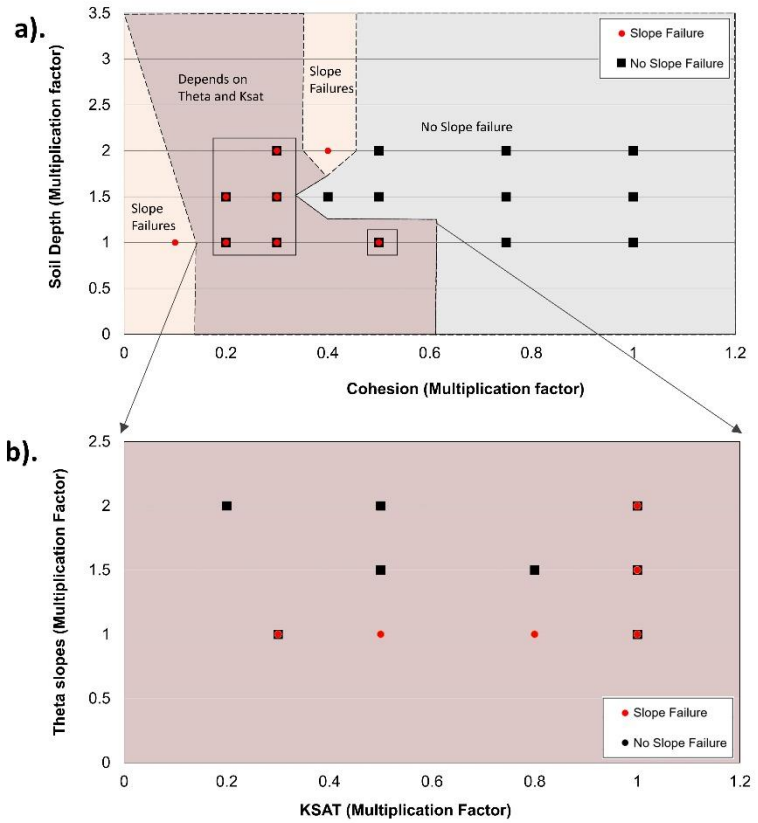

Figure 31. Relationship between calibration parameters and slope failure occurrence.

5.1.3. Influence of the Soil Depth Model

The model was used for the Mocoa case with two soil depth maps shown in Figure 13. Figure 32 shows the result of two identical runs, where the only difference was the input soil depth map. The results are shown in terms of slope failure and minimum safety factor. In Figure 32a, the soil depth map used is based on the model suggested by Catani, Segoni, and Falorni (2010) shown in Figure 13b. In Figure 32b, the soil depth map that used was constructed according to the model suggested by Stothoff (2008), shown in Figure 13a.

In the case of Figure 32a, the upper figure shows how the model assumes slope failure in the limit between soil units with a very big difference in depths, which in this case correspond to the boundary between rock units (with soil depths between 1-5 meters) and transported soil units, with soil depths up to 10 meters. Even though the failure patterns are inaccurate, the differences in slope stability do follow a logical pattern within slope units, as shown in the second figure. Nonetheless, the spatial variability in slope stability is unrealistically low, as the soil depth also varies very little within the slopes. Thus, the resulting slope failure

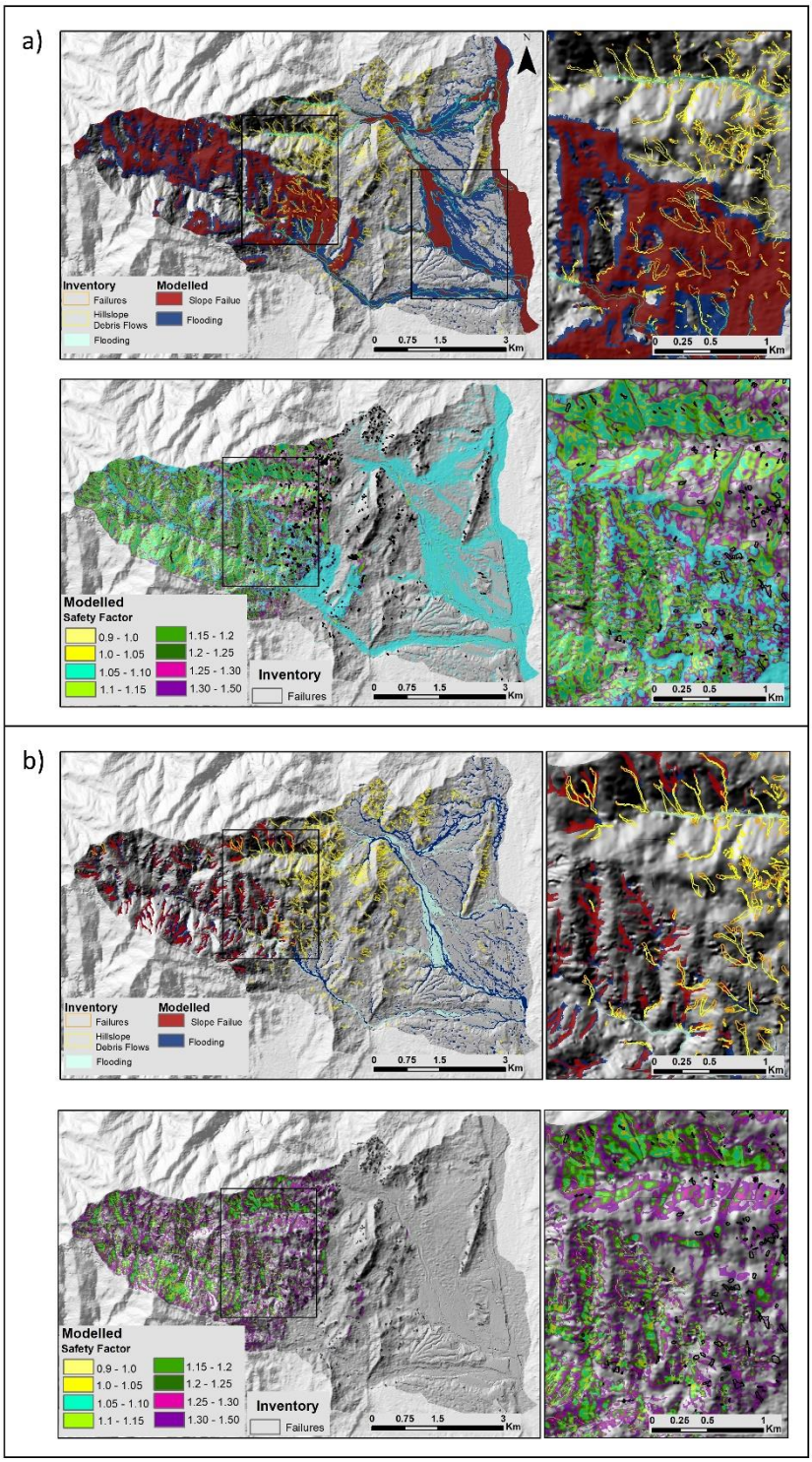

Figure 32. Slope Failure and Minimum Safety Factor outputs using a) The soil map of Figure 13b, and b)Figure 13a

pattern is very heterogeneous, modelling either too many failures in the more unstable soil units or no failures in the more stable ones.

For the case of Figure 32b, the upper figure shows how the slope failures pattern is more accurate and explains where landslides are likely to occur at some point. The bottom figure shows how the variations in slope stability values follow a very realistic pattern. The disadvantage of this soil depth map is that the depth values are not representative of the reality of the study area, but this can be solved by tuning the multiplication factor for soil depth in the calibration process.

In summary, the OpenLISEM model is very sensitive to the soil depth map since it determines the potential location of soil failures. However, absolute values are relative of lower importance compared to spatial patterns. In particular when calibration is carried out. The soil depth parameter will be adjusted to match more accurate simulation results. When working with the model, soil depth maps with sharp depth changes should be avoided, and standard soil depth models offer a good option to show areas with greater relative susceptibility to landslides.

5.1.3.1. Saturated Hydraulic Conductivity and Water Content of Slopes

These parameters were included in the calibration process because, as previously mentioned, the rainfall conditions of the previous months is a determinant factor for this type of disastrous event since they create conditions of a very high level of water saturation. This influences the stability of the slopes and increases the runout, expanding the flooding. Figure 33 shows the result of modelling with identical parameters and only varying the Ksat parameter, with a multiplication factor of 0.8, in Figure 33a, and 0.3 in Figure 33b. The Ksat influences the occurrence of the slope failure process and increases the water content of the flow, increasing the flooding extension. This is not the case for the Theta parameter. In the simulations where this parameter was varied, it did not influence the occurrence and extension of slope failures.

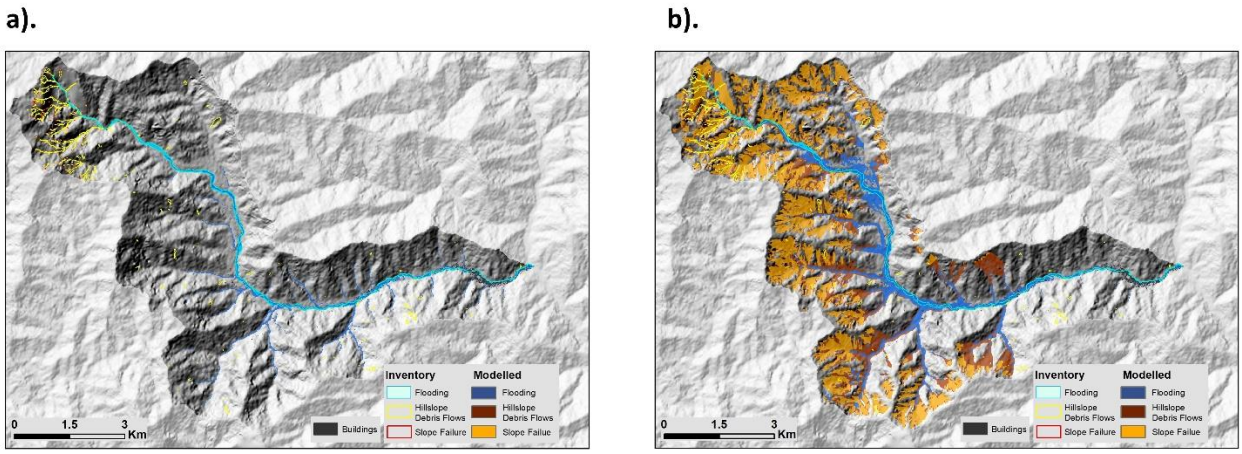

Figure 33. Results of modelling with different values of the Ksat parameter, with multiplication factors of a) 0.8 and b) 0.3

On the simulated scenarios, Ksat and Theta don't influence the flooding extent unless there are failures simulated in a run. Changing those parameters values in runs without any slope failure give identical flooding results.

These results indicate that, even though the slopes water content is an essential parameter in slope stability and flooding simulation, in OpenLISEM Hazard, such parameters have less importance than the other parameters. Making more simulations changing these parameters with limit equilibrium conditions may show better its influence on the modelling results. In theory, the direct effect of these parameters in the outcome of the model is difficult to predict since it influences long-term stability by saturating soils and adds more weight to the soil column, but also creates conditions for more runoff absorption from the soils, decreasing the flooding of channels and runoff in general.

5.2. Comparison between results using coarse and detailed resolution for the case of Mocoa

Since the study case of Mocoa was modelled with coarse and detailed input data, comparing their results can give an idea of the implications of the data resolution and quality into the modelling process.

Figure 34 shows the TPR and FPR for each subprocess and scale of study. The detailed resolution reached higher accuracies in the flood modelling. Figure 35 shows the frequency of flooding extent for both sets of modelling outputs. Generally, the high-resolution simulation shows significantly less flooded area. This can be attributed to high-resolution data better definition of channels and terrain depressions as water flow has

better connectivity through channels and valleys, and inundation decreases. Therefore, the DEM resolution is very critical in terms of flood modelling accuracy.

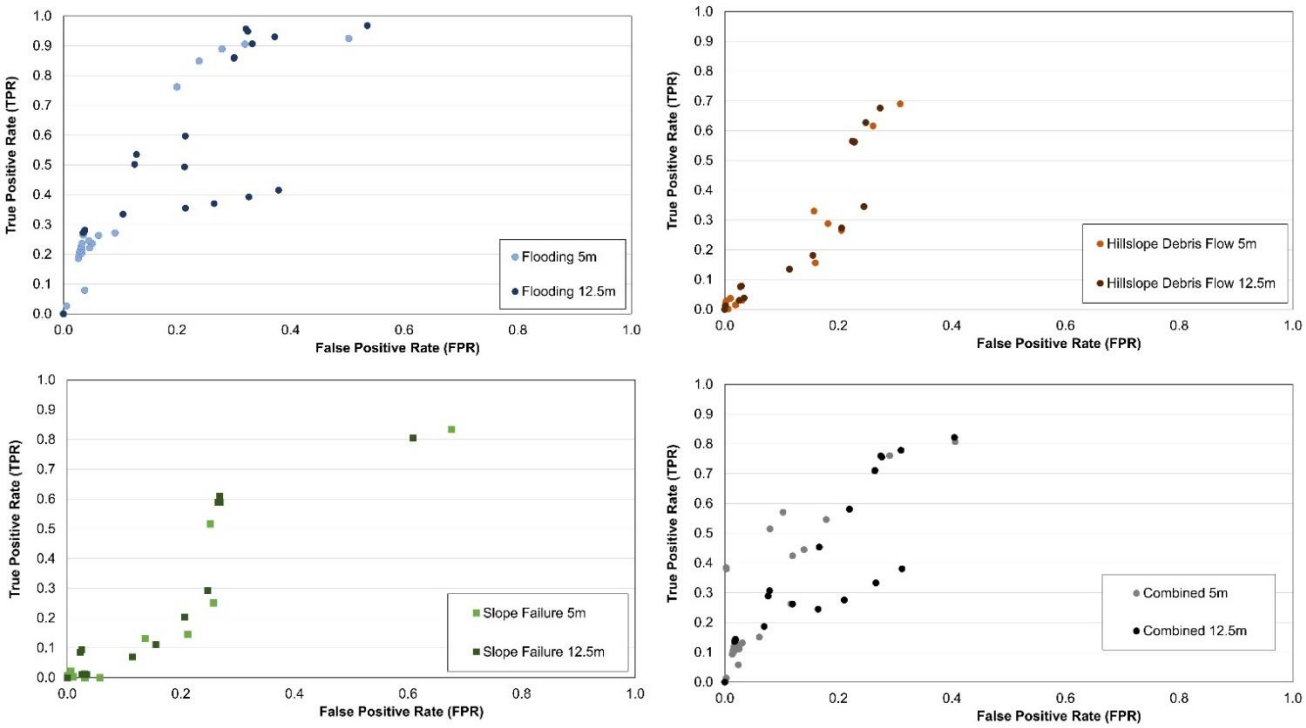

Figure 34. Comparison of accuracies for each subprocess for the detailed (5m) and coarse (12.5m) resolution for Mocoa

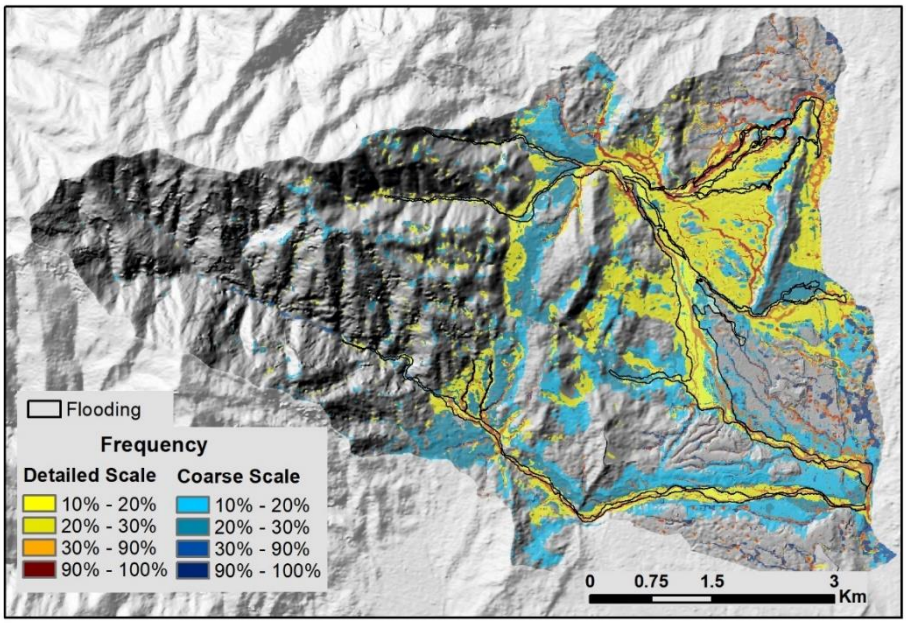

Figure 35. Comparison in flooding extents of modelling in the detailed and coarse resolution

There is no significant difference in terms of accuracies for the slope failure and hillslope debris flow runout processes. Not even with the more detailed soil unit map that was used in the detailed scale, the accuracies increased significantly. For the combined processes, the accuracies are also very similar, and the differences in detail of the input information do not improve the results significantly. The results show that, for the Mocoa event, the spatial resolution of the

elevation data did not limit the accuracy of the stability and failure model. Instead, the slope stability and runout processes could not reproduce the event's complex, critical, and sensitive aspects, such as the potential landslide damming in the upper channels.

5.3. Challenges of Multi-Hazard modelling and suggestions for improvement

When dealing with a study area with limited information concerning terrain properties and event inventories, multi-hazard modelling includes many uncertainties. Usually, the calibration procedure is the primary tool for a modeler to tune the model and achieve the best possible results. The analysis that was carried out in this research showed that the calibration procedure using a multi-hazard model, in particular, OpenLISEM has significant challenges, which include:

- The influence of the calibration parameters in the final output is not traceable for each subprocess. Figure 36 shows the interactions between the water, sediment and debris processes in the OpenLISEM Model. The model includes several parameters for each sub-process, but the scheme includes only the parameters influencing more than one modelling process. The calibration of such parameters is complex because they can affect the output differently, and tracing their influence becomes very difficult. For example, increasing the soil porosity can decrease the slope stability but increase infiltration, generating less flooding. So, if the modeler wanted to increase the flooding extent in the calibration process, a good solution would be decreasing the soil porosity. But on the other hand, this change would also trigger fewer landslides, which would reduce the amount of sediment in the flow, reducing the flooding extent.

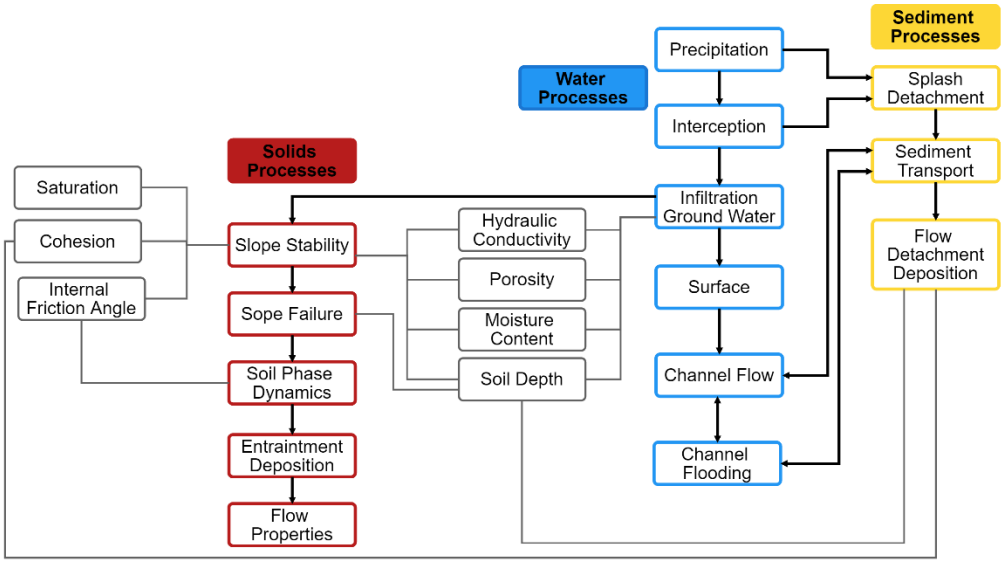

Figure 36. Graph showing the interactions between subprocesses and modelling parameters in the OpenLISEM Hazard model

- Multi-hazard models simulate the processes in a concatenated way, and they don't differentiate between the extent of slope and hydrological phenomena. For this reason, measuring the accuracy, and therefore the calibration of each subprocess is complex.

- The model consumes a lot of time and computational resources, so the calibration becomes a long process. Runs without any slope failure that triggers the subsequent chain processes take the same amount of time and do not contribute to the calibration processes.
- Usually, modelers are familiar with the processes and physical principles of slope stability, slope failure and flooding; therefore, calibrating the parameters related to these processes is a more straightforward step. Nonetheless, in a multi-hazard setting, there are several physical processes occurring in the entrainment and sediment transport, and calibrating the parameters involved in such processes is a more complicated task. For this reason, finding a balance between sediment failure, transport, and flooding is difficult. It was common to find the proper flood extent but with an over-estimation of slope failures or highly accurate slope failure models with very small flooding extents.

Based on these challenges, some of the improvements that multi-hazard models, including OpenLISEM, could include would be:

- Multi-hazard models carry many uncertainties related to each sub-process. The output of one multi-hazard model is related to one single scenario of several variables plus possible interactions. For this reason, a probabilistic approach could give a much better perspective of hazard. This approach to model slope failure could also be very useful to avoid the useless model runs that end up in a simulation with no failures and must be rejected later.
- In both study cases of this analysis, the antecedent soil moisture played a crucial role in the final output of the event. Including this variable in the model might provide additional insight into the causes of impact.
- The calibration of the parameters in OpenLISEM is done using multiplication factors for the whole study area. The option to calibrate specific soil units would allow the user to control relative differences within the study area. When many classes are present, the computational load of running many resulting simulations will become unrealistic. Instead, a new approach might need to be investigated, perhaps a co-linear variation of local parameter values according to class-specific uncertainties.
- The flow equations present in the multi-hazard models consider water and sediments to be perfectly mixed in the flow, which is not the case for landslides coming into the streams. When blockages occur, the sediments coming into the flow can cause blockages that increase the intensity and velocity of the flooding events. According to the reports of the Salgar and Mocoa events (PUJ 2016; SGC 2017a), in both events, there was evidence of several landslide blockages that influenced the behaviour of the flow, and such scenarios should also be considered in the model.

5.4. Suitability of the model for Colombia

Some of the most relevant factors for understanding the suitability of Multi-Hazard modelling for the context of Colombia are:

- Absolute soil depth values are not as relevant for the modelling process as their spatial variation within slopes, which ultimately determine the most unstable areas.
- The geotechnical characteristics are crucial parameters for modelling since they determine the occurrence of slope failures and the amount of material flowing into the channels. Nonetheless, their absolute values were not proven to be as relevant as their relative differences within the study area. For example, in the cases of Figure 31 that correspond to the Salgar study case, the slope failures started occurring when the Cohesion-Angle of friction was less than 60% of the original

values. For the case of Mocoa, this limit was located at around 40%. These changes might be attributed to either limitation of the method implemented in the model or missing processes such as loss of cohesive strength during very high saturation of fine soils. However, the calibration process allows us to understand the most susceptible areas for landslides and how the flow can behave with such sediment input.

- The resolution of the DEM was proven to be very important for the flood and slope failure modelling. In particular, when modelling with coarser DEM, the flooding extent was over-estimated. This could be especially an issue for land use planning in urban areas. The main disadvantage of using more detailed DEM is the increase in time consumption.
- The main obstacle of multi-hazard modelling is the large number of input parameters and the great effort needed to calibrate them, given the long computation time and the complex relationships between them and the sub-processes.

In this sense, the suitability of a multi-hazard model should be evaluated based on several critical aspects of the study case and areas. To start, multi-hazard models simulate one single scenario of several possibilities that could occur during a catastrophic event, such as a debris flow. The characteristics and peculiarities of the study area that may induce new possibilities during an event determine the suitability of using this model. Some events are very confined, meaning that there are factors that limit the spatial variability in probable outcomes. An example of this is steeply incised channels, which physically confine flood extent to a small area. When the knowledge of the study area and its level of confinement is reduced, the probability of getting very accurate results for modelling events with so many levels of freedom becomes very small. Using only a single model outcome for land use planning increases the risk of being incorrectly prepared for future disasters because of a more significant number of possible scenarios that were not contemplated.

In the case of Colombia, the basic hazard assessment required for land use planning is a first approximation to hazard that should be analysed further in detail when hazardous areas are planned to be developed. According to the review of data availability in the country, most municipalities lack detailed information that can allow the use of multi-hazard models with enough accuracy to contemplate different scenarios. For this reason, the most optimal option for the basic hazard assessment should consider all the uncertainties of the modelling. A good approach to basic hazard assessments could be coupled with physically-based models used sequentially. The fact that they are used in sequence allows the user to control the influence and uncertainties of each parameter in the output. Another interesting approach could be using physically-based models with a probabilistic approach, where the most critical parameters are included with a distribution function that allows the modelling of possible outcomes of diverse scenarios.

Empirical run-out models are a possible option for debris flow hazard assessment only when there is an interest in knowing the hazard for slope processes like hillslope debris flows. For most of the cases of debris flows in Colombia, the damages are caused mainly in the populated areas located in fans or valleys. The main interest of modelling these multi-hazard scenarios is to understand how the upslope processes influence the outcome of the flooding downstream. In this sense, the traditional hydraulic models can be useful for debris flow modelling, even though they ignore the sediment loads that increase density and impact pressure. The influence of the sediments could be assessed using multi-phase approaches for detailed studies.

In the case of basic hazard assessment analysis, the results of this work indicate that added uncertainties are not always worth accepting. The increment in the flooded volumes has been successfully done in a probabilistic way. However, both study cases in this work emphasize the importance of landslide and debris flow processes on flood dynamics and flood extent. If there is knowledge about the slope stability

phenomena that may be triggered in intense rainstorms, these calculations should include this. Multi-hazard setups might thus have been used in detailed investigations when good data is available. However, for the data-scarce, tropical and tectonically active areas like Colombia, the difficulties related to the calibration of multi-hazard modelling and the uncertainties of possible scenarios mean that such models could not be effectively be employed in this research.

5.5. Conclusions

The main objective of this research was to analyse the suitability of the multi-hazard OpenLISEM model for debris flow hazard assessment for land use planning in Colombia. The analysis shows that, while multi-hazard models show usefulness in research, their application for hazard assessment in areas with limited information like Colombia should not be undertaken without improved strategies for dealing with uncertainties. Other conclusions are addressed by answering the research questions:

1. Understand the main implications that modelling with limited input data may have when incorporating such results into land-use plans

The main limitation of using multi-hazard modelling with limited information is their lack of consideration to different and diverse scenarios. Being complex and compound events, debris flow phenomena include a series of sub-processes, each of them modelled with several parameters. In data-poor areas, such parameters are usually very uncertain. As a result, multi-hazard modelling results feature a combination of propagated uncertainties. A single, possibly calibrated simulation could be indicative of one single possible realization of an actual event. However, the variability in all potential outcomes and their uncertainty are not included. A possible solution to reduce the uncertainties would be using the multi-hazard model in a probabilistic framework, where the uncertainty of the parameters is considered, and the outputs can be evaluated based on the likelihood of their occurrence. In any case, the multi-hazard modelling gives sufficiently accurate results for a basic hazard assessment. Its probabilistic output can be used to define the areas that should be considered for more detailed analysis.

2. Assess the accuracy of the OpenLISEM Hazard model with varying quality and quantity of input information on the global, national, and local scale in Colombia

Measuring the accuracy of the debris flow processes separately came with some difficulties by dividing the output and decreasing their measured accuracy. A better approach to measuring the model's accuracy could be including all the processes and comparing their extent with the inventory of all processes. This methodology would hinder understanding how changing the calibration parameters influence which part of the results, although this was a difficult task, even for the separate analysis.

The highest accuracies that were achieved with the model for each case are shown in Table 9. The main difference in accuracies between the coarse and detailed scale in the Mocoa study area is the flooding extent, associated with a better resolution DEM. There were no significant differences in terms of accuracy for the slope stability and hillslope debris flow runout. Therefore, the national and global datasets proved to be sufficiently good to use when no better information is available. In general terms, the limited accuracies of the output of the multi-hazard model are not related to the resolution of the data but more to the uncertainties associated with calibrating the relationship between the subprocesses of the model. For basic hazard assessment in large areas with limited information, it would be better to use either consecutive

physically-based models, like slope stability coupled with hydraulic modelling, or even only hydraulic modelling. Using physically based models with a probabilistic approach might be a suitable option since it includes the uncertainties in the input information and possible scenarios. However, smart strategies need to be developed to cope with the computational costs of running many potential scenarios.

Table 9. The best accuracies that were achieved with the model for each study area

	TPR	**FPR**
Mocoa Detailed	0.76	0.29
Mocoa Coarse	0.58	0.22
Salgar	0.52	0.11

3. Review the knowledge about the drivers and the occurrence of debris flow processes in Colombia that may influence the methodologies used to model them.

Both study cases analysed in this research were triggered by a combination of intense precipitation and a longer preceding wet period. In both cases, the conditioning factor that contributed to such devastating outcomes was the moisture condition of the soils, given by long rainy seasons with high accumulated rainfall over the previous months. This condition is not added in the modelling process directly but is indirectly simulated by increasing the soil water content of the slopes. Another critical driver of the debris flow phenomena present in both study cases was channel blockages during the storm, which determined the behaviour and intensity of the events. This process is not implemented comprehensively in multi-hazard modelling.

6. REFERENCES

Alcrudo, F. 2004. *Mathematical Modelling Techniques for Flood Propagation in Urban Areas*.

Álvarez-Villa, Oscar David, Jaime Ignacio Vélez, and Germán Poveda. 2011. "Improved Long-Term Mean Annual Rainfall Fields for Colombia." *International Journal of Climatology* 31(14): 2194–2212.

Anderson, JL, and RW Decker. 1992. "Volcano Risk Mitigation through Training." *Geohazards*. http://link.springer.com/chapter/10.1007/978-94-009-0381-4_2 (August 9, 2017).

Arango-Carmona, Maria Isabel. 2019. "Assessing Channelized Debris Flow Susceptibility Using Triggering and Propagation Models for Tropical Mountainous Regions, a Case Study of the Northern Andes, Colombia." University of Geneva.

Aulitzky, H. 1982. "Preliminary Two-Fold Classification of Torrents." *Mitteilungen der Forstlichen Bundesversuchsanstalt* 144: 243–56.

Baum, Rex L., William Z. Savage, and Jonathan W. Godt. 2008. U.S. Department of the Interior U.S. Geological Survey *TRIGRS—A Fortran Program for Transient Rainfall Infiltration and Grid-Based Regional Slope-Stability Analysis, Version 2.0*.

Van Beek, L.P.H. 2002. "Assessment of the Influence of Changes in Land Use and Climate on Landslide Activity in a Mediterranean Environment."

Van Beek, L P H, and Th W J Van Asch. 2004. "Regional Assessment of the Effects of Land-Use Change on Landslide Hazard by Means of Physically Based Modelling." *Natural Hazards* 31(1): 289–304.

Bladé, E. et al. 2014. "Iber: Herramienta de Simulación Numérica Del Flujo En Ríos." *Revista Internacional de Metodos Numericos para Calculo y Diseno en Ingenieria* 30(1): 1–10.

Borga, Marco et al. 2014. "Hydrogeomorphic Response to Extreme Rainfall in Headwater Systems: Flash Floods and Debris Flows." *Journal of Hydrology* 518(PB): 194–205.

Bout, B. et al. 2018. *OpenLISEM - Multi-Hazard Land Surface Process Model Documentation and User Manual*. Enschede. https://blog.utwente.nl/lisem/.

Van den Bout, B. 2020. "Integrated Physically-Based Multi-Hazard Modelling." University of Twente.

Van den Bout, B, L. Lombardo, C. J. Van Westen, and V. G. Jetten. 2018. "Integration of Two-Phase Solid Fluid Equations in a Catchment Model for Flashfloods, Debris Flows and Shallow Slope Failures." *Environmental Modelling and Software* 105: 1–16.

Bruner, G.W. 2010. *HEC-RAS River Analysis System: Hydraulic Reference Manual*. Davis, CA.

Caballero, Humberto, and Isabel Mejía. 1988. "Algunos Comentarios Acerca Del Evento Torrencial de La Quebrada Ayurá (Envigado) Del 14-04-88 y Sus Implicaciones En La Evaluación de La Amenaza Al Municipio." *2 Conferencia de riesgos geológicos del Valle de Aburrá*.

Cadavid, Juan. 2014. *Informe de Asesoría Técnica de La Evaluación Del Cauce y La Cuenca Principal de La Quebrada La Liboriana Para Analizar La Amenaza Actual Por Avenidas Torrenciales*. Medellin.

Cadavid, M. F, and M. Hermelín. 2005. "El Evento Del 29 y 30 de Mayo de 2000 En La Estrella y Sabaneta (Antioquia)." In *Desastres de Origen Natural En Colombia 1979-2004*, ed. OSSO- Universidad EAFIT-. Medellin.

Catani, Filippo, Samuele Segoni, and Giacomo Falorni. 2010. "An Empirical Geomorphology-Based Approach to the Spatial Prediction of Soil Thickness at Catchment Scale." *Water Resources Research* 46(5): 1–15.

Chiang, Shou Hao et al. 2012. "Simulation of Event-Based Landslides and Debris Flows at Watershed Level." *Geomorphology* 138(1): 306–18.

Christen, M, J Kowalski, and P. Bartelt. 2010. "RAMMS: Numerical Simulation of Dense Snow Avalanches in Three-Dimensional Terrain." *Cold Regions Science and Technology* 63(1–2): 1–14. https://www.sciencedirect.com/science/article/pii/S0165232X10000844 (June 28, 2018).

Cobierno de Colombia. 2020. "Departamentos y Municipios de Colombia." *Datos Abiertos*. https://www.datos.gov.co/Mapas-Nacionales/Departamentos-y-municipios-de-Colombia/xdk5-pm3f.

Costa, J. E. 1988. "Rheologic, Geomorphic, and Sedimentologic Differentiation of Water Floods, Hyperconcentrated Flows, and Debris Flows." *Flood Geomorphology. John Wiley & Sons New York.*: 113–22.

Crozier, M. J. 2005. "Multiple-Occurrence Regional Landslide Events in New Zealand: Hazard Management Issues." *Landslides* 2(4): 247–56.

D'Ambrosio, Donato, Giulio Iovine, William Spataro, and Hideaki Miyamoto. 2007. "A Macroscopic

Collisional Model for Debris-Flows Simulation." *Environmental Modelling and Software* 22(10): 1417–36.
Deltares. 2013. *Sobek 1D/2D Modelling Suite for Integral Water Solutions, Unser Manual*.
Dietrich, William E., and David R. Montgomery. 1998. "SHALSTAB: A Digital Terrain Model for Mapping Shallow Landslide Potential." *NCASI (National Council of the Paper Industry for Air and Stream Improvement) Technical Report* 1998.
Fan, Linfeng, Peter Lehmann, Brian McArdell, and Dani Or. 2017. "Linking Rainfall-Induced Landslides with Debris Flows Runout Patterns towards Catchment Scale Hazard Assessment." *Geomorphology* 280: 1–15. http://dx.doi.org/10.1016/j.geomorph.2016.10.007.
Floors, Rogier et al. 2018. "From Lidar Scans to Roughness Maps for Wind Resource Modelling in Forested Areas." *Wind Energy Science* 3(1): 353–70.
Florez, Maria Teresa, and Luis Norberto Parra. 1988. "Avalancha de La Quebrada Ayurá Del 14 de Abril de 1988." *II Conferencia sobre riesgos geológicos en el Valle de Aburrá*.
Fonseca, Felipe Augusto. 2019. *Analysing Changing Multi-Hazard Risk to Flow.like Phenomena for Urban Planning*. Enschede.
Funk, Chris et al. 2015. "The Climate Hazards Infrared Precipitation with Stations - A New Environmental Record for Monitoring Extremes." *Scientific Data* 2: 1–21.
Gomes, Roberto A. T. et al. 2008. "Identification of the Affected Areas by Mass Movement through a Physically Based Model of Landslide Hazard Combined with an Empirical Model of Debris Flow." *Natural Hazards* 45(2): 197–209. http://link.springer.com/10.1007/s11069-007-9160-z (October 23, 2017).
Gomez, J et al. 2007. *Geological Map of Colombia*. Bogotá. https://www2.sgc.gov.co/ProgramasDeInvestigacion/Geociencias/Documents/Descargables/Gomez-et-al-2007_GMC_PDF.pdf (August 9, 2017).
Heim, and Albert. 1882. "Der Bergsturz von Elm." *Zeitschrift der Deutschen Geologischen Gesellschaft*: 74–115. https://www.schweizerbart.de/papers/zdgg_alt/detail/34/61670?l=EN (June 28, 2018).
Hermelín, Michel, C. Curvelo, and V.L Osorio. 1992. "Studio de Los Fenómenos Ocurridos En La Cuenca Del Río San Francisco a Raíz Del Aguacero Del 20 de Marzo de 1991." *Memorias II Conferencia Latinoamericana sobre Riesgo Geológico Urbano y II Conferencia Colombiana sobre Geología Ambiental* 2: 147–76.
Horton, P., M. Jaboyedoff, B. Rudaz, and M. Zimmermann. 2013. "Flow-R, a Model for Susceptibility Mapping of Debris Flows and Other Gravitational Hazards at a Regional Scale." *Natural Hazards and Earth System Sciences* 13(4): 869–85.
Hoyos, Carlos D et al. 2019. "Meteorological Conditions Leading to the 2015 Salgar Flash Flood: Lessons for Vulnerable Regions in Tropical Complex Terrain." *Natural Hazards and Earth System Sciences* 19(11): 2635–65.
Hsu, Kenneth J. 1975. "Catastrophic Debris Streams (Sturzstroms) Generated by Rockfalls." *Geological Society of America Bulletin* 86(1): 129–40.
Hungr, O., S. G. Evans, M. J. Bovis, and J. N. Hutchinson. 2001. "A Review of the Classification of Landslides of the Flow Type." *Environmental and Engineering Geoscience* 7(3): 221–38.
Hungr, O, S Leroueil, and L Picarelli. 2014. "The Varnes Classification of Landslide Types, an Update." *Landslides,* 11(2): 167–194.
IDEAM. 2010. *Leyenda Nacional de Coberturas Para La Tierra. Metodología Corine Land Cover Adaptada Para Colombia. Escala 1:100.000*. https://www.researchgate.net/publication/303960063_LEYENDA_NACIONAL_DE_COBERTURAS_DE_LA_TIERRA_METODOLOGIA_CORINE_LAND_COVER_ADAPTADA_PARA_COLOMBIA_ESCALA_1100000.
IDEAM, and CNM. 2018. *Guia Metodologica Para La Elaboración de Mapas de Inundación*. http://documentacion.ideam.gov.co/openbiblio/bvirtual/023774/GUIA_METODOLOGICA_MAPAS_INUNDACION_MARZO_2018.pdf.
IGAC – Instituto Geográfico Agustín Codazzi. 2018. *Catalogo de Información Geográfica Disponible Para Procesos de Ordenamiento Territorial*.
Iverson, Richard M. 1997. "The Physics of Debris Flows." *Reviews of Geophysics* 35(3).
Jakob, DM, and O Hungr. 2005. "Debris-Flow Hazards and Related Phenomena." http://link.springer.com/content/pdf/10.1007/b138657.pdf (August 9, 2017).
Jaramillo-Robledo, Alvaro, and Bernardo Chaves-Córdoba. 2000. "Distribución de La Precipitación En Colombia Analizada Mediante Conglometación Estadística." *Cenicafé* 51(2): 102–13.
Javeriana, Universidad. 2016. *Informe General de Avenidas Torrenciales En El Municipio de Salgar*.
Kanjanakul, Chollada, and Tanan Chub-uppakarn. 2013. "Comparison between Numerical and Limit

Equilibrium Methods for Slope Stability Analysis." In *18th National Conference on Civil Engineering (NCCE)*, , 104–10.
Kellogg, JN, V Vega, and TC Stailings. 1995. "Tectonic Development of Panama, Costa Rica, and the Colombian Andes: Constraints from Global Positioning System Geodetic Studies and Gravity." *Geological Society of*. http://specialpapers.gsapubs.org/content/295/75.abstract (August 9, 2017).
Lehmann, Peter, Jonas von Ruette, and Dani Or. 2018. "How Landslides Become Disasters." *Eos* 99. https://eos.org/science-updates/how-landslides-become-disasters (June 17, 2020).
Lupiano, Valeria et al. 2018. "Simulations of Flow-like Landslides Invading Urban Areas: A Cellular Automata Approach with SCIDDICA." *Natural Computing* 17(3): 553–68. https://doi.org/10.1007/s11047-017-9632-3 (October 21, 2020).
Ma, Chiyang. 2018. "Comparing and Evaluating Two Physically-Based Models : Openlisem and Scoops3D , for Landslide Volume Prediction." University of Twente.
McDougall, Scott, and Oldrich Hungr. 2004. "A Model for the Analysis of Rapid Landslide Motion across Three-Dimensional Terrain." *Canadian Geotechnical Journal* 41(6): 1084–97. https://cdnsciencepub.com/doi/abs/10.1139/t04-052 (October 24, 2020).
Mergili, M., J. Krenn, and H. J. Chu. 2015. "R.Randomwalk v1, a Multi-Functional Conceptual Tool for Mass Movement Routing." *Geoscientific Model Development* 8(12): 4027–43.
Mergili, Martin et al. 2014. "Spatially Distributed Three-Dimensional Slope Stability Modelling in a Raster GIS." *Geomorphology* 206: 178–95.
Mergili, Martin, Jan Thomas Fischer, Julia Krenn, and Shiva P. Pudasaini. 2017. "R.Avaflow v1, an Advanced Open-Source Computational Framework for the Propagation and Interaction of Two-Phase Mass Flows." *Geoscientific Model Development* 10(2): 553–69.
Mikola, Roozbeh Geraili. 2017. "ADONIS: A Free Finite Element Analysis Software with an Interactive Graphical User Interface for Geoengineers." In *Geo Ottawa*, http://www.geowizard.org/ (October 24, 2020).
Ministerio de Vivienda. 2014. *Decreto Numero 1807*. Bogotá, Colombia.
Nettleton, IM, S Martin, S Hencher, and R Moore. 2005. "Debris Flow Types and Mechanisms." *Scottish road network*. http://www.geoffice.it/files/download/0015327.pdf (August 9, 2017).
Nkwunonwo, UC, M Whitworth, and B Baily. 2020. "A Review of the Current Status of Flood Modelling for Urban Flood Risk Management in the Developing Countries." *Scientific African* 7. https://www.sciencedirect.com/science/article/pii/S2468227620300077 (October 21, 2020).
O'Brien, J. S., P. Y. Julien, and W. T. Fullerton. 1993. "Two-Dimensional Water Flood and Mudflow Simulation." *Journal of Hydraulic Engineering* 119(2): 244–61. http://ascelibrary.org/doi/10.1061/%28ASCE%290733-9429%281993%29119%3A2%28244%29 (October 21, 2020).
O'Brien, JS, and PY Julien. 1985. "Physical Properties and Mechanics of Hyperconcentrated Sediment Flows." *HD Delineation of landslides, flash flood and debris flow Hazards*.
O'Brien, Karen. 1982. *FLO-2D Simulating Mudflows Guidelines*.
Pabón, J., J. Eslava, and R. Gómez. 2001. "Generalidades de La Distribución Espacial y Temporal de La Temperatura Del Aire y de La Precipitación En Colombia." *Meteorología Colombiana*.
Papaioannou, George et al. 2018. "An Operational Method for Flood Directive Implementation in Ungauged Urban Areas." *Hydrology*.
Piedrahita, I, and M. Hermelín. 2005. "La Avenida Torrencial Del Río Tapartó Antioquia de 1993." In *Desastres de Origen Natural En Colombia 1979-2004*, ed. FONDO EDITORIAL UNIVERSIDAD EAFIT. Medellin, 109–20.
Poveda, Germán et al. 2007. "Linking Long-Term Water Balances and Statistical Scaling to Estimate River Flows along the Drainage Network of Colombia." 12(1): 4–13.
———. 2011. "Mixed Memory,(Non) Hurst Effect, and Maximum Entropy of Rainfall in the Tropical Andes." *Advances in Water Resources* 34(2): 243–56. https://www.sciencedirect.com/science/article/pii/S0309170810002162 (March 14, 2020).
Prada-Sarmiento, Luis Felipe et al. 2019. "The Mocoa Event on March 31 (2017): Analysis of a Series of Mass Movements in a Tropical Environment of the Andean-Amazonian Piedmont." *Landslides* 16(12): 2459–68.
Quan, Byron. 2012. 206 Thesis of University of Twente, ITC "Dynamic Numerical Run-out Modeling for Quantitative Landslide Risk Assessment." University of Twente.
Reid, Mark E, Sarah B Christian, Dianne L Brien, and S Henderson. 2015. "Scoops3D—Software to Analyze Three-Dimensional Slope Stability throughout a Digital Landscape." *US Geological Survey Techniques and*

Methods, book 14.
De Roo, APJ, and VC Jetten. 1999. "Calibrating and Validating the LISEM Model for Two Data Sets from the Netherlands and South Africa." *Catena* 37: 477–93. https://www.sciencedirect.com/science/article/pii/S034181629900034X (October 21, 2020).
Serdano-Cruz, Karime, Yesid Carvajal-Escobar, and Alvaro Javier Avila Diaz. 2013. "Análisis de Aspectos Que Incrementan El Riesgo de Inundaciones En Colombia." *Revista Luna Azul* (37): 219–238. http://www.redalyc.org/html/3217/321729206014/.
Servicio Geológico Colombiano (SGC). 2007. "Mapa Geológico de Colombia 2007." https://www.researchgate.net/publication/279450501_Mapa_Geologico_de_Colombia_2007 (May 31, 2021).
———. 2015a. "Guía Metodológica Para Estudios de Amenaza, Vulnerabilidad y Riesgo Por Movimientos En Masa." *Bogotá, DC, Colombia*.
———. 2015b. *Mapa Geológico de Colombia 2015*. Bogotá, Colombia. https://www.researchgate.net/publication/281209421_Mapa_Geologico_de_Colombia_2015 (May 31, 2021).
———. 2016. "Proyecto Mapa Nacional de Amenaza Relativa Por Movimientos En Masa. Escala 1:100.000." https://www2.sgc.gov.co/ProgramasDeInvestigacion/geoamenazas/Paginas/Proyecto-Mapa-Nacional-de-Amenaza-Relativa.aspx# (May 31, 2021).
———. 2017a. *Caracterización Del Movimiento En Masa Tipo Flujo Del 31 de Marzo de 2017 En Mocoa – Putumayo*.
———. 2017b. *Zonificación de Susceptibilidad y Amenaza Por Movimientos En Masa de Las Subcuencas de Las Quebradas Taruca, Taruquita, San Antonio, El Carmen y Los Ríos Mulato y Sangoyaco Del Municipio de Mocoa - Putumayo. Escala 1:25.000*. https://www.researchgate.net/publication/324175334_Zonificacion_de_susceptibilidad_y_amenaza_por_movimientos_en_masa_de_las_subcuencas_de_las_quebradas_Taruca_Taruquita_San_Antonio_El_Carmen_y_los_rios_Mulato_y_Sangoyaco_del_municipio_de_Mocoa_-_Putum.
———. 2018a. *Amenaza Por Movimientos En Masa Tipo Flujo de Las Cuencas de Las Quebradas Taruca, Taruquita, San Antonio y El Carmen y Los Ríos Mulato y Sangoyaco, Municipio de Mocoa, Escala 1:5.000*.
———. 2018b. *Evaluación de La Amenaza Por Movimientos En Masa En El Área Urbana, Periurbana y de Expansión Del Municipio de Mocoa – Putumayo. Escala 1:5.000*. http://recordcenter.sgc.gov.co/B22/532_18 AmeMovMasa Urbana Periurb Mocoa 5K/DOCUMENTO/PDF/Informe 5K Mocoa.pdf.
Servicio Geológico Colombiano (SGC), and Pontificia Universidad Javreiana (PUJ). 2020. *Documento Producto (Preliminar)*. Bogotá.
SGC. 2017. "GUÍA METODOLÓGICA PARA LA ZONIFICACIÓN DE AMENAZA POR MOVIMIENTOS EN MASA ESCALA 1: 25 000." : 1–160.
Shen, Ping et al. 2020. "Debris Flow Enlargement from Entrainment: A Case Study for Comparison of Three Entrainment Models." *Engineering Geology* 270(September 2019): 105581. https://doi.org/10.1016/j.enggeo.2020.105581.
Shen, Ping, Limin Zhang, Hongxin Chen, and Ruilin Fan. 2018. "EDDA 2.0: Integrated Simulation of Debris Flow Initiation and Dynamics Considering Two Initiation Mechanisms." *Geoscientific Model Development* 11(7): 2841–56. https://gmd.copernicus.org/articles/11/2841/2018/ (October 24, 2020).
Stothoff, Stuart. 2008. *Infiltration Tabulator for Yucca Mountain: Bases and Confirmation*. San Antonio, Texas. https://www.researchgate.net/publication/301780252_Infiltration_Tabulator_for_Yucca_Mountain_Bases_and_Confirmation.
Taboada, A, LA Rivera, A Fuenzalida, and A Cisternas. 2000. "Geodynamics of the Northern Andes: Subductions and Intracontinental Deformation (Colombia)." http://onlinelibrary.wiley.com/doi/10.1029/2000TC900004/full (August 9, 2017).
Trenkamp, R, JN Kellogg, and JT Freymueller. 2002. "Wide Plate Margin Deformation, Southern Central America and Northwestern South America, CASA GPS Observations." *Journal of South American*. http://www.sciencedirect.com/science/article/pii/S0895981102000184 (August 9, 2017).
UNGRD, and PUJ. 2017. *Definición Del Sistema de Información Hidrometeorológica*. Bogotá. https://repositorio.gestiondelriesgo.gov.co/bitstream/handle/20.500.11762/27207/Productos_Mocoa5. Definicion_Sistema_Informacion.pdf?sequence=4&isAllowed=y.
Unidad Nacional de Gestión del Riesgo de Desastres (UNGRD). 2015. *Guía de Integración de La Gestión Del Riesgo y El Ordenamiento Territorial Municipal*. Bogotá.
Unidad Nacional de Gestión del Riesgo de Desastres (UNGRD), and Pontificia Universidad Javeriana (PUJ). 2016. *Consultoría de Estudios y Diseño Para La Implementación Del Sistema de Alerta Temprana Por*

Avenidas Torrenciales En La Microcuenca de La Quebrada La Liboriana, Quebrada La Clara y Río Barroso Del Municipio de Salgar (Antioquia). Bogotá, Colombia.

———. 2018. *Informe General Del Ejercicio Con Las Consideraciones Supuestas Y Restricciones De Los Resultados Generados*. Bogotá, Colombia. https://repositorio.gestiondelriesgo.gov.co/bitstream/handle/20.500.11762/27207/Productos_Mocoa10_Informe_ general_ejercicio.pdf?sequence=10&isAllowed=y.

Urrea, Viviana, Andrés Ochoa, and Oscar Mesa. 2016. "Validación de La Base de Datos de Precipitación CHIRPS Para Colombia a Escala Diaria, Mensual y Anual En El Periodo 1981-2014." *Conference paper* (November).

Varnes, D. J. 1978. "Slope Movement Types and Processes. In 'Landslides: Analysis and Control'.(Eds RL Schuster, RJ Krizek)." *ransportation Research Board, National Research Council: Washington, DC*. 9: 12–33.

Velásquez, Nicolás, Carlos D Hoyos, Jaime I Vélez, and Esneider Zapata. 2020. "Reconstructing the 2015 Salgar Flash Flood Using Radar Retrievals and a Conceptual Modeling Framework in an Ungauged Basin." *Hydrol. Earth Syst. Sci* 24: 1367–92. https://doi.org/10.5194/hess-24-1367-2020 (October 22, 2020).

Westen, CJ, and MJT Terlien. 1996. "An Approach towards Deterministic Landslide Hazard Analysis in GIS. A Case Study from Manizales (Colombia)." *Earth Surface Processes and*. http://onlinelibrary.wiley.com/doi/10.1002/(SICI)1096-9837(199609)21:9%3C853::AID-ESP676%3E3.0.CO;2-C/full (September 9, 2017).

Xiao, Yi. 2020. "Analyzing the Predictive Capacity of a Physically-Based Debris Flow Model: A Case Study for Debris Flow in the Post-2008 Wenchuan Earthquake Area." University of Twente.

7. APENDICES

7.1. Apendix 1: Soil Properties of Mocoa according to SGC (2018b)

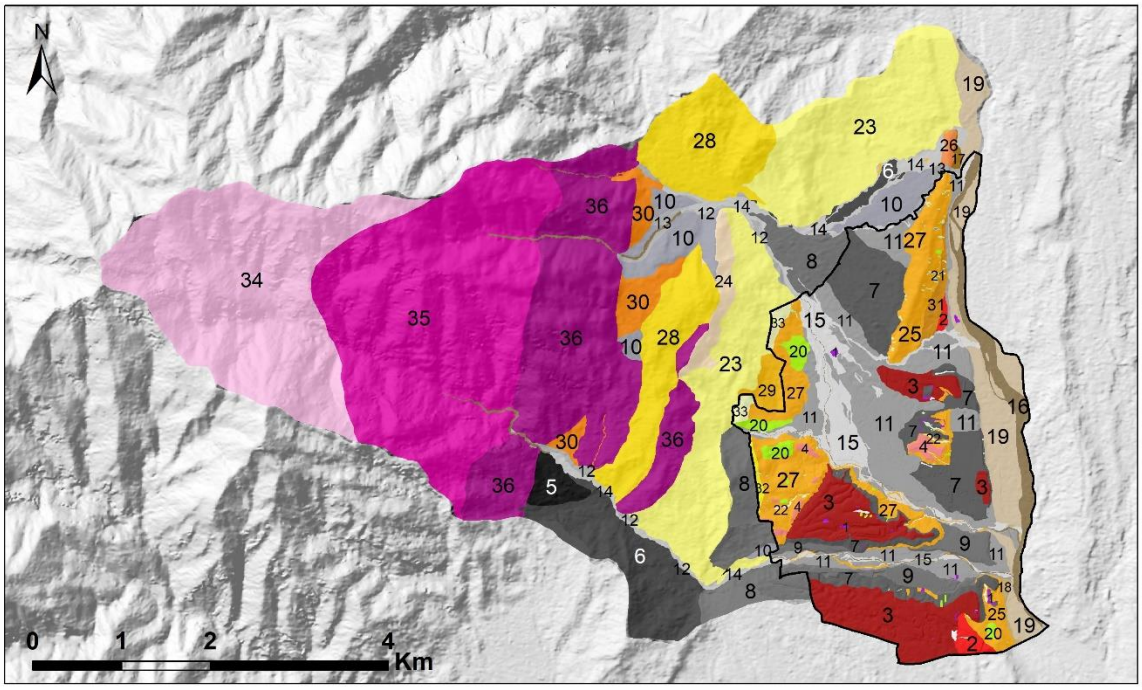

SOILS					ROCKS				
ANTROPIC	TRANSPORTED				SEDIMENTARY				IGNEOUS
	Fluvio-torrential		Alluvial	Coluvial	Conglomerate	Siltstone	Shale		Monzogranite
1 Stla	5 Staman	11 Stftgb	16 Stfca	20 Stci	23 Ricpi	25 Rmlv	27 Rmarr	32 Rmar	34 Rimgm
RESIDUAL	6 Staan	12 Stasac	17 Sttal	21 Stca	24 Ricps	26 Rmblv	28 Rbaro	33 Rrpi	35 Rbmgm
2 Srlv	7 Stftar	13 Stftsac	18 Stftal	22 Stl			29 Rmbar		36 Rmbgm
3 Srftar	8 Stftman	14 Stftac	19 Stflla				30 Rmbaro		
4 Srar	9 Stftargb	15 Stftb					31 Rmmlv		
	10 Stftan								

Number	Description	Code	Cohesion (kPa)	Internal Friction Angle (rad)	Soil Density (Kg/m3)
1	Transported soil, antropic	Stla	38.2	0.42	1800
2	Residual Soil of Villeta Fm. siltstones	Srlv	18	0.38	1800
3	Fluvio-torrential soil, clay matrix-supported	Stftar	22.54	0.43	1680
4	Residual Soil of Rumiyaco Fm. mudstones	Srar	18	0.38	1800
5	Fluvio-torrential soil, very old, matrix-suported	Staman	22.54	0.43	1800
6	Fluvio-torrential soil, old, matrix-supported	Staan	14.7	0.48	1800
7	Fluvio-torrential soil, clay rich	Srftar	27.4	0.47	1800
8	Fluvio-torrential soil, very old, clast-suported	stftman	27.4	0.47	1800
9	Fluvio-torrential soil, matrix-supported with boulders and gravel	Stftargb	14.7	0.49	1910

10	Fluvio-torrential soil, old, clast-supported	stftan	22.54	0.43	1680
11	Fluvio-torrential soil, clast-supported with boulders and gravel	Stftgb	12.9	0.61	1820
12	Fluvio-torrential soil, sub-actual, fine grained	Stasac	1	0.51	1800
13	Fluvio-torrential soil, sub-actual, coarse grained	stftsac	1	0.43	1800
14	Fluvio-torrential soil, actual	stftac	1	0.42	1800
15	Fluvio-torrential soil, flat surfaces covered with boulders, very recent	Stftb	1	0.51	1800
16	Alluvial soil, active riverbed	Stfca	1	0.42	1800
17	Alluvial soil, old terrace	Sttal	1	0.59	1810
18	Alluvial soil, very old terrace	stftal	1	0.60	1800
19	Alluvial soil, non-consolidated flat alluvial surfaces	Stflla	1	0.59	1810
20	Inactive colluvial soil	Stci	38.22	0.43	1820
21	Active colluvial soil	Stca	18	0.42	1820
22	Very fine grained washed colluvial deposits	Stl	38.22	0.42	1820
23	Conglomerates from Pepino Fm, Inferior Member	Ricpi	18	0.37	1800
24	Conglomerates from Pepino Fm, Superior Member, Intermediate Quality	Ricps	18	0.37	1800
25	Siltstones from Villeta Fm., Low quality	Rmlv	18	0.37	1800
26	Siltstones from Villeta Fm.	Rmblv	1	0.42	1800
27	Shales from Rumiyaco Fm., Low quality	Rmarr	18	0.37	2260
28	Shales from Orito Fm., Low quality	Rbaro	1	0.42	1800
29	Shales from Rumiyaco Fm.	Rmbar	18	0.37	1820
30	Shales from Orito Fm.	Rmbaro	18	0.37	1800
31	Shales from Rumiyaco Fm.	Rmmlv	18	0.38	1800
32	Shales from Villeta Fm.	Rmar	18	0.37	1800
33	Shales from Villeta and Rumiyaco Fms., very Low quality	Rrpi	22.54	0.37	1680
34	Mocoa Monzogranite, intermediate quality	Rimgm	18	0.38	1800
35	Mocoa Monzogranite, Low quality	Rbmgm	5	0.42	2000
36	Mocoa Monzogranite, very low quality	Rmbgm	18	0.41	1800

7.2. Apendix 2: Soil Properties of Mocoa according to UNGRD and PUJ (2018)

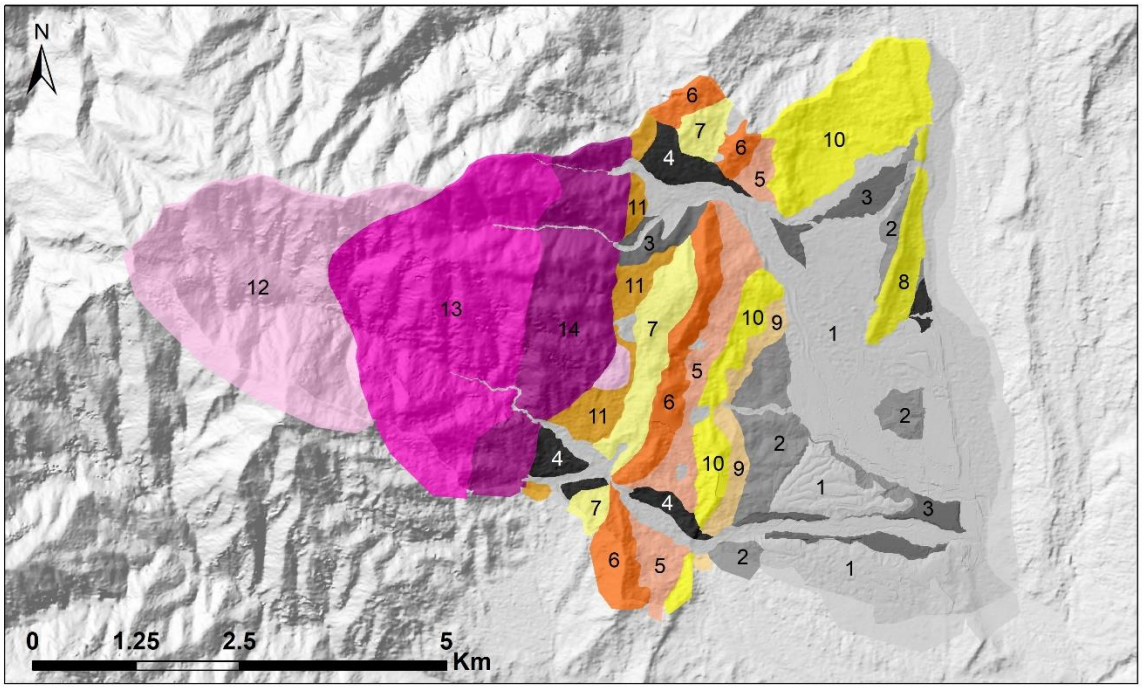

SOIL	ROCKS			
TRANSPORTED	SEDIMENTARY			IGNEOUS
	Conglomerate	Siltstone	Shale	Monzogranite
1 Stftsac	5 Rblpm	7 Rbaro	9 Rbar	12 Rmbgm
2 Stftar	6 Ricpc	8 Rblv	10 Rmbar	13 Rbmgm
3 Stftan			11 Rmbaro	14 Rmbmgm
4 Staman				

Number	Description	Code	Cohesion (Kpa)	Internal friction (rad)	Soil density (kg/m3)
1	Active transported soil	Stftsac	25	0.58	1800
2	Inactive transported soil	Stftar	50	0.58	1700
3	Old transported Soil	Stftan	45	0.58	1800
4	Very old transported soil	Staman	60	0.52	1600
5	Conglomerates from Pepino Fm. Intermediate Quality	Rblpm	65	0.49	1500
6	Conglomerates from Pepino Fm, Superior Member, Intermediate Quality	Ricpc	7	0.24	1600
7	Siltstone from the Orito Fm. Low Quality	Rbaro	65	0.49	1500
8	Silstone from the Villeta Fm. Low Quality	Rblv	10	0.17	1500
9	Shales Rumiyaco Fm. Low Quality	Rbar	65	0.49	1500
10	Shales from the Rumiyaco Fm. Very Low Quality	Rmbar	30	0.35	1700
11	Shales from the Orito Fm. Very Low Quality	Rmbaro	15	0.49	1500
12	Mocoa Monzogranite - Intermediate Quality	Rmbgm	100	0.33	1300
13	Mocoa Monzogranite - Low Quality	Rbmgm	10	0.35	1300
14	Mocoa Monzogranite - Very Low Quality	Rmbmgm	11.7	0.33	1300

7.3. Apendix 3: Soil Properties of Salgar

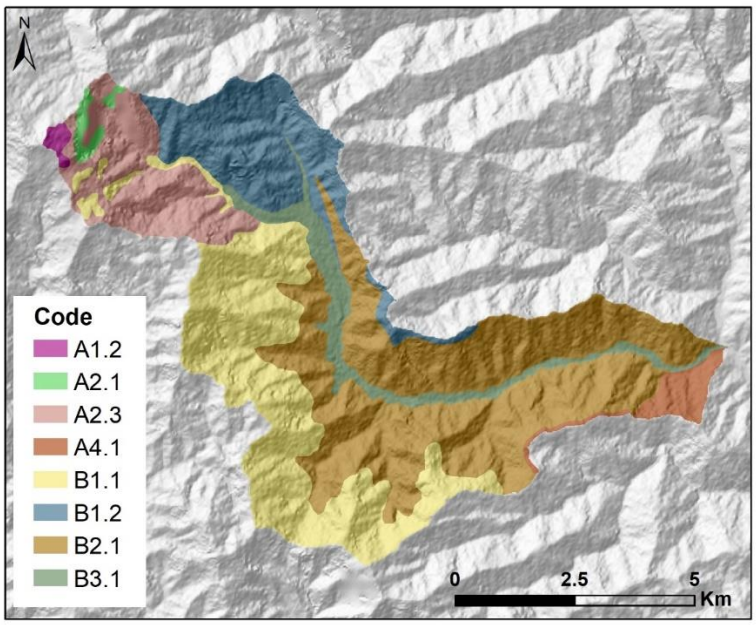

Code	Description	Cohesion (KPa)	Internal Friction Angle (rad)	Soil Density (Kg/m3)
A1.2	Branched crests, very high slopes, granitic rocks with layers of volcanic ash	16	0.61	1700
A2.1	Near vertical escarpment with severe mass movement processes	16	0.61	1700
A2.3	Moderately inclined slopes of granitic rocks with volcanic ashes	10	0.70	1900
A4.1	Moderately inclined slopes of sedimentary rocks with volcanic ashes	22	0.52	1500
B1.1	Moderately inclined slopes with severe mass movement processes	10	0.87	1800
B1.2	Moderately inclined slopes of shales, sandstones, and conglomerates with volcanic ashes	10	0.70	1800
B2.1	Moderately inclined slopes of sandstones, mudstones and meta-sedimentary rocks	16	0.52	1500
B3.1	Valley bottom	16	0.61	1600

7.4. Description of the runs for the Mocoa case on the detailed scale

Run	Soil Depth Map	soil units map	Other	Multiplication Factors			
				C-IFA	SD	Ksat	Theta
1	Catani	Detailed		0.75	1	1	1
2	Catani	Detailed		0.85	1	1	1
3	Catani	Detailed		0.8	1.1	1	1
4	Catani	Detailed		0.9	1.1	1	1
5	Catani	Detailed		1	1	1	1
6	Catani	Detailed		1	1	1	1
7	Catani	Detailed		0.3	1.1	1	1.5
8	Catani	Detailed		0.8	1	1	1
9	Catani	Detailed	Scars as sources	0	1	1	1
10	Catani	Detailed	Landslides as sources	0	1	1	1
11	Catani	Detailed	Landslides as sources	0.3	1	1	1
12	Catani	Detailed	Landslides as sources	0	1.1	0.5	1
13	Catani	Detailed	Landslides as sources	0	3	0.5	2
14	Catani	Coarse	Landslides as sources	0	2	0.5	2
15	Stothoff	Detailed		0.7	1	1	1
16	Stothoff	Detailed		0.85	1	0.5	0.5
17	Stothoff	Detailed		0.85	1	0.75	0.75
18	Stothoff	Detailed		0.85	1	1	0.5
19	Stothoff	Detailed		0.85	1	1	1
20	Stothoff	Detailed		0.8	1	1	1.2
21	Stothoff	Detailed		0.8	1	1	1.7
22	Stothoff	Detailed		0.8	1.15	1	1
23	Stothoff	Detailed		0.85	1	0.5	1
24	Stothoff	Detailed		0.85	1.1	0.2	1
25	Stothoff	Detailed		0.85	1.5	0.2	1
26	Stothoff	Detailed	Landslides as sources	0	5	0.5	2
27	Stothoff	Detailed	Landslides as sources	0.85	10	0.2	1
28	Stothoff	Coarse		0.8	1	1	1
29	Stothoff	Coarse		0.3	1.5	1	1.5
30	Stothoff	Coarse		0.8	2	1	1
31	Stothoff	Coarse		0.5	1.5	0.5	1.5
32	Stothoff	Coarse		0.4	1.8	0.4	1.8
33	Stothoff	Coarse		0.3	1.9	0.3	1.9
34	Stothoff	Coarse		0.2	2	0.2	2
35	Stothoff	Coarse		0.2	2.5	1	1
36	Stothoff	Coarse		0.4	2	1	1
37	Stothoff	Coarse		0.6	1.5	1	1
38	Stothoff	Coarse		0.7	1.5	1	1
39	Stothoff	Coarse		0.6	2	1	1
40	Stothoff	Coarse		0.5	1.5	1	1
41	Stothoff	Coarse		0.5	2	1	1
42	Stothoff	Coarse		0.5	1.8	1	1
43	Stothoff	Coarse		0.6	1	1	2
44	Stothoff	Coarse		0.6	1	1	2
45	Stothoff	Coarse	Solid Phase Internal Friction Angle * 0.5	0.3	1.5	1	2
46	Stothoff	Coarse	Dynamic Viscosity * 0.5	0.3	1.5	1	2
47	Stothoff	Coarse	Drag Force is is 2	0.3	1.5	1	2
48	Stothoff	Coarse	Soil Phase Fraction *0.5	0.3	1.5	1	2
49	Stothoff	Coarse	Release Volume *1	0.3	1.5	1	2
50	Stothoff	Coarse		0.3	1.5	1	2

7.5. Description of the runs for the Mocoa case on the coarse scale

Run	Soil Depth Map	soil units map	Other	Multiplication Factors			
				C-IFA	SD	Ksat	Theta
1	Stothoff	Detailed		0.75	1	1	1
2	Stothoff	Detailed		0.75	1.2	1	1
3	Stothoff	Detailed		0.7	1.25	1	1
4	Stothoff	Detailed		0.8	1.1	1	1
5	Stothoff	Detailed		0.7	1.1	1	1
6	Stothoff	Detailed		0.8	1.15	1	1
7	Stothoff	Detailed		0.8	1.15	1	1.5
8	Stothoff	Coarse		0.6	1	1	2
9	Stothoff	Coarse	Release volume * 0.5	0.6	1	1	2
10	Stothoff	Coarse	Dynamic viscosity *0.2	0.3	3	0.5	2
11	Stothoff	Coarse	Dynamic viscosity *0.5	0.3	1.5	1	2
12	Stothoff	Coarse	Drag Force *0.5	0.3	1.5	1	2
13	Stothoff	Coarse	Soil Phase Fraction *2	0.3	1.5	1	2
14	Stothoff	Coarse	Release Volume *0.5	0.3	1.5	1	2
15	Stothoff	Coarse		0.3	1.5	1	2
16	Catani	Coarse	Landslides as sources	0	5	0.5	2
17	Stothoff	Detailed		0.7	0.8	1.1	1
18	Stothoff	Detailed		0.3	1.5	0.5	2
19	Stothoff	Detailed		0.5	1.5	0.5	2
20	Stothoff	Detailed		0.5	1.5	1	2
21	Stothoff	Detailed	Transport capacity *4	0.7	2	1	2
22	Stothoff	Detailed	Transport capacity* 2	0.4	2	1	2
23	Stothoff	Detailed	Transport capacity *5	0.5	3	3	3
24	Stothoff	Detailed	Transport capacity* 10	0.3	1	3	2
25	Catani	Coarse		0.5	2	1	1
26	Catani	Coarse	Dynamic Viscosity *0.5	0.5	2	1	1
27	Catani	Coarse		0.4	2	1	1
28	Catani	Coarse		0.3	2	1	1
29	Catani	Coarse		0.3	2	1	1
30	Catani	Coarse		0.3	2	1	1
31	Catani	Coarse		0.3	2	1	1.5
32	Catani	Coarse	Drag Force *2	0.3	2	1	1
33	Catani	Coarse	Soil Phase Fraction *0.5	0.3	2	1	1
34	Catani	Coarse	Release Volume *2	0.3	2	1	1
35	Catani	Coarse		0.3	2	1	2

7.6. Description of the runs for Salgar

Run	Other	Multiplication Factors			
		C-IFA	SD	Ksat	Theta
1		1	1	1	1
2		1	1	1	1
3		1	1	1	1
4		0.75	1	1	1
5		0.5	1	1	1
6		0.3	1	1	1
7		0.1	1	1	1
8		0.2	1	1	1
9	Includes channel section	1	1	1	1
10	Includes channel section	0.2	1	1	1
11		0.75	1.5	1	1
12		0.5	2	1	1
13		0.5	1.5	1	1
14		0.4	1.5	1	1
15		0.4	2	1	1
16	Includes channel section	0.75	2	1	1
17	Includes channel section	0.3	2	1	1
18	Includes channel section	0.3	1.5	1	1
19		1	1.5	1	1
20		1	2	1	1
21	Includes channel section	1	3	1	1
22		0.5	2	1	2
23	Includes channel section	0.75	2	1	1.5
24	Includes channel section	0.5	1.5	1	2
25	Includes channel section	0.75	1.5	1	2
26	Includes channel section	0.3	1.5	1	1.5
27		0.3	1.5	1	1.5
28	Includes channel section	0.3	2	1	1.5
29	Includes channel section	0.3	1.5	1	2
30		0.4			
31		0.3	1	0.8	1.5
32	Includes channel section	0.3	1	0.5	2
33	Includes channel section	0.3	1	0.2	2
34		0.75	1	1	2
35	Includes channel section	0.5	1	1	2
36	Includes channel section	0.3	1	1	1.5
37	Includes channel section	0.3	1	1	2
38		0.2	1	1	1.5
39		0.3	1	1	1.5
40		0.3	1	1	2
41		0.3	1.5	0.8	1
42		0.3	1.5	0.5	1
43		0.3	1.5	0.3	1
44		0.3	2	0.8	1
45		0.3	2	0.3	1
46		0.2	1.5	0.8	1
47		0.2	1.5	0.3	1
48		1	2	0.5	2
49		0.5	2	0.5	1.5
50		0.5	1	1	2